
Molecular roles of the Prion Protein in zebrafish embryos and cultured cells

Dissertation

Zur Erlangung des Doktors der Naturwissenschaften (Dr. rer. nat.)

An der Universität Konstanz
Mathematisch-Naturwissenschaftliche Sektion
Fachbereich Biologie

Vorgelegt von
Aimilia Sempou

Dezember 2013

Kurzfassung

Das Prion Protein (PrP) ist ein glykosyliertes Protein an der Zelloberfläche, welches für seine Schlüsselrolle in übertragbaren krankhaften Veränderungen des Gehirns bekannt ist, den sogenannten Prion-Krankheiten oder "übertragbaren, spongiformen Enzephalopathien". Hierbei verliert PrP seine normale Konformation, aggregiert und verursacht Neurodegeneration. Die Umwandlung von normalem, zellulärem PrP (PrP^C) in eine missgefaltete, zur Aggregation tendierende Isoform (PrP^{Sc}) gilt als Kennzeichen dieser Krankheitsgruppe und ist ein wichtiger Auslöser für neuronalen Zelltod. Außerdem steht aber mittlerweile fest, dass die Anwesenheit von normalem PrP^C auf der Neuronenoberfläche ebenfalls eine Voraussetzung für die Einleitung des neurodegenerativen Prozesses ist. Aus diesem Grund wird die Hypothese weitgehend unterstützt, dass missgefaltetes/aggregiertes PrP^{Sc} seine neurotoxische Wirkung ausübt indem es eine physiologische Funktion/Aktivität von PrP^C auf der Zellmembran umwandelt oder destabilisiert. Die anerkannte Rolle von PrP als Signaltransduktionsmolekül würde mit einem solchen Szenario übereinstimmen. Jedoch sind die von PrP regulierten molekularen Signale noch größtenteils unbekannt. Unser Labor hat in einer früheren Studie entdeckt, dass das Zebrafisch-Ortholog PrP-1 als positiver Regulator von E-cadherin-vermittelter Zell-Zell-Adhäsion während der frühen Embryonalentwicklung (Gastrulation) fungiert. Dementsprechend blieben Embryonen, in denen PrP-1 ausgeschaltet war, früh in ihrer Entwicklung stehen, weil ihre Zellen nicht stark genug aneinander haften konnten um notwendige morphogenetische Bewegungen durchzuführen. Interessanterweise konnte überexprimiertes Säugetier-(Maus) PrP den Verlust der PrP-1 Funktion kompensieren, was darauf hindeutete, dass die Fähigkeit Zelladhäsion zu regulieren ein evolutiv konserviertes Merkmal von PrP ist. Das Ziel dieser Arbeit war die konservierten, zellulären Signalwege zu identifizieren, durch die PrP E-cadherin-Adhäsion in der Gastrula reguliert. Es konnte gezeigt werden, dass die Src Tyrosinkinasen Fyn und Yes im Signalweg unterhalb von PrP aktiviert werden und dabei die Endozytose von Adhäsionskomplexen verhindern, die aus transmembranem E-cadherin und seinem intrazellulären Bindepartner β -catenin bestehen. Dementsprechend ähnelten sich die Phänotypen von Zebrafischembryonen mit einem PrP-1 oder einem Fyn/Yes knockdown, während die von PrP-1 knockdown verursachten Entwicklungsdefekte sich durch exogene Fyn- und Yes- Expression überwinden ließen. Interessant ist auch unser Befund, dass PrP-Depletion die Lokalisierung von β -catenin an der Plasmamembran beeinträchtigt, wogegen eine PrP-Überexpression diese Lokalisierung übermäßig fördert. Dadurch wirkt PrP der, neben der Zelladhäsion, zweiten Funktion von β -

catenin als Transkriptionsaktivator im Zellkern stark entgegen. Die unnatürliche Stabilisierung von β -catenin an der Plasmamembran und die daraus resultierende Unfähigkeit in den Nucleus zu translozieren, inhibiert die Entwicklung von dorsalem Embryonalgewebe, dessen Ausbildung auf β -catenin-vermittelte Transkription angewiesen ist. Wir zeigen weiterhin, dass die subzelluläre Lokalisierung von PrP (Maus oder Zebrafisch) und seine Fähigkeit die Gastrulation zu beeinflussen sowohl von seiner Verankerung an der Zellmembran als auch von seiner repetitiven und globulären Domäne abhängt. Als ebenso wichtig für die Funktionalität von PrP (Maus) im Zebrafish Embryo erwies sich eine kurze positiv geladene Region im N-Terminus, die in anderen Studien als essentiell für die neuroprotektive Wirkung des Proteins erachtet wurde. Im Gegensatz dazu, zeigte sich kein Effekt auf die Aktivität von Maus-PrP bei Deletion der zentralen Region des Proteins, die laut anderer Studien Einfluss auf neurotoxische Ereignisse in transgenen Mäusen hat. Interessanterweise verursachten aber Zebrafisch PrP Mutanten mit fehlender zentralen Region ähnliche Toxizität in Säugetierzellen wie die entsprechende Maus Deletionsmutante. Aufgrund jüngster Erkenntnisse, dass PrP^C nicht nur wichtig für Prion-Erkrankungen ist, sondern auch als Rezeptor für neurotoxische A β -Oligomere in der Alzheimer-Krankheit fungiert, untersuchten wir die Effekte dieser toxischen Spezies auf PrP-abhängige Signalwege in embryonalen Zebrafischzellen. Wir fanden heraus, dass die Behandlung von Zellen mit A β -Oligomeren eine PrP-1-vermittelte Aktivierung von Src Kinasen und die Erhöhung der zellulären Mengen von E-cadherin verursachte und damit ein PrP "gain-of-function" Szenario nachahmte. Insgesamt heben diese Befunde die bemerkenswerte funktionelle Konservierung von PrP innerhalb der Vertebratengruppe, in Bezug auf seine Fähigkeit komplexe intrazelluläre Signale zu regulieren, hervor. Diese sind von besonderer Wichtigkeit für die Fachgebiete der Entwicklungsbiologie, der neurodegenerativen Erkrankungen, sowie auch der Zelladhäsion.

Abstract

The prion protein (PrP) is a cell surface glycoprotein, best known for its key role in infectious brain disorders in which it misfolds, forms aggregates and triggers neurodegeneration. Although the misfolding and aggregation of PrP in the brain constitute hallmarks of these disorders, it has become clear that normally folded PrP molecules contribute to neuronal death via an activity carried out on neuronal surfaces. Thus, aggregates of misfolded PrP trigger neurodegeneration possibly by subverting the function of normal PrP molecules. A physiological role of PrP in signal transduction is consistent with this thesis, but the exact nature of PrP's function and the underlying molecular mechanisms have remained elusive. Our laboratory identified the zebrafish orthologue PrP-1 as a positive regulator of E-cadherin based cell-cell adhesion during early embryonic development. Due to their impaired tissue cohesiveness, PrP-1 knockdown embryos failed to undergo morphogenesis and became arrested at gastrulation. Interestingly, mammalian (mouse) PrP could compensate for PrP-1 loss of function, indicating that the control of cell adhesion is a basic, conserved function of PrPs. The goal of my thesis was to elucidate the conserved cellular and molecular mechanisms by which PrP exerts its regulation over E-cadherin-based adhesion in the zebrafish gastrula. Our morpholino knockdown experiments revealed that the Src tyrosine kinases Fyn and Yes act downstream of PrP-1 to prevent the endocytosis of cell surface adhesion complexes, composed of transmembrane E-cadherin and its intracellular binding partner β -catenin. Accordingly, downregulation of Fyn/Yes or PrP-1 produce similar gastrulation phenotypes and defects in cell adhesion, whereas the exogenous expression of these kinases in PrP-1 knockdown embryos leads to developmental recovery. We further show that zebrafish and mouse PrPs positively regulate the activity of Src kinases and that these have an unexpected, positive effect on E-cadherin-mediated cell adhesion *in vivo*. In addition, while PrP knockdown disrupts the cell surface localization of E-cadherin, PrP mRNA overexpression enhances it, thereby sequestering β -catenin at the plasma membrane and antagonizing its parallel role as a transcription activator in the nucleus. This, in turn, leads to impaired development of embryonic dorsal structures, which largely depends on β -catenin nuclear signaling. Through mutational analysis, we found that the ability of PrP to localize at cell-cell contacts and influence zebrafish gastrulation phenotypes depends on its anchorage at the plasma membrane as well as on its repetitive and globular domains. In addition, we show that a small polybasic stretch within PrP's N-terminus, reportedly encoding neuroprotective properties, is essential to the role of PrP during zebrafish gastrulation. Conversely, PrP activity was not affected by deletion of a central

stretch that controls neurotoxicity in transgenic mice, although the corresponding zebrafish mutant PrPs were toxic to mammalian cells. Finally, in light of the recent identification of PrP^C as a receptor for neurotoxic A β oligomers in Alzheimer's disease, we assessed the effects of these species on PrP-mediated signaling in zebrafish embryonic cells. These experiments revealed that exposure to A β oligomers leads to the PrP-1-dependent activation of Src kinases and a simultaneous increase in the levels of E-cadherin, thus mimicking a PrP gain-of-function scenario. Taken together, these findings highlight the remarkable functional conservation of vertebrate PrPs in the regulation of complex intracellular signals relevant to the fields of development, neurodegeneration and cell adhesion.

Abbreviations

AD	Alzheimer's disease
AJ(s)	adherens junction(s)
BSE	bovine spongiform encephalopathy
CA	constitutively active
CJD	Creutzfeldt-Jakob disease
GPI	glycosylphosphatidylinositol
GSS	Gerstmann-Sträussler-Scheinker syndrome
MO	morpholino
OE	overexpression
SFK(s)	Src family kinase(s)
WT	wildtype

Table of Contents

Kurzfassung	3
Abstract	5
Abbreviations	7
Table of Contents	8
1 Introduction	12
1.1 Prion diseases.....	12
1.2 The nature of prions	13
1.3 Prion protein sequence and structure	14
1.4 The role of PrP ^C in prion and other neurodegenerative diseases.....	16
1.5 PrP cell biology and physiological function- An overview	17
PrP expression and general cell biology	17
Studies in mice.....	18
Studies in cells	19
1.6 Insights into PrP function from the zebrafish	20
1.7 E-cadherin-mediated adhesion and its regulation.....	28
Regulation of the expression levels of AJ proteins	29
Regulation by phosphorylation of AJ components.....	30
Regulation via endocytosis/degradation	31
Regulation by local modulation of actin dynamics	31
2 Aims of this study	33
3 Materials	34
3.1 Organisms/Cell lines	34
3.2 Zebrafish media	34
3.3 Morpholino antisense oligonucleotides (Gene Tools, LLC)	34
3.4 Morpholino working solutions.....	35
3.5 Synthetic mRNAs.....	35
3.6 Plasmid vectors and DNA constructs.....	36
3.7 Cell culture media and reagents.....	37
3.8 Chemical Inhibitors.....	38
3.9 Other solutions and buffers.....	38
3.10 Antibodies for immunofluorescence (IF) and Western blot (WB) analysis	40
3.11 Protein and DNA markers	42

3.12	Enzymes	42
3.13	Kits	42
3.14	Other Materials/Chemicals	42
3.15	Laboratory equipment	43
3.16	Software	43
4	Methods	44
4.1	Maintenance of adult zebrafish	44
4.2	Embryo microinjection	44
4.3	Morpholinos	44
4.4	mRNAs	44
4.5	Molecular Cloning	45
	Cloning of mouse PrP cDNAs into pCS2+	45
	The 3F4 epitope	46
	Generation of Fyn and Yes -EGFP and cloning into pCS2+	46
	Generation of zebrafish PrP-1 and -2 Δ CR constructs	46
4.6	Chemical inhibitors	47
4.7	Assessment of embryonic phenotypes (live pictures and quantifications)	47
4.8	Immunostainings of zebrafish embryos	48
4.9	Immunofluorescence profiles and quantification (zebrafish embryos)	48
4.10	Western Blots with zebrafish embryo lysates	48
	Preparation of embryo lysates for Western Blot (General protocol)	48
	Preparation of embryo lysates for Western Blot detection of the 120 kDa E-cadherin isoform	49
	SDS gel electrophoresis and Western Blot analyses	49
4.11	Treatment of zebrafish embryonic cells with Aβ₁₋₄₂ peptide	50
4.12	HEK cells	51
	Culture conditions	51
	Drug-based cell assay (DBCA)	51
	Western Blot	51
4.13	MCF-7 cells	52
	Culture conditions	52
	Immunostainings	52
	Western Blots	52
5	Results	54
5.1	PrP-1 regulates the turnover of selected AJ components at the plasma membrane	54
5.2	Convergence of SFK and PrP-1 knockdown phenotypes	57
5.3	Fyn and Yes act downstream of PrP-1 to maintain embryonic AJ stability	60

5.4	PrP-1 modulates the levels and activation state of SFKs	61
5.5	PrP gain-of-function in the zebrafish embryo	63
5.6	PrP expression triggers SFK activation and translocation to cell-cell contacts in human MCF-7 cells	68
5.7	Contribution of PrP domains and glycosylation to PrP localization and regulation of E-cadherin based cell-cell adhesion (Solis et al, 2013)	70
	Differential subcellular localization of PrP deletion mutants in MCF-7 cells	72
	Differential subcellular localization of PrP deletion mutants in zebrafish embryos	73
	Functional tests through rescue assays.....	76
	Functional tests through overexpression assays	77
5.8	Functionality of neurotoxic mouse PrP mutants in zebrafish embryos	78
	Localization of mouse PrP mutants in zebrafish embryos	81
	Functional tests through rescue assays.....	83
	Functional tests through overexpression assays	83
	Zebrafish Δ CR PrPs act cytotoxically in a drug-based cell assay	84
5.9	Treatment of zebrafish embryonic cells with Aβ₁₋₄₂ oligomers activates the PrP-1/SFK pathway affecting AJ protein levels	86
6	Discussion	89
6.1	Regulation of AJ stability by PrP-1	89
6.2	Fyn and Yes act downstream of PrP-1 during gastrulation	91
6.3	SFK-mediated changes in cell-cell adhesion	93
6.4	Regulation of SFKs by PrP	96
6.5	PrP overexpression: adhesion vs. β-catenin signaling	97
6.6	Roles of different PrP domains in PrP localization and function	100
	Glycosylation and GPI-anchorage	100
	Hydrophobic domain	101
	Repetitive and globular domains.....	101
	Physiological vs. pathological functions of PrP domains	103
6.7	Functionality of mouse PrP mutants with a known impact on neuronal survival 104	
	Subcellular localization in zebrafish embryos	104
	The N-terminal polybasic residues 23-31 but not the central region affect PrP's function during zebrafish gastrulation	106
6.8	Neurotoxic Aβ oligomers induce changes in SFK activation and AJ protein levels in a PrP-1-dependent way	107
7	Conclusions and Outlook	109
8	References	111

9 Acknowledgements 141

1 Introduction

1.1 Prion diseases

The cellular prion protein (PrP^C) is a neuronal cell-surface glycoprotein that entered the spotlight of research when its misfolded form, scrapie PrP (PrP^{Sc}), was identified as the causative agent of a group of fatal brain diseases collectively termed transmissible spongiform encephalopathies (TSEs) (Bolton et al, 1987; Bolton et al, 1982; Bueler et al, 1993). TSEs, also referred to as prion diseases, have been reported since the 1700s and include a variety of neurodegenerative illnesses, ranging from scrapie in sheep and bovine spongiform encephalopathy (BSE) in cattle to Kuru and Creutzfeldt-Jakob disease (CJD) in humans. Prions are proteinaceous infectious particles composed of aggregated PrP^{Sc}, which can be isolated from the brains of TSE afflicted individuals and the term was introduced by Stanley Prusiner and his coworkers, who successfully isolated the infective agent in the 1980s (Prusiner, 1982). Although different TSEs vary in their clinical progression, they all appear to be linked to PrP^{Sc}, are transmissible and share characteristic histopathological traits, including spongiform vacuolation of the brain, neuronal death and astrocytosis (DeArmond et al, 1987). In humans these may result in characteristic cognitive and motor deficiencies, such as rapidly progressing dementia, depression, blindness, speech impairment and cerebellar ataxia.

Depending on their etiology, TSEs can be classified into different categories. Sporadic TSEs, exemplified in humans by CJD and some cases of Gerstmann-Sträussler-Scheinker syndrome (GSS), appear randomly, have unknown causes and no apparent link to genetic or external factors. Although the incidence of CJD is rare, causing the death of one in one million individuals per year worldwide, its rapid progression and lethality within a year after its onset place it among the most severe known neurological illnesses. The second type of TSEs, familial prion diseases, is connected to autosomal dominant alterations of the PrP gene, which increase the probability of PrP misfolding. These illnesses, which include familial CJD, most cases of GSS, as well as fatal familial insomnia (FFI), typically manifest themselves early during life and have long durations. Finally, acquired TSEs are caused by direct exposure to prion-contaminated material. Kuru, a neurological condition reported in the 1950s among Papua New Guinea natives is an example of an acquired TSE. Its spread among the affected tribes took place via cannibalistic rituals in which families ate the brains of their deceased relatives. More recently, in the 1990s, individuals in the UK developed a novel TSE named variant CJD (vCJD) after ingesting prion-contaminated meat, this

occurrence being strongly regarded as the spread of BSE (“mad cow disease”) to humans (Bruce et al, 1997).

1.2 The nature of prions

Since the identification of PrP^{Sc} as the infective element behind TSEs, intensive research has provided insights into the molecular basis of these disorders. The initial key event is the conformational rearrangement of PrP^C, a protein found normally in the central nervous system (CNS), into its rogue isoform PrP^{Sc} (Bendheim et al, 1992). Unlike its cellular counterpart, PrP^{Sc} tends to aggregate and form amyloid deposits in the brain, triggering via poorly defined mechanisms neuronal loss (Prusiner, 1998). Remarkably, although prions form in other tissues as well, such as lymphoid organs and skeletal muscle, it is only in neurons where they cause damage (Bosque et al, 2002; Glatzel et al, 2003). It is now widely accepted that the accumulation of prions relies on the ability of PrP^{Sc} to replicate by binding and conferring its rogue conformation onto PrP^C (Bolton & Bendheim, 1988; Prusiner, 1998) (Figure 1). In fact, the transmissibility of TSEs across species relies on the physical interaction between PrP^C and PrP^{Sc} molecules of different animals (Prusiner, 1991). Although the exact dynamics of PrP conversion await full elucidation, it has become clear that mismatches in the primary sequences of donor PrP^{Sc} and host PrP^C reduce the efficiency of the process, making transmission of prions less likely between different species than within the same one (Priola & Chesebro, 1995; Prusiner et al, 1990).

Altogether, the majority of experimental data strongly suggests that PrP^{Sc} is infectious on its own, is not part of any type of virus or microorganism, and does not require nucleic acids for its replication. This “protein-only” hypothesis, originally proposed by S. Prusiner (Prusiner, 1982), is supported by the repeated failure to detect nucleic acids physically associated with prions, the strong link between the PrP gene and disease susceptibility, as well as the existence of familial forms of TSEs (Weissmann, 2004). However, direct proof for the protein-only hypothesis is yet to be provided, since a *de novo* generation of prions from full length PrP^C -without use of infectious material derived from animals- remains unaccomplished (Benetti & Legname, 2009). In fact, some researchers still defend the idea that TSE infectivity does not rely on PrP^{Sc}, but rather on a viral particle, and that PrP amyloid aggregates represent the host’s reaction to infection (Manuelidis, 2003).

Notwithstanding the controversy it generated, the protein-only hypothesis has recently gained more momentum due to indications that other protein misfolding diseases (PMDs), such as Alzheimer’s (AD), Parkinson’s or Huntington’s may be infectious and involve similar mechanisms of transmission. For example, brain homogenates from Alzheimer’s patients

were shown to induce aggregation of host A β peptide when injected into mouse brains or administered peripherally, an event that depended on the presence of pre-formed A β aggregates in the inoculum (Meyer-Luehmann et al, 2006). Similarly, Tau aggregates from brain extracts of AD patients induced the aggregation of native mouse Tau and caused brain pathology (Clavaguera et al, 2009). The evidence for misfolded proteins acting infectious is even more striking in the case of two systemic amyloid diseases, namely secondary reactive amyloidosis and mouse senile amyloidosis. These illnesses, associated with the deposition of amyloid-A and apolipoprotein A-II aggregates, respectively, have been demonstrated to be transmissible between individuals both via blood transfusion or oral administration (Lundmark et al, 2002; Xing et al, 2001). Altogether, these exciting findings strengthen the credibility of a protein-only hypothesis, but also raise important questions about what mechanisms are common or distinct behind these different pathologies.

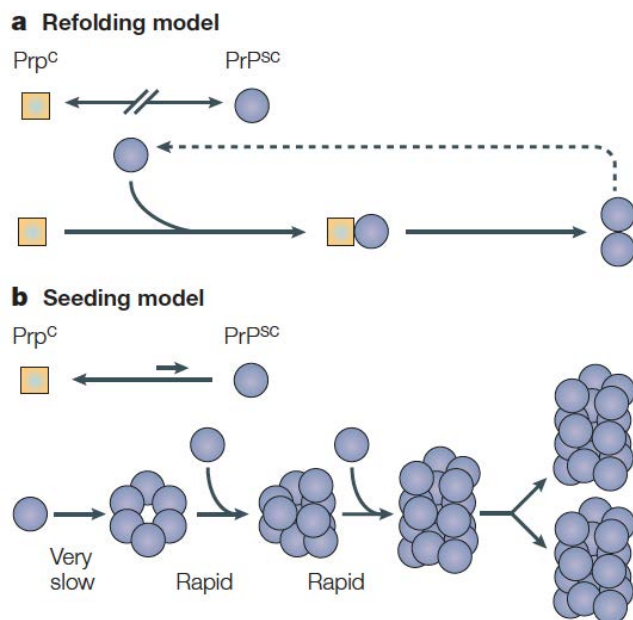


Figure 1 Two possible models for conversion of PrP^C to PrP^{Sc}. **a.** A spontaneous conversion of PrP^C to PrP^{Sc} is kinetically regulated, so that PrP^{Sc} is not formed at detectable levels under physiological conditions. Conversion can be induced by interaction with exogenous PrP^{Sc}, possibly enabled by an enzyme or chaperone, or can occur spontaneously as a rare event in the case of certain PrP mutations. **b.** Both PrP isoforms exist in equilibrium, the PrP^C conformation being kinetically favored. PrP^{Sc} is stabilized only upon addition to an already formed PrP^{Sc} aggregate (seed). Seed formation is rare, but once it occurs, PrP^{Sc} monomers are added rapidly. The exponential replication of PrP^{Sc} can be explained if aggregates are constantly split, and monomers can be added to an increasingly larger surface. (From Weissmann 2004, Nat Rev Microbiol 2: 861-871)

1.3 Prion protein sequence and structure

PrPs are sialoglycoproteins anchored to the outer leaflet of the plasma membrane via a glycosylphosphatidylinositol (GPI) anchor. Among mammals they display >90% amino acid (aa) sequence identity and share a characteristic protein domain composition (Figure 2a and b) (López Garcia et al, 2000; Lysek et al, 2005). An N-terminal signal peptide targets the protein to the ER, whereas the adjacent positively charged residues (KKRPKP in mouse

PrP) support its localization to clathrin-coated pits and thus its constitutive endocytosis (Shyng et al, 1995b; Sunyach et al, 2003). Adjacent to this region is a succession of five proline- and glycine-rich octapeptide repeats, which stimulate endocytosis upon binding to copper (Hornshaw et al, 1995; Pauly & Harris, 1998; Taylor et al, 2005). The short central hydrophobic core is highly conserved and may act as a transmembrane domain in some PrP conformers. These represent minimal fractions of total cellular PrP and result from altered translocation in the ER (PrP^{Ctm} and PrP^{Ntm}) (Hegde et al, 1998; Hegde et al, 1999; Stewart & Harris, 2001). Finally, the C-terminal hydrophobic region serves as a signal for the addition of the GPI anchor and becomes cleaved after the latter is attached. The GPI anchorage of the protein is also essential for a further posttranslational modification, namely the N-glycosylation of two sites in the C-terminus (Chesebro et al, 2005b).

According to nuclear magnetic resonance (NMR) spectroscopy data, PrP^C can be roughly divided into two structural halves: a N-terminal flexible random-coil domain and a more structured C-terminal globular domain (each approximately 100 aa). The globular domain contains three α -helices interposed by two β -sheets, and is stabilized by a single disulfide bond between cystein residues 179 and 214 (Knaus et al, 2001; Riek et al, 1997). Remarkably, although PrP primary sequences are highly divergent between vertebrate classes (30% similarity or below), structural modeling indicates that the N-terminal repetitive and C-terminal globular domains as well as the α -helix/ β -sheet arrangement have been maintained through evolution (Calzolari et al, 2005; Rivera-Milla et al, 2006). NMR spectroscopy and crystallography have provided detailed information on the structural organization of PrP^C, yet the insufficient purity of PrP^{Sc} preparations and the insoluble character of PrP^{Sc} aggregates render them unsuitable for similar analyses. Nevertheless, the limited insights gained through these methods indicate that the misfolded prion protein has a high content of β -sheets and that it may be organized in trimers (Caughey et al, 1991; Govaerts et al, 2004; Wille et al, 2002).

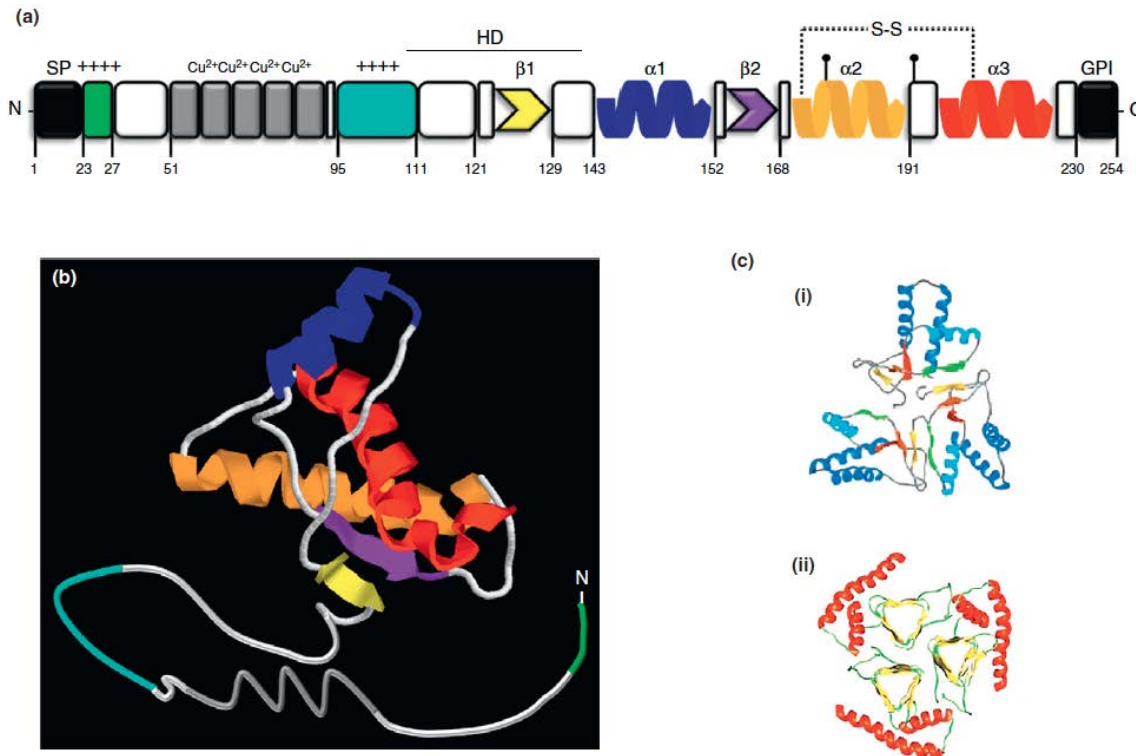


Figure 2 Structure of PrP^C and PrP^{Sc}. **a.** Schematic drawing of PrP^{Sc}. Residue numbering corresponds to the mouse PrP sequence. Black (SP): N-terminal signal peptide for ER translocation that is removed in the ER lumen; green: polybasic domain; gray: octarepeats that can bind copper and other bivalent metal ions; cyan: central positively charged region; HD: hydrophobic domain; β1 (yellow) and β2 (purple): short β-strands; α1 (blue), α2 (orange) and α3 (red): α-helices; S-S: disulfide bond; black (GPI): signal for GPI attachment, which is removed during biosynthesis. **b.** Three-dimensional structure of PrP^C, as deduced from NMR spectroscopy. Colors correspond to the structural elements described in (a). **c.** Two models of aggregated PrP^{Sc} molecules. i) The core of the PrP^{Sc} aggregate consists of parallel and antiparallel β-strands, organized in a spiral. ii) The core is formed by left-handed β-helices. (From Biasini *et al* 2012, Trends in neurosciences 35: 92-103)

1.4 The role of PrP^C in prion and other neurodegenerative diseases

After the prion hypothesis was put forward, increasing amounts of experimental data provided evidence for the role of PrP^C in TSEs. For instance, PrP knockout mice proved to be resistant to prion infection, and were unable to propagate PrP^{Sc} when infected with it (Brandner *et al*, 1996; Bueler *et al*, 1993). Even more astonishing was the finding that genetic ablation of PrP^C in neurons of mice with already established clinical prion disease reversed neurodegeneration and upheld symptom progression despite the ongoing propagation of PrP^{Sc} in surrounding brain tissue (Mallucci *et al*, 2003). Equally compelling was another study showing that mice expressing PrP without a GPI anchor -and therefore lacking attachment to the plasma membrane- did not manifest clinical prion disease, even though they preserved the ability to replicate prions (Chesebro *et al*, 2005b). Altogether, these crucial findings strengthened the notion that PrP^{Sc} requires host PrP^C to replicate, and moreover, that the onset of neurodegeneration entails the presence of PrP^C on the surface of neurons. An important role of PrP^C in prion disease is also suggested by the fact that PrP mutations can lead to neurotoxicity in transgenic mice and familial cases of disease, even

without detectable formation of prions (Aguzzi et al., 2008; Solomon et al., 2010b). Hence, alterations in PrP^C function may precede PrP^{Sc} formation and contribute to the onset of prion-induced neuronal death. Such alterations, brought on by the conformational change, could consist in a loss, an enhancement or even a subversion of the protein's physiological role. Another indication that PrP^C activity can contribute to neuronal dysfunction was provided by recent findings that the same protein participates in abnormal signaling during Alzheimer's disease. Concretely, PrP^C was found to function as a receptor for A β ₁₋₄₂ oligomeres, which are peptide aggregates that form in the brains of AD patients, causing neuronal impairment (Lauren et al, 2009; Um et al, 2012). In these studies the PrP^C-A β interaction was shown to activate a cytosolic kinase of the Src family, Fyn, leading to altered localization of the NMDA receptor on the surface of neurons and a subsequent destabilization of dendritic spines. Overall, these findings have emphasized the need to understand the physiological role/activity of PrP in order to further understand how this contributes or is affected in disease.

1.5 PrP cell biology and physiological function- An overview

PrP expression and general cell biology

Given the central role of PrP^C in prion-induced neuronal damage, large efforts have been aimed at understanding its physiological function and the molecular networks influenced by it. Consistent with the neurodegenerative phenotype observed in prion diseases, PrP expression is abundant in neurons of the adult brain and spinal cord (Harris et al, 1993c). However, detection of the protein in other cell types, including glia cells and lymphocytes, indicates that PrP's function is not exclusively neuronal (Ford et al, 2002; Moser et al, 1995). Interestingly, PrP expression in the CNS starts already during embryonic development, suggesting that it plays a role in the process of neuronal differentiation (Manson et al, 1992). At the subcellular level, PrP localizes typically at the plasma membrane, in compartments of the secretory pathway, and in endocytic vesicles following endocytosis via clathrin-coated pits (Westergard et al, 2007). Cell surface PrP is mainly concentrated in domains of the plasma membrane rich in cholesterol and sphingolipids ("lipid rafts") known to play a role in several cellular processes including protein sorting and transmembrane signaling (Gorodinsky & Harris, 1995; Simons & Ikonen, 1997). In particular, lipid rafts have been proposed to function as signaling platforms, since they contain GPI anchored and transmembrane proteins, and at the same time associate with their cytoplasmic leaflet to intracellular signaling molecules such as Src kinases and G-proteins (Simons & Ikonen, 1997).

Studies in mice

Despite the vast available knowledge on the basic cell biology of PrP, linking the protein to concrete physiological functions has been and remains a challenging task. This is partly due to the fact that aside from their resistance to prion infection, PrP knockout mice display no overt phenotypes, save for subtle abnormalities in olfactory physiology, neurogenesis, the maintenance of peripheral myelin, and muscle regeneration (Bremer et al, 2010; Le Pichon et al, 2009; Steele et al, 2006; Stella et al, 2010). More importantly, it remains unclear how these defects correlate with the extensive neurodegeneration caused by prion disease in the CNS. The absence of a strong phenotype in developing or adult mice stands in contrast to the astonishing defects observed in transgenic mice expressing various deleted versions of PrP (Solomon et al, 2010b) and has been largely attributed to genetic compensation and/or developmental plasticity (Collinge, 1997; Málaga-Trillo & Sempou, 2009). Remarkably, although the use of PrP deletion mutants itself has not uncovered a specific function of PrP, it has revealed that the protein has both neuroprotective and neurotoxic properties encoded in its sequence. For example, transgenic mice expressing N-terminally deleted PrP constructs ($\Delta 32-121$, $\Delta 32-134$) developed spontaneous neurodegeneration even without infection with prions and with no signs of protein aggregation (Shmerling et al, 1998). This effect was observed only in mice with a *PrP^{0/0}* background and consistently rescued by introduction of a wildtype *PrP* allele. At the same time, shorter deletions ($\Delta 32-80$, $\Delta 32-93$, $\Delta 32-106$) did not trigger appreciable pathology, indicating that the region critical for neurotoxicity consisted of residues C-terminally to 106. This hypothesis was tested almost a decade later with the generation of mice expressing PrP ΔCR ($\Delta 105-125$; CR: central region), which displayed the most severe neurodegenerative phenotype among all mutants tested before and died soon after birth (Li et al, 2007). Specifically, neurons expressing this PrP mutant were shown to die due to an abnormal influx of ionic currents through the plasma membrane (Solomon et al, 2010a). Interestingly, there are indications that the central region is conformationally modified in PrP^{Sc} and the same is true for PrP carrying an octapeptide insertional mutation (PG14) found in familial disease cases (Biasini et al, 2008). Recent studies have revealed that another small region of PrP is relevant for neurotoxicity: Co-deletion of polybasic residues 23-31, previously implicated in PrP endocytosis, abrogated the neurotoxicity of mutants $\Delta 32-134$ and ΔCR (Solomon et al, 2011; Westergard et al, 2011b), whereas deletion of the same residues in wildtype PrP abolished its ability to suppress neurodegeneration triggered by PrP $\Delta 32-134$ (Turnbaugh et al, 2011). Altogether, these data suggested that alterations in the function of PrP^C have a strong impact on neuronal viability, and led to hypotheses as to how PrP might exert these effects. For example, the conserved central region of PrP could interact with another protein conveying a neuroprotective signal or suppressing a neurotoxic one. In this case, the rescuing activity of WT PrP would derive from its ability to bind to that signaling partner (Biasini et al, 2012). On

the other hand, both the protective and the toxic effects of the protein would depend on a basic cell biological feature of PrP dictated by its N-terminal polybasic domain, such as its association to specific domains of the plasma membrane or its endocytosis. However, while these studies confirmed the neuroprotective character of PrP and partially mapped its sequence determinants, they have not succeeded in unraveling the cellular pathways by which PrP exerts its activity.

Studies in cells

Studies in cultured cells have revealed a plethora of potential physiological roles for PrP^C, including lymphocyte activation, cell cycle regulation/proliferation, synaptic function, neuronal differentiation/survival and cell-cell adhesion (Cashman et al, 1990; Chen et al, 2003; Collinge et al, 1994; Devanathan et al, 2010; Kanaani et al, 2005; Llorens et al, 2013; Mange et al, 2002; Santuccione et al, 2005). These functions are consistent with a role of PrP at the cell surface and in some cases involve its interaction with transmembrane molecules. For example, a PrP-NCAM (neuronal cell adhesion molecule) interaction was found to stimulate neurite outgrowth (Santuccione et al, 2005), whereas binding of PrP to the epidermal growth factor receptor (EGFR) was shown to enhance cell cycle progression (Llorens et al, 2013). At the same time, PrP has been reported to support cell survival, in one case by affecting the expression levels of pro- and anti-apoptotic proteins, like Bax and Bcl-2 respectively (Chen et al, 2003), and in others by binding to stress-inducible protein 1 (ST-1) and activating a cAMP/protein kinase A (PKA) pathway (Chiarini et al, 2002; Zanata et al, 2002). Interestingly, PrP has also been reported to act against oxidative stress, possibly by causing detoxification of reactive oxygen species (Linden et al, 2008). Such a role would be compatible with the observation that the brains of PrP knockout mice undergo biochemical changes indicative of oxidative stress and are more sensitive to hypoxia or ischemia (McLennan et al, 2004; Spudich et al, 2005; Westergard et al, 2007; Wong et al, 2001). However, for this to be true, PrP would have to possess or regulate the activity of an anti-oxidant enzyme, a hypothesis that until today lacks solid proof. Although the *in vivo* relevance of these findings as well their putative connection to neurodegeneration is unclear, important information can be extracted from them. For example, the ability of PrP to modulate central intracellular signaling pathways, such as those involving MAP kinases, PI3K/Akt, PKA and members of the Src family of tyrosine kinases (SFKs) (Chen et al, 2003; Linden et al, 2008; Mouillet-Richard et al, 2000) (Figure 3). Among the latter, SFKs present a particularly interesting signaling partner due to their involvement in neurological disease. For instance, their activation levels are altered in scrapie-sick mouse brains (Nixon, 2005) and they have also been shown to mediate PrP^C-dependent neuronal impairment in mouse AD models (Um et al, 2012).

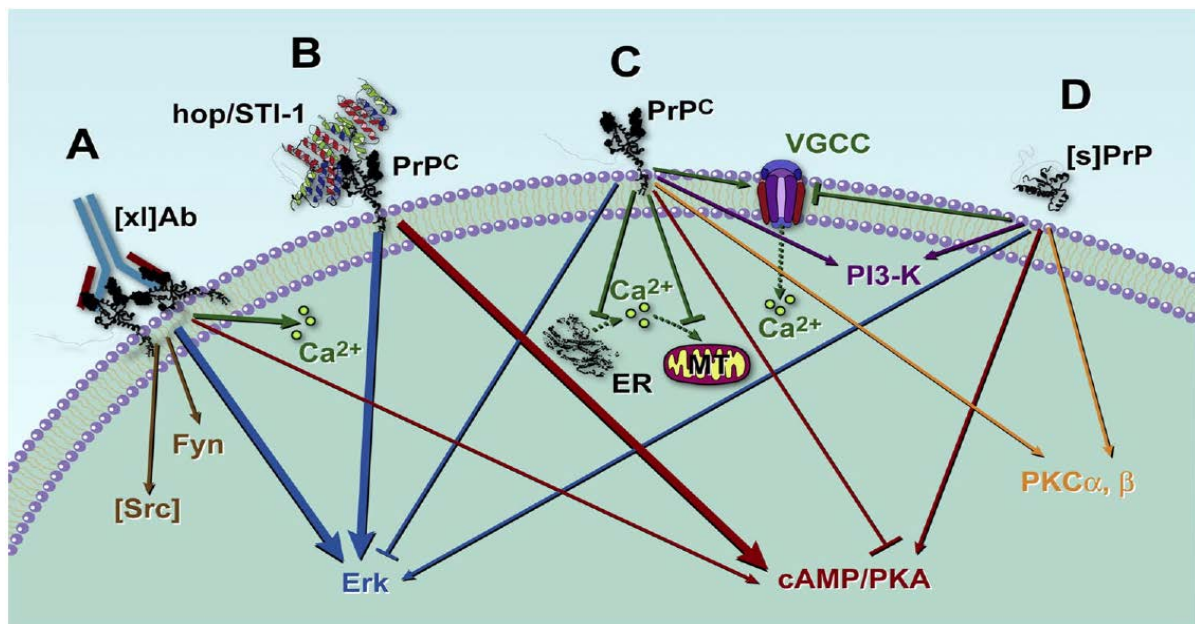


Figure 3 Overview of molecular signaling pathways influenced by PrP. Different methods have been used to alter PrP function: **A.** Antibody crosslinking ([xI]Ab); **B.** Engagement of PrP with a ligand (hop/STI-1); **C.** Modulation of PrP expression levels; **D.** Application of soluble PrP ([s]PrP) to cells. [Src]: unidentified member of the Src family besides Fyn; VGCC: voltage-gated calcium channel; ER: endoplasmic reticulum; MT: mitochondria; arrows indicate activation, hammers indicate inhibition, and each pathway is marked by a different color. From Linden 2008, *Physiol Rev* 88: 673-728

1.6 Insights into PrP function from the zebrafish

The absence of a clear phenotype in PrP knockout mice and the need to validate the numerous roles reported for PrP *in vitro*, made it urgent to search for new models to study its function. Our laboratory chose to investigate the physiological role of PrP *in vivo* in the zebrafish (*Danio rerio*) due to its many experimental advantages such as its external development, its optical clarity during embryonic and larval stages, and the possibility to perform cellular and biochemical analyses. During the last decade the zebrafish has emerged as a powerful model in the fields of development, cancer and neurobiology, since it is anatomically simpler than mice but, unlike *Drosophila* or *C. elegans*, is a vertebrate and shares 70% of the protein-coding human genes (Howe et al, 2013). In addition, forward and reverse genetics approaches are now routinely practiced in zebrafish, with a large variety of transgenic lines and mutants being available to study gene regulation and function.

Table 1 highlights some important stages during zebrafish embryonic and larval development, and is meant to serve as a short guide to understand the phenotypes described throughout this study.


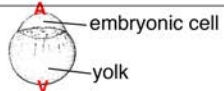

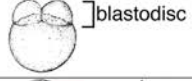



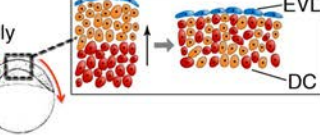
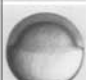
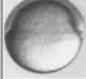
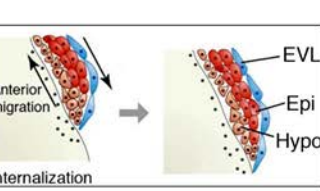



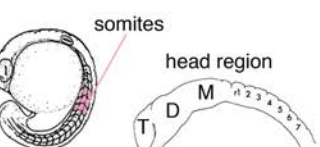





Hours	Stage	Schematic illustration	Description
	0.2 1-cell		one-cell stage following fertilization of the egg A: animal pole, V: vegetal pole
	0.75 2-cell		cleavage period (0.75-2 hpf): successive cleavages of embryonic cells (blastomeres), which form the blastodisc overlying the yolk
	3.3 High		translocation of cytoplasmic β-catenin into the nuclei of marginal blastomeres , leading to transcription of dorsalis genes; this process defines the position of future dorsal tissues
	4.7 30% epiboly		During epiboly , the blastoderm (previously blastodisc) becomes progressively thinner and spreads over the yolk, eventually engulfing it completely. The necessary increase of the blastoderm's surface is achieved by movement of deeper cells to more superficial layers (radial intercalation). At this stage, the blastoderm can be subdivided into an outer protective epithelium (EVL: enveloping layer) and underlying deep cells (DC), from which all embryonic tissues will descend. Epiboly signifies the beginning of gastrulation , which encompasses all morphogenetic cell movements leading to the formation of the germ layers (endo-, meso- and ectoderm).
	5.3 50% epiboly		
	6 Shield		At 50% epiboly, deep cells on the dorsal side of the embryo start accumulating locally at the margin of the blastoderm. There, these cells internalize forming a new layer (hypoblast) under the more superficial layer of deep cells (epiblast). Whereas the hypoblast will later give rise to meso- and endoderm, the epiblast is the precursor of ectodermal tissues. While internalization occurs, the newly formed hypoblast cells start to converge towards the dorsal side of the gastrula and extend along the anterior-posterior axis. Altogether, these morphogenetic movements lead to the formation of a local thickening on the dorsal side of the embryo, which represents the embryonic organizer and is referred to as the shield . The formation of the anterior-posterior axis becomes increasingly visible towards the end of epiboly, and is well-defined by the bud stage (A: anterior; P: posterior).
	10 Bud		
	18-somite		During the segmentation period (10-24 hpf), the basic organization of muscles along the trunk is established (somites), while in the head region neuromeres become visible, progressively differentiating into distinct brain regions (T: telencephalon, D: diencephalon, M: mesencephalon and rhombomeres: r1-7). Primary organogenesis takes place and the tail forms.
	24		At 24 hpf, blood circulation and pigmentation are initiated, and fins begin to form. By 48 hpf, primary organ morphogenesis is complete and cartilage starts to develop in the head.
	48		
			Zebrafish reach adulthood after 3-4 months of development. In captivity they grow up to 4 cm in length. (Photograph by Philippe Mourrain, University of Stanford)

Table 1 Important stages of early zebrafish development. Pictures of live embryos and schematic drawings are from Kimmel *et al*, 1995 and Montero & Heisenberg, 2004, and have been partially modified. The scale bar in the picture of the one-cell embryo indicates 250 μ m.

Previously, our group identified and characterized duplicated genes in zebrafish coding for PrP-1 and PrP-2 (Rivera-Milla *et al*, 2006). Although fish PrPs show low sequence identity to their mammalian counterparts (approximately 16%) and are considerably longer (approx. 600 aa vs. 250 aa in mammals), they share with them key structural and biochemical

properties, such as protein domain composition, patterns of N-glycosylation and attachment to the plasma membrane via a GPI anchor (Figure 4A). Sequence similarity varies along the different protein domains, with the hydrophobic core being the most conserved stretch and the repetitive region the most variable one. It is noteworthy that even though the globular domains of zebrafish and mammalian PrPs differ significantly in their aa sequence, their structural fold is conserved, suggesting that they carry out an important function (Rivera-Milla et al, 2006) (Figure 4B).

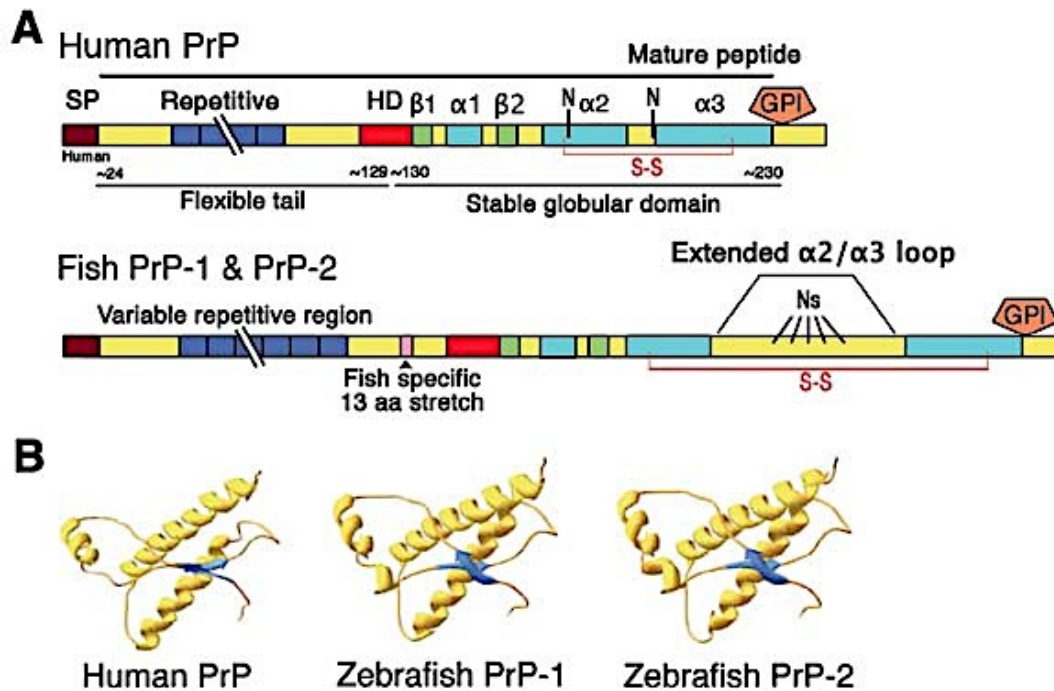


Figure 4 Evolutionary conservation of PrP domain architecture and structure. **A.** Domain composition of human and zebrafish PrPs. Tandem repeats are presented in blue, hydrophobic domains (HD) in red, β -strands in green, α -helices in cyan. SP= signal peptide; orange pentagons= GPI anchors; N= glycosylation sites; and S-S= disulfide bridges. Breakpoints in repetitive regions indicate length variation. **B.** Conservation of 3-D structures of human (experimental) and zebrafish (predicted) PrP-1 and -2 globular domains. Figure (modified) from Rivera-Milla et al 2006, FASEB J 20: 317-319)

While both zebrafish PrPs are expressed in the brain of adult zebrafish, their spatiotemporal expression during early development is tightly regulated. On one hand, *PrP-1* mRNA transcripts are detected at high levels ubiquitously in the embryo during the blastula-gastrula stages (2.5-10 hours postfertilization [hpf]), maintaining low levels after completion of gastrulation in the forebrain and eyes (Figure 5A and B). On the other hand, transcription of *PrP-2* mRNAs begins during somitogenesis, reaching its highest levels at the pharyngula stage (30 hpf) in the developing nervous system (Figure 5C and D). Concretely, *PrP-2* transcripts are found mostly in the brain and discrete neuronal populations of the central and peripheral nervous system (Figure 5D), thus strongly resembling the embryonic distribution of mouse and chicken *PrP* mRNAs (Harris et al, 1993a; Manson et al, 1992) (Figure 5D and E). Altogether, the differential expression of zebrafish *PrPs* indicates that these proteins fulfill

specialized functions during distinct developmental phases: PrP-1 is expressed at early stages, in which cells are largely undifferentiated, divide constantly and make massive coordinated morphogenetic movements to form elementary embryonic structures. Differently, PrP-2 expression begins later and is targeted to emerging neuronal structures.

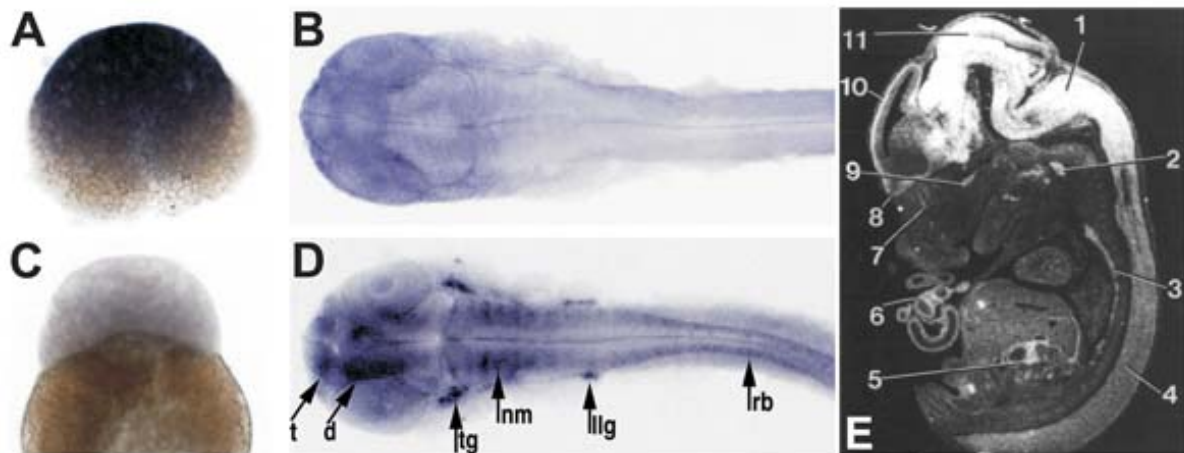


Figure 5 Zebrafish and mouse PrP expression during embryonic development. A-D. Differential expression of PrP-1 and PrP-2 during early zebrafish development, detected by *in situ* hybridization. Strong detection of PrP-1 but not PrP-2 mRNA at the midblastula stage, at 2.5 hpf (A and C respectively; lateral views). At pharyngula stages (30 hpf), PrP-1 transcript levels are detected at lower levels (B), whereas PrP-2 is strongly transcribed in defined neural structures (D). B and D, dorsal views; d, diencephalon; llg, lateral line ganglion; nm, neuromeres; rb, Rohon-Beard sensory neurons; t, telencephalon; tg, trigeminal ganglion (From Malaga-Trillo et al 2009, PLoS Biol 7(3): e55). **E.** Expression of PrP in a 13.5-day mouse embryo detected by *in situ* hybridization. Strong detection of PrP mRNA in the developing brain. Transcripts are also detected in several other neuronal populations of the central and peripheral nervous system, as well as in peripheral tissues. Neuronal structures: 1, rhombencephalon; 2, superior cervical sympathetic ganglion; 3, sympathetic trunk and ganglia; 4, spinal cord; 8, olfactory lobe; 9, optic nerve; 10, telencephalic cortex; 11, mesencephalon (From Manson et al 1992, Development 115(1): 117-122)

To investigate the function of PrP during embryonic development, the expression of zebrafish PrP-1 or PrP-2 was blocked by the morpholino knockdown approach (Málaga-Trillo et al, 2009). Morpholinos are modified antisense oligonucleotides that bind mRNAs to prevent their translation. They are introduced in the embryo by microinjection at the one-cell stage and become distributed to all embryonic tissues through successive cell divisions. Notably, individual knockdowns of PrP-1 and -2 generated distinct phenotypes, which correlated with the localization patterns of the respective mRNAs in the embryo. Specifically, PrP-1 knockdown embryos (morphants) ceased to develop after reaching the stage of 50% epiboly (6 hpf), and did not survive beyond gastrulation (Figure 6A and B), whereas PrP-2 morphants developed into larval stages, but displayed severe morphological defects in the head area, particularly in their eyes and brain (Figure 6D-G). Importantly, the specificity of the PrP-1 knockdown phenotype was confirmed by the ability of PrP-1 mRNA to rescue the developmental arrest (Figure 6C). Remarkably, partial rescues could also be achieved with PrP-2, but also mouse PrP mRNA, indicating that both zebrafish PrPs as well as mammalian PrP share a common basic function.

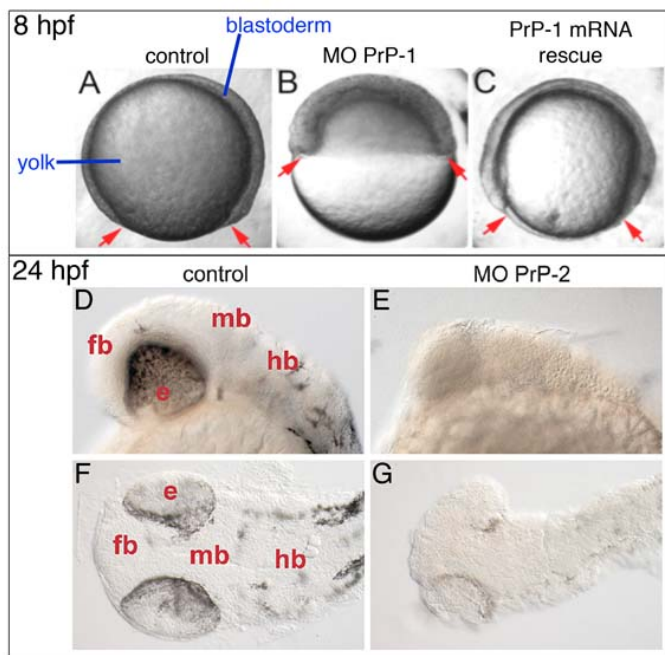


Figure 6 Morpholino knockdowns of zebrafish PrP-1 and PrP-2. **A-C.** Embryos at 8 hpf (gastrula stage). Control embryos (A) reach approximately 80% epiboly, demonstrating normal progression of the blastodermal margin (red arrows). PrP-1 morphants undergo early developmental arrest and fail to develop beyond 50% epiboly (B). The PrP-1 knockdown phenotype can be rescued by microinjection of zebrafish *PrP-1*, *PrP-2* or *mouse PrP* mRNA (C, and not shown). **D-G.** Control (D and F) and PrP-2 morphant embryos (E and G) at 24 hpf (prim-5 stage) from lateral (D and E) and dorsal (F and G) perspectives. PrP-2 morphants display severe defects in the head region. fb: forebrain; mb: midbrain; hb: hindbrain; e: eye. (From Malaga-Trillo *et al* 2009, PLoS Biol 7(3): e55)

In further experiments, the PrP-1 knockdown phenotype was characterized more thoroughly. The developmental arrest during early gastrulation was found to result from reduced tissue cohesiveness within the blastoderm of PrP-1 morphants (Figure 7). The blastoderm represents the embryonic tissue, which initially develops on top of the yolk, and can be subdivided into several layers of deep cells (DCs) and an overlying epithelial monolayer (EVL: enveloping layer). Deep cells give rise to the embryo *per se*, whereas the EVL acts as a protective cover throughout early development. In PrP-1 morphants, the loss of adhesion between embryonic cells prevented them from performing movements essential for epiboly. This is a morphogenetic process that marks the beginning of germ layer formation (gastrulation) and entails the spreading of the blastoderm over the yolk (Figure 6A and B). These abnormalities could only be observed in DCs, but not the EVL, suggesting that cell-cell adhesion in the latter is regulated differently or is reinforced by additional PrP-1-independent mechanisms.

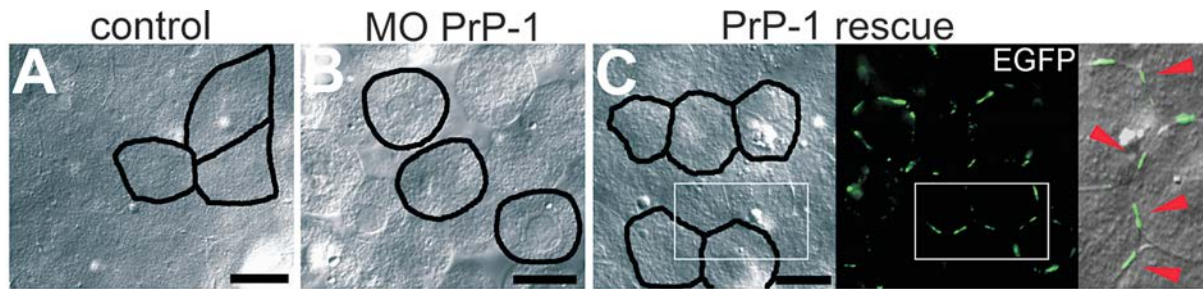


Figure 7 Impaired cell-cell adhesion in the blastoderm of PrP-1 knockdown embryos (deep cell layer). Whereas tissue compactness is normal in control embryos, with cells displaying polygonal shapes (A), the blastoderm in PrP-1 knockdown embryos consists of round and detached cells (B). Tissue cohesiveness in PrP-1 morphants can be restored by expression of PrP-1-EGFP, which accumulates at sites of cell-cell contact (C). Scale bars indicate 10 μ M. (From Malaga-Trillo *et al* 2009, PLoS Biol 7(3): e55)

Throughout gastrulation, embryonic cells have to remain in contact while performing organized movements. At this stage, cell-cell contacts are largely mediated by homophilic, Ca^{2+} -dependent interactions of the adhesion molecule E-cadherin (see next section). E-cadherin depletion in zebrafish embryos has been shown to lead to the loss of cell-cell adhesion and epibolic arrest in DCs without affecting the cohesiveness or the movement of the EVL (Babb & Marrs, 2004; Kane *et al*, 2005; Shimizu *et al*, 2005). To assess whether PrP-1 affects Ca^{2+} -dependent cell-cell adhesion, aggregation assays were performed (Málaga-Trillo *et al*, 2009) (Figure 8). In these, embryos were mechanically dissociated into single-cell suspensions, and the cells were allowed to re-aggregate in the presence or absence of Ca^{2+} . In medium containing Ca^{2+} , control cells re-aggregated forming large and small clusters, whereas PrP-1 knockdown cells showed a reduced ability to form clusters of either size. Notably, cells derived from embryos overexpressing PrP-1 displayed an increased tendency to form large aggregates compared to control cells. This confirmed the hypothesis that PrP-1 has a positive influence on Ca^{2+} -dependent adhesion. In the absence of Ca^{2+} , formation of large clusters was abolished in all of the tested groups, indicating that it was strongly Ca^{2+} -dependent, whereas small clusters still assembled. However, the number of the latter was reduced upon PrP-1 knockdown even under these conditions, suggesting that besides supporting Ca^{2+} -dependent cell-cell adhesion, PrP-1 contributes to contact formation via an additional mechanism that does not involve Ca^{2+} .

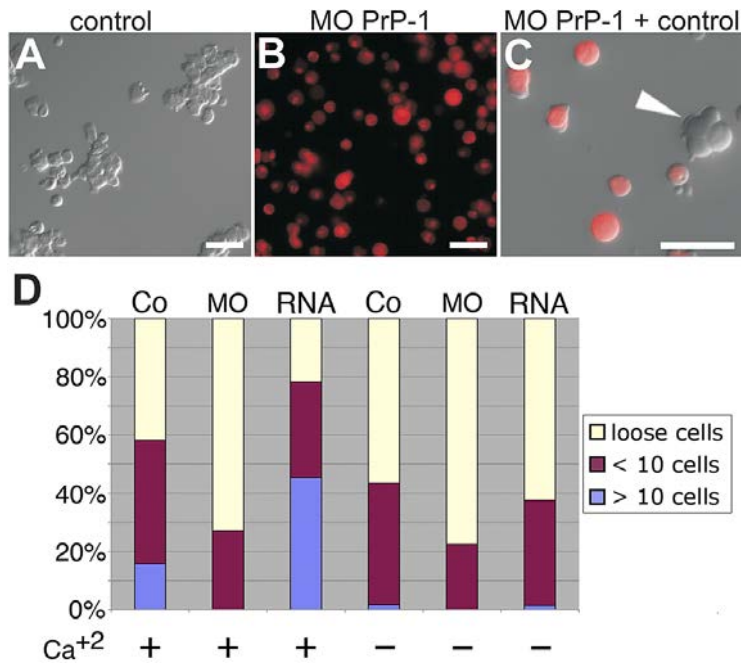


Figure 8 Aggregation assays with cells from mechanically dissociated 6 hpf embryos, in medium with or without Ca²⁺ (re-aggregation time: 45 min). **A.** Cells from control embryos re-aggregate forming small and large clusters. **B.** PrP-1 morphant cells show a reduced ability to re-aggregate (morpholinos are fluorescent due to a Lissamine-tag). **C.** PrP-1 morphant cells are excluded from aggregates when co-cultured with control embryo cells. **D.** Quantification of small (<10 cells) and large (>10 cells) clusters of cells derived from control, PrP-1 morphant and PrP-1 overexpressing embryos, in the presence or absence of Ca²⁺. Scale bars indicate 20 μ M. (From Malaga-Trillo *et al* 2009, PLoS Biol 7(3): e55)

Subsequent analyses showed that the tissue defects caused by PrP-1 depletion were linked to a reduced presence of E-cadherin on the surface of DCs (Málaga-Trillo *et al*, 2009). While in control embryos E-cadherin localized primarily at the plasma membrane, its distribution in PrP-1 morphants appeared mainly cytosolic (Figure 9A and D). At the same time, the levels of the mature, membrane-bound E-cadherin isoform (Figure 9G; Western blot: 120 kDa band) were strongly reduced in lysates of PrP-1 knockdown embryos. Consistently, an abnormal localization was also observed for β -catenin, an intracellular binding partner of E-cadherin and a stabilizing component of adhesive complexes (Figure 9B and E). Like E-cadherin, the presence of β -catenin at the plasma membrane was strongly reduced upon PrP-1 knockdown, with the protein accumulating largely in cytosolic pools. Concomitant defects were observed in the localization of F-actin, since its normally homogeneous distribution along cell-cell contacts appeared to a great degree irregular (Figure 9C and F). When analyzed for similar defects, the EVL of PrP-1 morphants showed mild or no defects in the localization of AJs. Also, unlike DCs, EVL cells were connected by additional adhesion complexes, namely tight junctions, which were not affected in the absence of PrP-1 (not shown). This suggested that cell-cell adhesion in the EVL is controlled by different and additional mechanisms than that in DCs. Altogether these results demonstrated that PrP-1 is required during epiboly in DCs for the maintenance of proper cell surface localization of E-cadherin adhesive complexes.

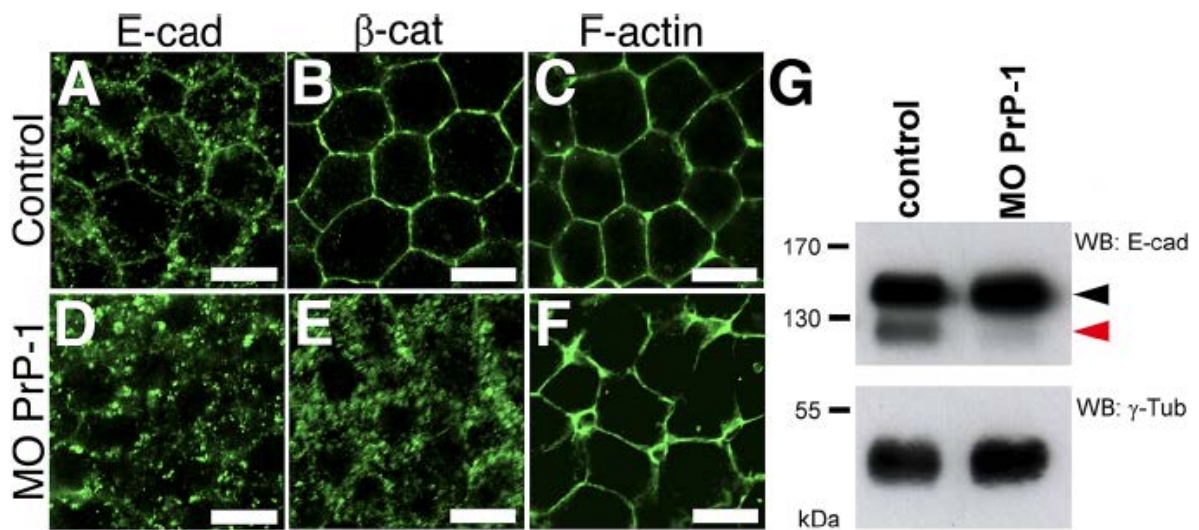


Figure 9 Regulation of E-cadherin mediated cell-cell adhesion by PrP-1. A-F. Immunofluorescence of E-cadherin and β -catenin, and phalloidin staining of F-actin in DCs of 6 hpf control and PrP-1 morphant embryos. Scale bars indicate 10 μ M. **G.** Western blot analysis of 6 hpf embryo extracts, showing a reduction in the levels of mature, membrane-bound E-cadherin (120 kDa isoform; red arrowhead) upon PrP-1 knockdown, but no changes in those of the E-cadherin precursor (140 kDa; black arrowhead). (From Malaga-Trillo *et al* 2009, PLoS Biol 7(3): e55)

In the same study, mouse and zebrafish PrPs were expressed in mouse neuroblastoma (N2a) cells and found to accumulate at cell-cell contact sites. Remarkably, accumulation could only be observed when both cells in contact expressed PrP, suggesting an affinity between PrPs on opposing cell membranes. Similar experiments were performed in *Drosophila* embryonic S2 cells, which lack cell adhesion molecules and grow as single-cell suspensions. Strikingly, PrP expression led to aggregation of these cells, with PrP strongly accumulating at cell-cell contact sites (Figure 10A-C). Untransfected cells were excluded from aggregates, suggesting that adhesion depended on homophilic binding of PrP molecules on opposing cell membranes. This finding showed that PrP itself has basic adhesive properties independently of the presence of bona fide adhesion molecules, which are likely to be responsible for small cluster formation in the embryo aggregation assays described above. Remarkably, affinity between zebrafish and mouse PrPs was also evident and led to contact formation between S2 cells, implying that interactions are possible even between PrPs of distantly related species (Figure 10D). Moreover, PrP expression in these cells led to the recruitment of activated SFKs, F-actin and reggie/flotillin microdomains at sites of cell-cell contact, suggesting that PrP homophilic interactions can elicit intracellular signaling (Figure 10E-G).

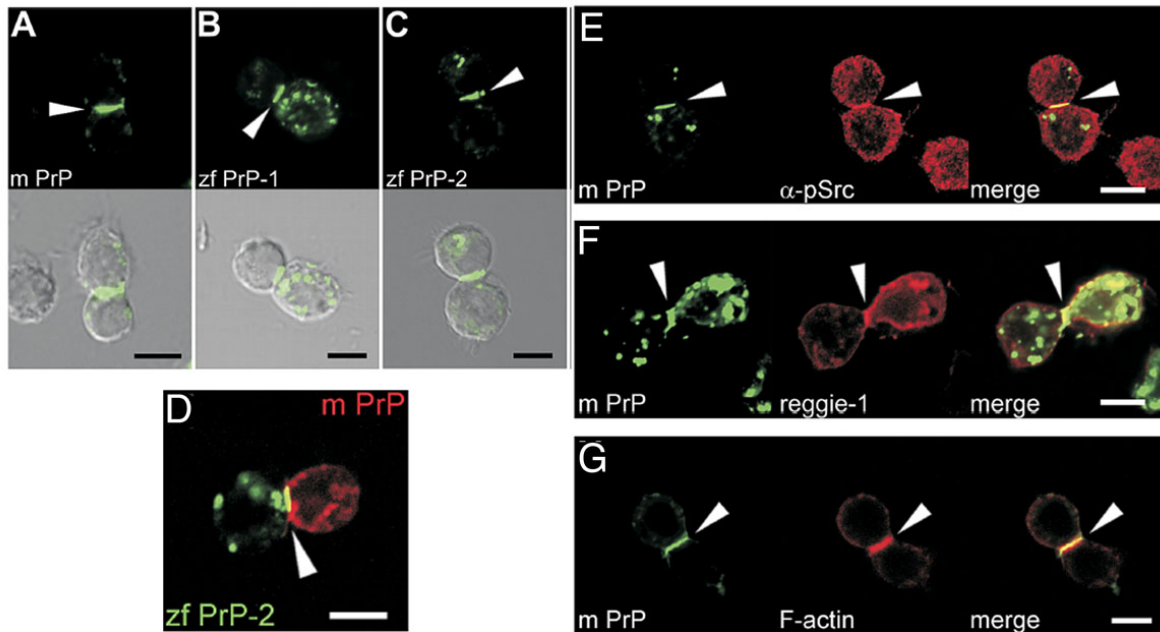


Figure 10 Adhesion and cell signaling in *Drosophila* S2 cells upon PrP expression. A-C. Expression of EGFP-tagged mouse PrP (A), zebrafish PrP-1 and PrP-2 (B and C) in normally non-adhesive S2 cells induces cell contact formation. D. Contact formation between cells expressing different PrPs (EGFP-tagged zebrafish [zf] PrP-2 and DsRed-tagged mouse [m] PrP). E-G. Accumulation of activated (phosphorylated) Src-kinase (E), Reggie-1 (F) and F-actin (G) at PrP-induced cell contacts. Scale bars indicate 5 μm. (From Malaga-Trillo *et al* 2009, PLoS Biol 7(3): e55)

Overall, these data provided unprecedented evidence that lack of PrP can be detrimental for an organism. Thus, in the zebrafish embryo, PrP-1 supports cell-cell adhesion by positively regulating E-cadherin adhesive complexes at the plasma membrane, an activity that is shared by mammalian (mouse) PrP. The strong phenotype caused by PrP-1 depletion and the fact that zebrafish and mammalian PrPs share a basic function which can be assayed in the gastrula, make the zebrafish a valuable tool in deciphering conserved molecular networks influenced by PrP. Furthermore, the observation that PrPs engage in *trans*-homophilic binding and thereby trigger signaling, suggests that these interactions are responsible for the ability of PrP to regulate E-cadherin.

1.7 E-cadherin-mediated adhesion and its regulation

Epithelial cadherin (E-cadherin) is a transmembrane protein able to engage in Ca^{2+} -dependent homophilic *trans*-interactions intracellularly anchored to the actin cytoskeleton, thus forming adhesive junctions between adjacent cells (adherens junctions=AJs; Figure 11). Besides E-cadherin, AJs are composed of cytosolic proteins that interact directly or indirectly with its cytoplasmic tail and mediate its connection to F-actin, thereby stabilizing the contact point. One such molecule is β -catenin, which has a binding site on E-cadherin and serves as a link to the actin-binding protein α -catenin. The latter can homodimerize and in this state bind and bundle actin filaments.

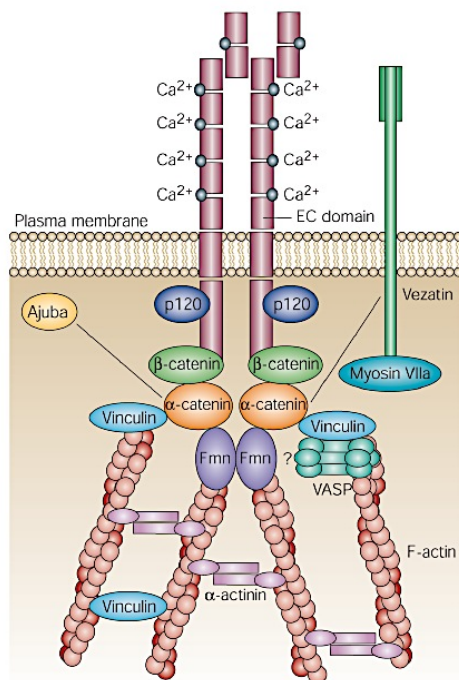


Figure 11 The AJ protein complex. Binding of extracellular Ca^{2+} confers E-cadherin molecules a conformation, which allows them to dimerize at the plasma membrane. E-cadherin homodimers on opposing cell surfaces of neighboring cells can interact and establish a stabilized cell-cell contact by engaging the actin cytoskeleton intracellularly. This implies the interaction of the E-cadherin cytoplasmic domain with β -catenin, which in turn binds the actin binding protein α -catenin. Another catenin, p120, binds the juxtamembrane domain of E-cadherin and is proposed to affect its endocytosis. A plethora of other proteins, which are not shown, are known to influence the integrity of the AJ complex. (From Kobiela & Fuchs 2004, *Nat Rev Mol Cell Biol* 5(8): 614-625)

Depending on whether cells need to form compact tissues or stay in loose contact and perform movements, the stability of AJs can be finely regulated via several mechanisms:

Regulation of the expression levels of AJ proteins

Downregulation of E-cadherin at the transcriptional level has been reported mainly in tumors and developing tissues, in which cells lose their epithelial characteristics (adhesive and stationary) to become mesenchymal (non-adhesive and highly motile/invasive) in a process called epithelial-to-mesenchymal transition (EMT) (Bolos et al, 2003; Cheng et al, 2001; Leptin, 1991; Nieto, 2002). Under the same conditions, β -catenin is transcriptionally upregulated, but due to the concomitant reduction in cell-surface E-cadherin, it loses its function at AJs and enters the nucleus to act as a transcription factor for tumorigenic genes (Bandapalli et al, 2009). As in the case of E-cadherin, a reduction in α -catenin expression correlates with the dissociation of AJs and the invasive behavior of cancer cells. Accordingly, prostate cancer cells lose their motility and resume cell-cell adhesion upon re-expression of α -catenin, an effect that is dependent on E-cadherin co-expression (Ewing et al, 1995).

Regulation by phosphorylation of AJ components

Changes in cell-cell adhesion are often not connected with altered biosynthesis of AJ proteins but with changes in the integrity of AJ complexes, which in turn, are determined by their state of phosphorylation. Studies addressing this type of regulation have been traditionally carried out in tumor cell lines or in cell-free *in vitro* systems. In these, tyrosine phosphorylation of β -catenin, regulated by a variety of kinases and phosphatases, has been repeatedly linked to the disassembly of AJs. For example, cytosolic kinases such as the SFKs (Src, Fyn) and Fer, as well as the EGFR can catalyze the phosphorylation of at least three different tyrosine residues in β -catenin, thus reducing its affinity to either E-cadherin or α -catenin (Hoschuetzky et al, 1994; Piedra et al, 2001; Piedra et al, 2003). On the other hand, binding of β -catenin to E-cadherin is supported by the phosphorylation of three serine residues within the β -catenin binding domain of the latter, mediated by kinases CK2 and GSK3 β (Huber & Weis, 2001). Tyrosine phosphorylation regulates the binding of another member of the catenin family, p120, to the cytosolic tail of E-cadherin. However, in this case, phosphorylation increases the affinity of the two proteins, leading to the stabilization of E-cadherin at the plasma membrane (Ishiyama et al, 2010) (see paragraph on endocytosis/degradation below). Interestingly, phosphatase activity can also influence AJ dynamics. For example, protein tyrosine phosphatase 1B (PTP1B) can bind to the cadherin cytoplasmic domain and is responsible for β -catenin dephosphorylation, thus promoting the affinity of adhesive complexes (Balsamo et al, 1996). Altogether, these findings reveal an intricate mechanism for the regulation of AJs (Figure 12). At the same time they raise the question which of these regulatory steps are more critical than others and whether they are engaged variably in different adhesive states of cells. Along these lines, AJ regulation has been proposed to vary between cells that are in the process of forming a new contact and others that share an established/stable one (Nelson, 2008). Also, more recent data have revealed that these regulatory mechanisms might not be identical to those found in non-oncogenic cells. For example, although β -catenin phosphorylation by SFKs leads to AJ disassembly in oncogene-transformed cells, it correlates with increased cell-cell adhesion in mouse keratinocytes, *in vivo* and *in vitro*, as well as in developing *Drosophila* embryos (Calautti et al, 1998; Takahashi et al, 2005).

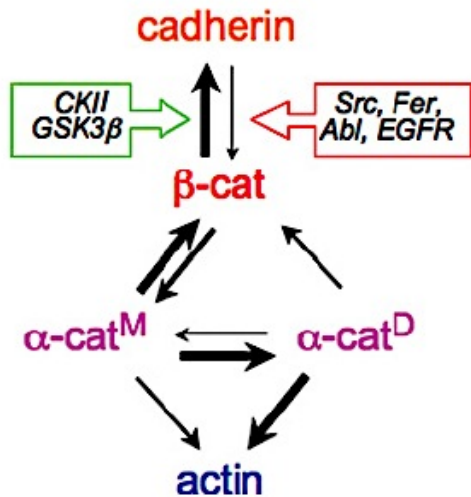


Figure 12 Interactions between proteins of the AJ complex, as revealed by studies in cancer cell lines. The thickness of the arrows indicates the strength of protein-protein interactions (thick arrows mean increased interaction). $\beta\text{-cat}$: β -catenin; $\alpha\text{-cat}^M$: α -catenin monomer; $\alpha\text{-cat}^D$: α -catenin dimer. Green box: kinases that increase binding affinity of β -catenin to E-cadherin/ red box: kinases that reduce it. (From Nelson 2008, *Biochem Soc Trans* 36: 149-155)

Regulation via endocytosis/degradation

Another mechanism contributing to the regulation of AJ stability at the cell surface consists in the modulation of E-cadherin endocytosis and degradation. For example, in cells performing EMT, binding and ubiquitination of membrane-bound E-cadherin by E3 ubiquitin-ligases such as MDM2 and Hakai lead to its endocytosis and subsequent depletion in lysosomes (Fujita et al, 2002; Palacios et al, 2005; Yang et al, 2006). Notably, Hakai binding is promoted by Src-mediated phosphorylation of E-cadherin but competitively abolished when p120 binds to E-cadherin (Miyashita & Ozawa, 2007). p120 has also been reported to protect E-cadherin from binding of AP-2, a clathrin adaptor protein and initiator of endocytosis (Ishiyama et al, 2010). However, a recent study has questioned the relevance of p120 in this regulation, and additionally indicated that the proteasome might contribute to ubiquitin-mediated degradation of cell-surface E-cadherin equally to lysosomes (Hartsock & Nelson, 2012).

Regulation by local modulation of actin dynamics

It is widely accepted that the link between E-cadherin and the actin cytoskeleton is essential for strong cell-cell adhesion (Tsukita et al, 1992). This link is regulated via inside-out signaling, meaning that changes in actin dynamics can affect the stability of cell surface E-cadherin and vice versa. An example for cytoskeleton regulation by upstream AJ proteins is the binding of α -catenin homodimers to actin, which not only promotes filament bundling, but antagonizes the activity of actin nucleator Arp2/3 thus preventing actin polymerization (Drees et al, 2005). Such regulation is necessary when cells need to make strong cell-cell contacts, whereas actin polymerization is required for dynamic membrane movements -such as lamellipodia formation- and cell migration (Pollard & Borisy, 2003). The small cytosolic

GTPases of the Rho family (Rho, Rac, Cdc42) can also influence AJ stability by mediating local actin rearrangements (Fukata et al, 1999). These molecules can crosstalk to each other, receive signaling input from AJs at the plasma membrane, and in some cases interfere directly with E-cadherin/ β -catenin complexes, thus creating a complex regulatory network (Wheelock & Johnson, 2003).

Remarkably, while E-cadherin mediated adhesion is mostly relevant to epithelial tissues, the mechanisms involved in its regulation are also employed for other members of the cadherin family, such as the neuronal cell-adhesion molecule N-cadherin. The latter is involved in synapse stabilization (Arikath, 2010) and neuronal differentiation (Zhang et al, 2013) and associates intracellularly with the same catenin network as E-cadherin

2 Aims of this study

The goal of this thesis was to dissect the molecular pathways by which PrP-1 regulates cell-cell adhesion in the zebrafish gastrula. Since expression of mouse PrP could be previously used to compensate for defects caused by zebrafish PrP-1 depletion, we argued that the zebrafish gastrula could be used as an *in vivo* model to study basic functions of PrP conserved from fish to mammals. Based on the previous data from our laboratory in zebrafish embryos and cultured cells (Málaga-Trillo et al, 2009), we formulated and tested the hypothesis that PrP-1 mediates its effects on AJs via SFK signaling (Málaga-Trillo & Sempou, 2009) and, furthermore, investigated the participation of catenins (β -catenin, p120) in these events. In addition, we asked which domains of PrP are required for this regulation, and whether mutations/deletions commonly associated with PrP neurotoxicity in mammals are also capable of influencing this function. In the same context, we tested whether A β_{1-42} oligomers, whose binding to PrP induces neuronal impairment in Alzheimer's disease, could alter PrP-induced signals in the gastrula, thus making these relevant to the study of this disorder and its cellular causes. Since mechanisms of cell adhesion/communication (such as the cadherin/catenin system) and SFKs, are widely conserved across species and employed in a plethora of cell types- including neurons- we propose that these findings altogether may help understand alterations in PrP function that contribute to disease.

3 Materials

3.1 Organisms/Cell lines

Name	Source
Zebrafish (wildtype)	Bred and maintained at the TFA of the University of Konstanz
HEK293 (human embryonic kidney) cells	ATCC CRL-1573
MCF-7 (human mammary epithelial) cells	ATCC HTB-22

3.2 Zebrafish media

Name	Recipe
60x E3 embryo medium	300 mM NaCl 10.2 mM KCl 19.8 mM CaCl ₂ 19.8 mM MgSO ₄ autoclaved
50x Danieau buffer	2.9 M NaCl 35 mM KCl 20 mM MgSO ₄ 30 mM Ca(NO ₃) ₂ 250 mM HEPES pH 7.6 filter sterilized
30% Danieau buffer	50x Danieau buffer, diluted in water

3.3 Morpholino antisense oligonucleotides (Gene Tools, LLC)

Name	Sequence	Stock solution in water
MO-PrP-1-1	GGTCCATAAAAAGGTTGAAGAAGCG 3' Lissamine	1 mM
MO-PrP-1-2	TCTCTCCCGCAGCACTCTCTGCTCA 3' Lissamine	1 mM
MO-Fyn	TGTCCTTACATTGCACACAGCCCAT 3' Lissamine	1 mM
MO-Yes	CCTCTTTACTCTTGACACAGCCCAT 3' Lissamine	1 mM

3.4 Morpholino working solutions

Name	Recipe
MO-PrP-1	0.5 ng/nl MO-PrP-1-1 0.5 ng/nl MO-PrP-1-2 0.125% (v/v) phenol red solution in 1x Danieau buffer
MO-Fyn/Yes	1.6 ng/nl MO-Fyn 1.6 ng/nl MO-Yes 0.125% (v/v) phenol red solution in 1x Danieau buffer

3.5 Synthetic mRNAs

Note: Variations in microinjection concentrations reflect differences in the quality of mRNA synthesized in different rounds of *in vitro* transcription.

mRNA	Concentration in injection solution	
	Rescue or hypomorph experiments [ng/μl]	Overexpression [ng/μl]
WT=wildtype; CA=constitutively active		
zebrafish Fyn WT -EGFP	11	-
zebrafish Yes WT-EGFP	11	-
zebrafish Fyn CA -EGFP	1	-
zebrafish Yes CA-EGFP	1	-
mouse PrP*	20	40-80
Δ23-31 mouse PrP*	15	30-60
ΔCR mouse PrP	15	30-60
Δ23-31/ΔCR mouse PrP	10	20-40
Δ32-134 mouse PrP (F35)	-	100
Δ23-134 mouse PrP (C3)	-	100
Δ23-111 mouse PrP (C1)	-	100
PG14 mouse PrP*	-	100
zebrafish PrP-1 (untagged)	100	200
EGFP-WT PrP-1	300	-
EGFP-PrP-1 Δ48-340 (ΔRep)	100	-
EGFP-PrP-1 Δ394-567 (ΔGlob)	300	-
EGFP-PrP-1 Glyc-	100	-

*These constructs contained a 3F4 epitope (see Methods section)

3.6 Plasmid vectors and DNA constructs

Name (ZF = zebrafish; mo = mouse; WT = wildtype; CA = constitutively active)	Source	Restriction sites used for cloning	Vector modifications
General			
1. pCS2+	Dr. Z. Varga	-	
2. EGFP-pCS2+	Alejandro Pinzon-Olejua	EcoRI/XbaI	
3. pCRII-TOPO	Invitrogen		
4. pEGFP-N1	Clontech		
zebrafish cDNAs			
5. ZF WT Fyn-EGFP-pCS2+	Insert originally in pBsK vector from Dr. Jeroen den Hertog	See Methods	
6. ZF CA Fyn-EGFP-pCS2+	Generated from 5.	See Methods	
7. ZF WT Yes-EGFP-pCS2+	Insert originally in pBsK vector from Dr. Jeroen den Hertog	See Methods	
8. ZF CA Yes-EGFP-pCS2+	Generated from 7.	See Methods	
9. EGFP-ZF WT PrP-1-pCS2+	Málaga-Trillo et al, 2009 Solis et al, 2013		
10. EGFP-Δ48-340 ZF PrP-1-pCS2+ (ΔRep)	Solis et al, 2013		
11. EGFP-Δ394-567 ZF PrP-1-pCS2+ (ΔGlob)	Solis et al, 2013		
12. EGFP-ZF PrP-1 Glyc ⁻ -pCS2+	Solis et al, 2013		
13. ZF WT PrP-1-pCS2+			
14. ZF WT PrP-2-pCS2+			
15. ZF Δ374-393 PrP-1-pCS2+ (ΔCR)	Generated from 13. by inverse PCR and blunt end ligation		
16. ZF Δ295-314 PrP-2-pCS2+ (ΔCR)	Generated from 14. by inverse PCR and blunt end ligation		
mouse cDNAs			
17. EGFP-WT moPrP-pCS2+	Málaga-Trillo et al, 2009 Solis et al, 2013		
18. WT moPrP -pCS2+ (with 3F4 epitope)	Insert originally in pcDNA vector from Dr. D.A. Harris	HindIII/BamHI	SP6 promoter was re-inserted with cloning oligo at SalI/HindIII

19. Δ 105-125 moPrP-pCS2+ (Δ CR)	Insert originally in pcDNA vector from Dr. D.A. Harris	HindIII/BamHI	SP6 promoter was re-inserted with cloning oligo at NdeI/HindIII
20. Δ 23-31 moPrP-pCS2+ (with 3F4 epitope)	Insert originally in pcDNA vector from Dr. D.A. Harris	HindIII/XhoI	SP6 promoter was re-inserted with cloning oligo at Sall/HindIII
21. Δ 23-31/ Δ CR moPrP-pCS2+	Insert originally in pcDNA vector from Dr. D.A. Harris	HindIII/BamHI	SP6 promoter was re-inserted with cloning oligo at NdeI/HindIII
22. Δ 32-134 moPrP-pCS2+ (F35)	Insert originally in pcDNA vector from Dr. D.A. Harris	HindIII/XbaI	SP6 promoter was re-inserted with cloning oligo at NdeI/HindIII
23. Δ 23-134 moPrP-pCS2+ (C3)	Insert originally in pcDNA vector from Dr. D.A. Harris	HindIII/XbaI	SP6 promoter was re-inserted with cloning oligo at NdeI/HindIII
24. Δ 23-111 moPrP-pCS2+ (C1)	Insert originally in pcDNA vector from Dr. D.A. Harris	HindIII/XbaI	SP6 promoter was re-inserted with cloning oligo at NdeI/HindIII
25. PG14 moPrP-pCS2+ (with 3F4 epitope)	Insert originally in pcDNA vector from Dr. D.A. Harris	HindIII/BamHI	SP6 promoter was re-inserted with cloning oligo at Sall/HindIII

3.7 Cell culture media and reagents

Reagent	Company
α -minimum Eagle's medium (MEM α)	Gibco (Life Technologies)
Dulbecco's modified Eagle's medium (DMEM)	Gibco (Life Technologies)
OptiMEM	Gibco (Life Technologies)
Penicillin/Streptomycin (10000 U/ ml)	Gibco (Life Technologies)
MEM Non-Essential Amino Acids (100X)	Gibco (Life Technologies)
L-Glutamine	Gibco (Life Technologies)
Trypsin (0.25%) –EDTA, phenol red	Gibco (Life Technologies)
Lipofectamine 2000	Invitrogen
X-tremeGENE HP transfection reagent	Roche
(3-(4,5-dimethylthiazol-2-yl)-2,5-diphenyltetrazolium bromide (MTT)	Molecular Probes (Life Technologies)
Zeocin (100 mg/ml)	Invitrogen

3.8 Chemical Inhibitors

Substance	Company	Stock solution (Further dilutions of stocks were made in water)	Concentration in injection solution	Concentration in embryo (approx. injection volume: 1/3 of embryo)
Dynasore (Dynamamin Inhibitor I)	Calbiochem	50 mM in 100% DMSO	150 μ M/ 30 μM	50 μ M/ 10 μM
MG132	Calbiochem	20 mM in 100% DMSO	30 μ M	10 μ M
Chloroquine	Sigma	10 mM in water	300 μ M	100 μ M
ammonium chloride (NH ₄ Cl)	Calbiochem	0.5 M in water	150 mM	50 mM
PP2 (4-Amino-5-(4-chlorophenyl)-7-(<i>t</i> -butyl)pyrazolo[3,4-d]pyrimidine)	Calbiochem	11 mM in 100% DMSO	15 μ M	5 μ M
PP3 (4-Amino-7-phenylpyrazol[3,4-d]pyrimidine)				

3.9 Other solutions and buffers

Name	Recipe
Immunostainings	
4% PFA	4% (w/v) PFA in PBS
PBS-T	0.1% (v/v) Triton X-100 in PBS
PBS-DT	0.1% (v/v) Triton X-100 1% (v/v) DMSO in PBS
Blocking solution (zebrafish)	10% (v/v) goat serum in PBS-DT
Blocking solution (MCF-7 cells)	1% bovine serum albumin (BSA) in PBS
Mounting media for microscopy (zebrafish)	25%, 50% and 80% (v/v) glycerol in PBS
Mounting media for microscopy (MCF-7 cells)	16% mowiol 33% glycerol 0.1% thimerosal in PBS, pH 8-8.5
Preparation of Western blot samples	
Pronase stock solution	30 mg/ml Pronase in water; self-digested for 3 h at 37°C

Pronase working solution	1 mg/ml in 30% Danieau buffer
Deyolking buffer (Link et al, 2006)	55 mM NaCl 1.8 mM KCl 1.25 mM NaHCO ₃
Wash buffer (Link et al, 2006)	110 mM NaCl 3.5 mM KCl 2.7 mM CaCl ₂ 10 mM Tris/HCl pH 8.5
Lysis buffer	20 mM Tris-HCl pH 7.5 2 mM EDTA 100 mM NaCl 5 mM MgCl ₂ 1% (v/v) Triton X-100 10% (v/v) Glycerol Supplemented with Protease and Phosphatase Inhibitor cocktail (Thermo Scientific) before use
6x SDS sample buffer	320 mM Tris-HCl pH 6.8 10% (v/v) SDS 51% (w/v) Sucrose 0.02% (w/v) Bromophenol blue 30% (v/v) β-Mercaptoethanol
SDS-PAGE (Sambrook et al, 1989)	
Stacking gel buffer	1 M Tris-HCl pH 6.8 0.75% (v/v) SDS
Resolving gel buffer	1.5 M Tris-HCl pH 8.8 0.4% (v/v) SDS
1x Tris-glycine electrophoresis buffer	25 mM Tris 250 mM Glycine (electrophoresis grade, pH 8.3) 0.1% (w/v) SDS

Western blot (Sambrook et al, 1989)	
1x Transfer buffer	19.8 mM Tris 145 mM Glycine 20% methanol
Blocking solution	3% (w/v) low-fat milk in TBS-T
TBS-T	0.1% (v/v) Tween in 1x TBS
10x TBS	200 mM Tris pH 7.6 1.37 M NaCl

Molecular cloning (Sambrook et al, 1989)	
6x DNA loading buffer for agarose gels	0.25% (w/v) Bromophenol blue 0.25% (w/v) Xylene cyanol FF 15% (w/v) Ficoll (type 400) in water
50x Tris-acetate-EDTA (TAE) buffer	2 M Tris acetate 1 M Glacial acetic acid 0.5 M EDTA
1x TAE buffer	0.04 M Tris acetate 0.02 M Glacial acetic acid 0.0001 M EDTA
Luria-Bertani (LB) medium	1% (w/v) Bacto tryptone 0.5% (w/v) Bacto yeast extract 1% (w/v) NaCl pH 7, autoclaved
LB agar	1% (w/v) Bacto tryptone 0.5% (w/v) Bacto yeast extract 1.5% (w/v) Bacto agar 1% (w/v) NaCl pH 7, autoclaved

3.10 Antibodies for immunofluorescence (IF) and Western blot (WB) analysis

Primary antibodies

Name	Company	Dilution for IF	Dilution for WB
Goat polyclonal anti-Actin	Santa Cruz Biotechnology	-	1:500
Rabbit polyclonal anti- α -tubulin	Abcam	-	1:5000
Mouse monoclonal anti- β -catenin	BD Biosciences	1:250	1:2000
Rabbit polyclonal anti- β -catenin	Sigma-Aldrich	1:500	1:2000
Mouse monoclonal anti-E-cadherin	BD Biosciences	1:250	1:1000
Mouse monoclonal anti-EGFP	Roche, Switzerland	-	1:2000
Mouse monoclonal prion 3F4	Covance (USA)	-	1:2000
Mouse monoclonal prion 6D11	Covance (USA)	-	1:1000
Human monoclonal prion D18 (0.8 μ g/ μ l)	Dennis R. Burton (The Scripps Research Institute, La Jolla, CA)	-	1:1000
Mouse monoclonal prion 6H4	Prionics, Switzerland	1:500	-

Rabbit polyclonal anti-zebrafish PrP-1 globular 983 (affinity-purified; 9 mg/ml; batch from 04.09.2007)	-	-	1:1000
Rabbit polyclonal anti-zebrafish PrP-2 globular 981 (affinity-purified; batch from 20.06.2008)	-	-	1:1000
Rabbit polyclonal anti-Src	Cell Signaling Technology	1:100	1:1000
Anti-phospho antibodies			
Rabbit polyclonal anti-phospho- β -catenin (Y142)	Abcam	-	1:250-1:500
Rabbit polyclonal anti-phospho Src (Y416)	Cell Signaling Technology	1:250	1:500
Rabbit polyclonal anti-phospho Src (Y527)	Cell Signaling Technology	1:250	1:500
Mouse monoclonal anti-phospho-tyrosine	Cell Signaling Technology	1:500	1:2000

Secondary antibodies for Immunofluorescence

Name	Company	Dilution
Monoclonal goat anti-mouse IgG (H+L) Alexa Fluor 488	Jackson ImmunoResearch (UK)	1:1000
Monoclonal donkey-anti-mouse IgG (H+L) Cy3	Jackson ImmunoResearch (UK)	1:1000
Goat anti-mouse IgG (H+L) Cy5	Invitrogen	
Polyclonal goat anti-rabbit IgG (H+L) Alexa Fluor 488	Jackson ImmunoResearch (UK)	1:1000
Polyclonal donkey anti-rabbit IgG (H+L) Cy3	Jackson ImmunoResearch (UK)	1:1000
Goat anti-rabbit IgG (H+L) Cy5	Invitrogen	1:1000

Secondary antibodies for Western blot analysis

Name	Company	Dilution
Goat anti-human IgG HRP	Invitrogen	1:5000
Polyclonal goat anti-mouse IgG (H+L) HRP	Invitrogen	1:5000-1:20000
Polyclonal goat anti-rabbit IgG (H+L) HRP	Jackson ImmunoResearch (UK)	1:5000-1:20000
Polyclonal rabbit anti-goat IgG (H+L) HRP	Jackson ImmunoResearch (UK)	1:5000

3.11 Protein and DNA markers

Name	Company
Page Ruler Prestained Protein Ladder	MBI-Fermentas
Lambda DNA/HindIII Marker, 2	MBI-Fermentas

3.12 Enzymes

Molecular cloning	Company
Platinum Pfx DNA polymerase	Invitrogen
Calf intestine alkaline phosphatase (1u/μl)	MBI-Fermentas
Restriction enzymes	MBI-Fermentas and New England Biolabs
T4 DNA Ligase (5 u/μl)	MBI-Fermentas
Other enzymes	
Pronase (Protease Type XIV: bacterial, from <i>Streptomyces griseus</i>)	Sigma-Aldrich

3.13 Kits

Name	Company
QIAprep Spin Miniprep kit	Qiagen
QIAquick gel extraction kit	Qiagen
QIAquick PCR purification kit	Qiagen

3.14 Other Materials/Chemicals

Bovine serum albumin (BSA)	Sigma-Aldrich
Bradford Reagent	Sigma-Aldrich
4',6-Diamidino-2-phenylindole (DAPI)	Sigma-Aldrich
Dimethyl sulfoxide (DMSO)	Sigma-Aldrich
Dulbecco's phosphate buffered saline (DPBS)	Biochrom (Germany)
Goat serum	Invitrogen
Milk powder (non-fat)	Migros (Zürich, Switzerland)
Phenol red solution 0.5% in DPBS	Sigma-Aldrich
Ponceau S solution	Sigma-Aldrich

SuperSignal West Pico chemiluminescent substrate	Thermo Scientific
Triton X-100	Sigma-Aldrich
Tween 20	Sigma-Aldrich
Hyperfilm ECL	GE Healthcare
Whatman filter paper	Schleicher & Schuell (Dassel, Germany)
Hybond-C Extra Nitrocellulose membrane (0.45 µM pore size)	Amersham Biosciences

3.15 Laboratory equipment

Microscopes

Name	Specification	Manufacturer
Steromicroscope	Stemi 2000-C	Zeiss (Göttingen, Germany)
Fluorescence steromicroscope	LUMAR. V12	Zeiss (Göttingen, Germany)
Confocal laser scanning microscope	LSM 510	Zeiss (Göttingen, Germany)

Microinjection

Name	Specification	Manufacturer
Glass capillaries	1 mm x 4 in	World Precision Instruments (USA)
Micromanipulator	-	Bachofer (Reutlingen, Germany)
Microinjector	FemtoJet Express	Eppendorf
Vertical pipette puller	Model 720	David Kopf Instruments (USA)

3.16 Software

Name	Company/Organization
Adobe Photoshop CS5	Adobe System
Adobe Acrobat Reader Adobe Acrobat Pro	Adobe System
Axiovision 4.7.2	Zeiss (Göttingen, Germany)
Endnote X4	Thomson ISI Researchsoft (USA)
ImageJ	National Institute of Health, USA
Microsoft Office 2008 (Word, Excel)	Microsoft Germany
ZEN 2012	Zeiss (Göttingen, Germany)

4 Methods

4.1 Maintenance of adult zebrafish

Wild type zebrafish (*Danio rerio*) were bred and maintained at the Experimental Animal Facility (Tierforschungsanlage-TFA) of the University of Konstanz following standard procedures (Westerfield, 1993).

4.2 Embryo microinjection

The microinjection set-up consisted of a stereomicroscope to monitor the procedure, a micromanipulator holding the glass needle, and a pneumatic microinjector connected to an air compressor. Embryos were injected manually at 400-1500 hPa for 0.2 s. After injection, the eggs were flushed into a 94 mm-diameter petri dish with pre-warmed E3 medium and placed in an incubator at 28.5°C to continue development.

4.3 Morpholinos

Two Lissamine-tagged, non-overlapping morpholinos were used to target sequences in the 5' UTR of *PrP-1* (Málaga-Trillo et al, 2009): MO-PrP1-1: 5'-GGTCCATAAAAAGGTTGAAGAAGCG-3' and MO-PrP1-2: 5'-TCTCTCCCGCAGCACTCTCTGCTCA-3'. Morpholinos against zebrafish *Fyn* and *Yes* (Jopling & den Hertog, 2005) targeted sequences close to the start ATG of the respective cDNAs: *Fyn*: 5'-TGTCCTTACATTGCACACAGCCCAT-3' and *Yes*: 5'-CCTCTTTACTCTTGACACAGCCCAT-3'. Desiccated morpholinos were initially diluted in water to a 1 mM stock solution, which was stored (without aliquoting) at -20°C. Prior to each experiment, morpholino stock solutions were thawed at room temperature and heated for 10 min at 50°C to dissolve precipitates, before being used to prepare 10 or 20 µl microinjection solutions. These consisted of 0.5 ng/nl (PrP-1-1 and -2, each) and 1.6 ng/nl (*Fyn* and/or *Yes*, each) in 1X Danieau buffer and 0.125% (v/v) Phenol Red. A volume of 5 nl was microinjected into the yolk of embryos at the one- to four-cell stage.

4.4 mRNAs

Capped mRNAs were synthesized by *in vitro* transcription using the mMessage mMachine SP6 kit (Ambion). The synthesis was performed using 1 µg plasmid DNA as template,

previously linearized by *Apal* restriction digest. After synthesis, the mRNA was purified by lithium chloride precipitation. Typically, each synthesis yielded between 20 and 30 µg mRNA product. This was resuspended in 20 µl water and stored at -80°C in 5 µl aliquots. Prior to injection, mRNAs were thawed on ice, heated for 10 min at 60°C, and mixed into microinjection solutions containing 0.05 M KCl and 0.125% Phenol Red. These were kept on ice until injected into embryos. The amounts of injected mRNAs varied between experiments, depending on the quality of the synthesized mRNA and the desired protein expression levels (see Materials section, paragraph 3.5). mRNAs were injected into the cell of one-cell stage embryos using a volume of 5 nl per embryo.

4.5 Molecular Cloning

Cloning of mouse PrP cDNAs into pCS2+

To synthesize mRNAs *in vitro*, the respective cDNAs were cloned into a pCS2+ vector using the multiple cloning site between the SP6 promoter region and the SV40 polyA sequence. The cloning sites used for each cDNA and details to cloning procedures are reported in the Materials section, paragraph 3.6. Some cDNAs were inserted into pCS2+ using the *HindIII* restriction site -positioned upstream of the SP6 promoter- in which case the promoter had to be restored in the vector by an additional cloning step. This entailed the insertion of annealed, 5'-phosphorylated cloning oligos containing the SP6 promoter sequence into the already modified pCS2+ vector. Depending on the sequence of each cDNA, two different types of 5'-phosphorylated oligos were designed and purchased from Eurofins MWG Operon: ones with 5'-*NdeI/HindIII*-3' and ones with 5'-*Sall/HindIII*-3' sticky ends. The oligos were composed of two separately purchased strands, which were then annealed to generate a double-stranded linker oligo. The single-stranded oligos were designed as follows (nucleotides corresponding to sticky ends of restriction sites are in capital letters):

5'-*NdeI/HindIII*-3':

5' -TATGgatttaggtgacactatagaatacaagctacttgttctttttgcaA-3'

5' -AGCTTtgcaaaaagaacaagtagcttgattctatagtgtcacctaatacCA-3' and

5'-*Sall/HindIII*-3':

5' -TCGACgatttaggtgacactatagaatacaagctacttgttctttttgcaA-3'

5' -AGCTTtgcaaaaagaacaagtagcttgattctatagtgtcacctaatacG-3'

10 µl of each single-stranded oligo (100 µM) were mixed together, denatured for 2 min at 94°C and left to anneal for 30 min at 60°C. The annealed products were then placed on ice and used immediately for ligation.

The 3F4 epitope

Untagged mouse PrP cDNAs with an intact central region contained three point mutations at positions 322 (C to A), 324 (C to G) and 331 (G to A), enabling the recognition of the respective protein product by the 3F4 prion antibody, which normally recognizes hamster PrP. The original and modified DNA/protein sequences were the following:

DNA (mouse PrP): 5' – CTC AAG CAT GTG –3' protein: L K H V
 DNA (3F4-modified): 5' – **ATG** AAG CAT **ATG** –3' protein: **M** K H **M**

Generation of *Fyn* and *Yes* -EGFP and cloning into pCS2+

Plasmids encoding zebrafish wildtype (WT) *Fyn* and *Yes* cDNAs, a kind gift of Dr. Jeroen den Hertog, were used to create C-terminally tagged EGFP fusion constructs. The following PCR primers (Eurofins MWG Operon) were designed to remove stop codons:

Fyn-F-(EcoRI): 5' –CGAATTCATGGGCTGCGTACAGTG–3'
Fyn-R-(ApaI): 5' –GGGGCCCAGAGGTTGTCCCCGGGTTGG–3'
Yes-F-(EcoRI): 5' –CGAATTCATGGGCTGCGTAAAAAGC–3'
Yes-R-(ApaI): 5' –GGGGCCCACAGGTTGTCTCCGGGCTGATA–3'.

Constitutively active (CA) forms were generated by mutating Tyr residues 531 in *Fyn* and 540 in *Yes* to Phe using instead the following reverse primers:

Fyn CA-R-(ApaI): 5' –GGGGCCCAGAGGTTGTCCCCGGGTTGGAAC–3'
Yes CA-R-(ApaI): 5' –GGGGCCCACAGGTTGTCTCCGGGCTGAAAC–3'.

PCR products were cloned into pCRII-TOPO, digested with *EcoRI*//*ApaI* and subcloned into pEGFP-N1. For expression in zebrafish embryos, inserts lacking 9 bp upstream of the EGFP stop codon were excised with *EcoRI*//*BsrGI*, and inserted into the corresponding sites of pCS2+-EGFP, thereby restoring the full-length fusion constructs. pCS2+-EGFP was constructed by inserting EGFP into the *EcoRI*//*XbaI* sites of pCS2+.

Generation of zebrafish PrP-1 and -2 Δ CR constructs

The central regions of zebrafish PrP-1 (residues 374-393) and PrP-2 (residues 295-314) were deleted by inverse PCR amplification of whole pCS2+ plasmids containing inserts WT PrP-1 or WT PrP-2 (Imai et al, 1991), and subsequent blunt-end ligation.

Inverse PCRs were performed in 50 μ l reactions containing 0.3 μ M of each primer, 0.3 mM of each

dNTP, 1 u Platinum Pfx DNA polymerase , 1 mM MgSO₄, and approximately 120 pg plasmid DNA as template (either ZF WT PrP-1-pCS2+ or ZF WT PrP-2-pCS2+). The following primer pairs were used:

PrP-1-ΔCR-Rev: 5' – TTTGGATTTTGCAGAAGGGTTGTAGC –3'

PrP-1-ΔCR-Fwd: 5' – GGCTATGGAATAGGAAACTTTCAACG –3' and

PrP-2-ΔCR-Rev: 5' – CTTTGATTTGTAAGAAGGGGCCATAC –3'

PrP-2-ΔCR-Fwd: 5' – GGATATGGCCTGGGAAGTTTCCCCCG –3'

All primers were 5' phosphorylated. PCRs were performed as follows:

Initial denaturation: 4 min at 94°C

35 cycles of:	Denaturation	30 s at 94°C
	Annealing	30 s at 62°C
	Extension	6 min at 68°C

Final extension: 10 min at 68°C

After amplification, the template DNA was digested by adding 25 units of *DpnI* to each reaction and incubating for 1 h at 37°C. PCR products were then separated in an agarose gel and purified with the QIAquick gel extraction kit. Blunt end ligations were performed overnight at 16°C using 100 ng purified PCR product.

4.6 Chemical inhibitors

Chemical inhibitors were injected at the concentrations reported in the Materials section, paragraph 3.8, in the same solution as morpholinos or mRNAs (described above). To avoid precipitation, stock solutions of inhibitors in DMSO were heated for 5 min at 37°C prior to further dilution in water -also heated at 37°C.

4.7 Assessment of embryonic phenotypes (live pictures and quantifications)

In each experiment, a total of approximately 200 embryos were examined for their phenotype under a stereomicroscope. Representative images of live embryos were acquired with a LUMAR.V12 microscope and processed using Adobe Photoshop CS5. Staging of embryos was performed as previously described (Kimmel et al, 1995). All graphs showing percentages of embryonic phenotypes depict values of at least three independent experiments. Statistical significance was assessed by unpaired two-tailed student's t-tests.

4.8 Immunostainings of zebrafish embryos

For immunostainings, embryos were fixed overnight at 4°C in 4% PFA-PBS, washed three times in PBS and dechorionated. They were then permeabilized by successive washes in PBS-T (three times) and PBS-DT (once), and blocked in 1% goat serum-PBS-DT for 2 h at room temperature. Primary antibodies were diluted as indicated in the Materials section in 1% goat serum-PBS-DT and incubations were performed overnight at 4°C. Embryos were then washed three times in PBS-DT and incubated overnight with secondary antibodies and DAPI reagent (diluted 1:500). All secondary antibodies were diluted 1:1000 in 1% goat serum-PBS-DT. Subsequently, the embryos were washed three times in PBS-T, mechanically deyolked (for flat mounts) and placed sequentially in 20%, 50% and 80% glycerol-PBS. Embryos were mounted with or without yolk in 80% glycerol-PBS between two glass coverslips and imaged using a confocal laser-scanning microscope. All wash, blocking and antibody incubation steps were performed with 15-20 embryos in 2 ml plastic tubes or in glass wells on a shaker. Wash steps were performed in volumes of 500 µl for 5 min. Blocking and antibody incubations were carried out in volumes between 100 and 500 µl.

4.9 Immunofluorescence profiles and quantification (zebrafish embryos)

For the E-cadherin and β -catenin immunofluorescence profiles of 6 hpf embryos, the fluorescence intensity was measured with Zeiss Zen software along manually drawn lines crossing from the ventral to the dorsal side of laterally imaged, whole-mounted embryos. To study β -catenin translocation, embryos were fixed at the High stage (at approximately 3 hpf) and stained with a mouse monoclonal anti- β -catenin antibody (see Materials section). Z-sections of whole embryos were generated and marginal cells with nuclear β -catenin were counted. The data of three independent experiments (N=5) were statistically evaluated by unpaired two-tailed student's t-tests. The same embryo images were used to determine ratios of plasma membrane vs. cytosolic β -catenin fluorescence in dorsal blastomeres. For this, whole cell/cytoplasm areas were outlined and the corresponding fluorescence (integrated densities) measured and subtracted using Image J. Ten cells per embryo were analyzed (N=15) in three independent experiments and values were assessed for statistical significance by unpaired two-tailed student's t-tests.

4.10 Western Blots with zebrafish embryo lysates

Preparation of embryo lysates for Western Blot (General protocol)

Up to 100 zebrafish embryos were dechorionated in 25 ml beakers using 10 ml of 1 mg/ml Pronase (in 30% Danieau buffer). Incubations with Pronase were carried out by placing the

beakers halfway into a 30°C water-bath for 20 min. Pronase working solutions were stored at -20°C and used up to four times. After enzymatic digestion, chorions were washed off the embryos by four to five successive washes in 30% Danieau buffer. Throughout these washes, special caution was taken to continuously keep embryos covered by liquid by holding the beakers in a tilted position between pouring out the buffer and refilling with new one. To assist dechorionation, embryos retaining their chorions after the washing procedure were passed once through a glass Pasteur pipette. For dissociation into single cells, embryos were transferred with the glass pipette into 1.5 ml tubes and most of the Danieau buffer was removed. Deyolking buffer was then added (2 µl/embryo) and the embryos were mechanically deyolged by resuspension using a 200 µl pipette. Dissociated embryonic cells were then pelleted by centrifugation at 1500 rpm for 30 s, the yolk-containing supernatant was discarded, and the cells resuspended in wash buffer (3 µl/embryo) using a 1000 µl pipete. The deyolking and washing procedure was carried out twice. Embryo cells were pelleted in a final centrifugation step at 2000 rpm for 2 min, resuspended in ice-cold lysis buffer (0.5 µl/embryo) and left to lyse 10 min on ice. Cell debris was pelleted by centrifugation of lysates at 14000 rpm for 10 min at 4°C. The cleared lysates were transferred into clean tubes and frozen at -80°C until further use, or loaded immediately onto SDS gels whenever the Western Blot analysis was aimed at detecting phosphorylated proteins.

Preparation of embryo lysates for Western Blot detection of the 120 kDa E-cadherin isoform

Although embryo dissociation by two consecutive rounds of deyolking and washing was normally performed at room temperature with solutions pre-heated at 28°C, we found that a better detection of the E-cadherin 120 kDa isoform could be achieved in Western Blots by dissociating the embryos on ice. For this, the latter were placed on ice directly after being dechorionated and washed in Danieau buffer. Then they were deyolged and washed in ice-cold deyolking and wash buffer, respectively, as described above. Only one round of this procedure on ice was sufficient to dissociate the embryos into cells and effectively remove the yolk. Cell lysates were prepared as described above.

SDS gel electrophoresis and Western Blot analyses

The protein concentration of embryo lysates was measured using the Bradford reagent and a standard BSA concentration curve. For the measurement, 2 µl lysate were added to Bradford reagent (diluted 1:2 with water) and the OD was measured at 570 nm. After determining lysate concentrations, different samples were adjusted to the same concentration by adding the appropriate volume of lysis buffer. 20 µg of embryo lysate were mixed with 6x SDS sample buffer and loaded into 3 mm-wide slots of 10% or 12% SDS gels

(the latter were used exclusively for mouse PrP due to its low molecular weight). Protein transfer to a nitrocellulose membrane was performed either for 2.5 h at 90 V or overnight at 37 V. To visualize transferred proteins, membranes were stained with a 0.1% Ponceau S/5% acetic acid solution for 2 min on a shaker and then rinsed with water.

Membranes were blocked in 3% non-fat milk-TBS-T for 30 min at room temperature and briefly rinsed in TBS-T, before being incubated with primary antibodies overnight at 4°C. As an exception, membranes were incubated for only 1 h at room temperature with an antibody against α -tubulin due to its high immunoreactivity. Primary antibodies were all diluted in 3% BSA-TBS-T and stored between uses at 4°C after addition of ammonium azide. After primary antibody incubation, membranes were washed three times for 5 min in TBS-T. Secondary antibodies were diluted in 3% non-fat milk-TBS-T and incubated with membranes overnight at 4°C, or for α -tubulin detection, for 1-2 h at room temperature. The membranes were then finally washed three times for 5 min in TBS-T before being incubated for 2 min with HRP substrate (1.5 ml for a 6 cm x 8 cm membrane). Bands of specific proteins were visualized by capturing the chemiluminescence on photographic film for 1s to 5 min. Films were developed directly after exposure in an automatic film-processing machine. All abovementioned washing and antibody incubation steps were performed on a shaker. Antibody dilutions are reported in the Materials section. Western Blot bands were quantified by standard procedure using ImageJ.

4.11 Treatment of zebrafish embryonic cells with A β ₁₋₄₂ peptide

A total of 300 4 hpf control or PrP-1 morphant embryos was divided into groups of 100 embryos, dechorionated as described in paragraph 4.10 (100 embryos/beaker), washed in Danieau buffer and transferred into 1.5 ml tubes (100 embryos/tube). The embryos were deyolked by resuspension in 200 μ l deyolking buffer (preheated at 28°C; details described in paragraph 4.10). After centrifugation at 1300 rpm for 30 s, the dissociated cells were resuspended in 200 μ l fresh deyolking buffer, and embryos of the same type (control or PrP-1 knockdown) were pooled into one tube. Cells were then pelleted again at 1300 rpm for 1 min, the deyolking buffer was removed, and the pellet was resuspended thoroughly in 620 μ l wash buffer (preheated at 28°C; details described in paragraph 4.10). Without delay, the cells in suspension (control or PrP-1 knockdown) were divided into three fresh 1.5 ml tubes and centrifuged at 1300 rpm for 2 min. The pellets were finally resuspended in 200 μ l of 30% Danieau buffer (control) or buffer containing 500 nM monomeric or oligomeric A β peptide. Cells were left to incubate in the tubes in vertical position at 28.5°C for 1 h (a hole was punched with a syringe into the lid of each tube), before being pelleted by centrifugation at 1300 rpm for 2 min, and disrupted in 40 μ l ice-cold lysis buffer. After resuspension in lysis

buffer, cells were left for 5 further minutes on ice and the lysates were then processed as described in paragraph 4.10. Without prior storage, 15 µg of protein were directly loaded per lane of 10% SDS gels and analyzed as described above.

Monomeric (fresh) A β was provided by Dr. S. Schildknecht at the University of Konstanz, whereas oligomeric Abeta was synthesized and provided by D. A. Harris at the University of Boston School of Medicine.

4.12 HEK cells

Culture conditions

HEK293 cells (ATCC CRL-1573) were grown in medium containing α -minimum Eagle's medium/Dulbecco's modified Eagle's medium (1:1), supplemented with 10% fetal bovine serum, 2 mM glutamine, non-essential amino acids and penicillin/streptomycin. Cells were trypsinized with 0.25% Trypsin-EDTA prior to subculturing in 25 cm² flasks or 24-well plates.

Drug-based cell assay (DBCA)

For the DBCA, one confluent 25 cm² flask was distributed into the wells of a 24-well plate. After approximately 15 h, cells were transfected for 5-6 h using 1.8 µl Lipofectamine and 0.8 µg plasmid DNA (WT or Δ CR PrPs in pCS2+) per well in 0.5 ml OptiMEM. The OptiMEM was then replaced with 1 ml regular growth medium, and cells were further incubated without treatment for 18 h. The medium was subsequently removed and fresh medium containing 0.5 mg/ml Zeocin was added to the cells. After a 24 h incubation in Zeocin, the medium was removed and replaced with 300-400 µl PBS containing 1 mg/ml (3-(4,5-dimethylthiazol-2-yl)-2,5-diphenyltetrazolium bromide (MTT). Cells were left to metabolize MTT for 20 min at 37°C, the MTT solution was then removed, and the cell carpet was lysed in 500 µl DMSO (99.9%). 100 µl of cell lysate were transferred into a 96-well plate and the OD was measured at 570 nm in an ELISA reader.

Western Blot

To verify the expression of untagged WT and Δ CR PrPs, HEK cells were plated and transfected as described above. After transfection, cells were washed twice in PBS, and then resuspended in 100 µl lysis buffer (per well). Lysates were further processed as described in paragraph 4.10 and stored at -80°C until further use. 15 µg of protein lysate were loaded per lane of 12% SDS minigels and analyzed by Western Blot using the anti-mouse PrP antibody 6D11 or anti-zebrafish PrP-1 and -2 polyclonal antibodies. Western Blots were performed as described in paragraph 4.10.

4.13 MCF-7 cells

Culture conditions

MCF-7 cells (ATCC HTB-22) were grown in medium containing Dulbecco's modified Eagle's medium containing 10% fetal bovine serum, 2 mM glutamine and penicillin/streptomycin. Cells were trypsinized with 0.25% Trypsin-EDTA prior to subculturing in 75 cm² flasks, 12-well plates (for immunostaining) or 6-well plates (for Western blots).

Immunostainings

For immunostainings, 175.000 cells were plated per well of a 12-well plate onto 20 mm-diameter Poly-L-Lysine-coated coverslips, and were left to grow 15-18 h prior to transfection. Transfections with pCS2+ plasmids encoding EGFP-tagged PrPs were performed using 4.5 µl X-tremeGENE HP transfection reagent and 1.5 µg plasmid DNA per well, overnight in 1 ml regular growth medium. The cells were then fixed in 500 µl 4% PFA-PBS at room temperature for 20 min, washed three times in PBS and permeabilized with 500 µl ice-cold PBS-T for exactly 1 min. To completely remove the PBS-T, cells were washed three times in PBS, and then blocked in 500 µl 1% BSA-PBS at room temperature for 30 min. Incubations with primary antibodies, diluted in 1% BSA-PBS, were performed overnight at 4°C. Cells were then washed three times in PBS, before being incubated with secondary antibodies together with DAPI reagent (1:500) in 1% BSA-PBS. Antibody dilutions are reported in the Materials section. Finally, the cells were washed twice in PBS and once in water and the coverslips were mounted between 76 x 26 mm microscope slides (bottom) and 40 x 24 mm cover slips (top) in 16% mowiol. Confocal images were acquired with a confocal laser-scanning microscope. To measure the percentage of Src kinases and E-cadherin localized at cell contacts, whole cells and cell contact sites were separately outlined in ImageJ and their fluorescence intensity (integrated density) was measured. The ratios of cell contact to whole cell fluorescence were depicted as percentages in graphs. The statistical significance of these values was evaluated by unpaired two-tailed student's t-tests. 30 cells were evaluated per experiment.

Western Blots

For Western Blots, 900.000 cells were plated per well of a 6-well plate and left to become confluent overnight. The transfection procedure was the same as the one used for immunostainings, using double the amounts of transfection reagent, plasmid DNA and medium per well. After overnight transfection, the cells were washed twice in PBS and lysed in 300 µl ice-cold lysis buffer per well using a cell-scraper. Lysates were further processed as described in paragraph 4.10. To detect phosphorylated Src kinases, lysates were not

stored, but loaded directly (15 $\mu\text{g}/\text{lane}$) onto 10% SDS minigels. Western Blots were performed as reported in paragraph 4.10.

5 Results

5.1 PrP-1 regulates the turnover of selected AJ components at the plasma membrane

During gastrulation, AJs promote tissue cohesiveness while allowing for coordinated morphogenetic movements of the deep cells (see Introduction, Table 1) (Montero & Heisenberg, 2004). These include “radial intercalation” (deep cells relocating to more superficial layers, causing a thinning of the blastoderm over the yolk) and “convergence-extension” (massive movement of cells from throughout the gastrula toward the dorsal side, and subsequent redistribution along the anterior-posterior axis). Such rearrangements, which give rise to the body axis and germ layers (ecto-, meso- and endoderm), rely on the ability of each cell to down- and up-regulate AJ function at the cell surface (Montero & Heisenberg, 2004; Niessen et al, 2011). In this way, cells are allowed to move while remaining flexibly attached in a tissue. Accordingly, embryonic cells with depleted E-cadherin not only display lack of cell-cell adhesion, but also a clear inability to perform migratory movements (Babb & Marrs, 2004; Kane et al, 2005; Schepis & Nelson, 2012; Shimizu et al, 2005).

As outlined in paragraph 1.7 of the Introduction, AJ function entails the maintenance of E-cadherin molecules at the cell surface, their association with α -, β -, p120-catenin, and their dynamic anchorage to the actin cytoskeleton (Niessen et al, 2011). Our laboratory previously reported that upon knockdown of PrP-1 in early zebrafish embryos, E-cadherin and β -catenin lose their cell surface localization and accumulate in the cytosol. This defect leads to a dramatic loss of adhesion between blastomeres and the subsequent embryonic arrest at the 50% epiboly stage (approx. 6 hpf). The reduced cell surface levels of E-cadherin in PrP-1 morphant embryos were also detected in Western blot experiments where the levels of the mature, membrane-bound E-cadherin isoform appeared clearly diminished (Málaga-Trillo et al, 2009). The latter sets itself apart from a larger E-cadherin polypeptide (140 kDa), which is a proteolytically unprocessed, biosynthetic intermediate residing mostly in intracellular vesicles and without a verified adhesive function (Babb & Marrs, 2004; Ozawa & Kemler, 1990). In this thesis, we asked which molecular mechanisms trigger the downregulation of plasma membrane E-cadherin in PrP-1 knockdown embryos. Since the 140 kDa E-cadherin precursor polypeptide is present at similar levels in the lysates of control and PrP-1 knockdown embryos, we reasoned that defective biosynthesis of the protein was not the

reason for its reduced localization at the plasma membrane. Alternatively, this effect may be explained by defects in the transport of the protein to or from the plasma membrane. Given the reduced levels of mature E-cadherin in morphant embryos, we tested the hypothesis that PrP-1 controls the internalization and degradation of E-cadherin. To address this scenario, we microinjected embryos with PrP-1 morpholinos in the presence or absence of Dynasore, an inhibitor of dynamin-dependent endocytosis, and examined the subcellular localization of AJ components at 6 hpf (50% epiboly). Whole-mount immunofluorescence analysis of deep cells revealed that treatment with as little as 10 μ M Dynasore was sufficient to restore the localization of both E-cadherin and β -catenin at the plasma membrane and prevented their abnormal cytosolic accumulation (Figure 13A). Complementary Western blot analyses further showed that Dynasore restored the levels of mature E-cadherin (120 kDa) in a dose-dependent manner (Figure 13B).

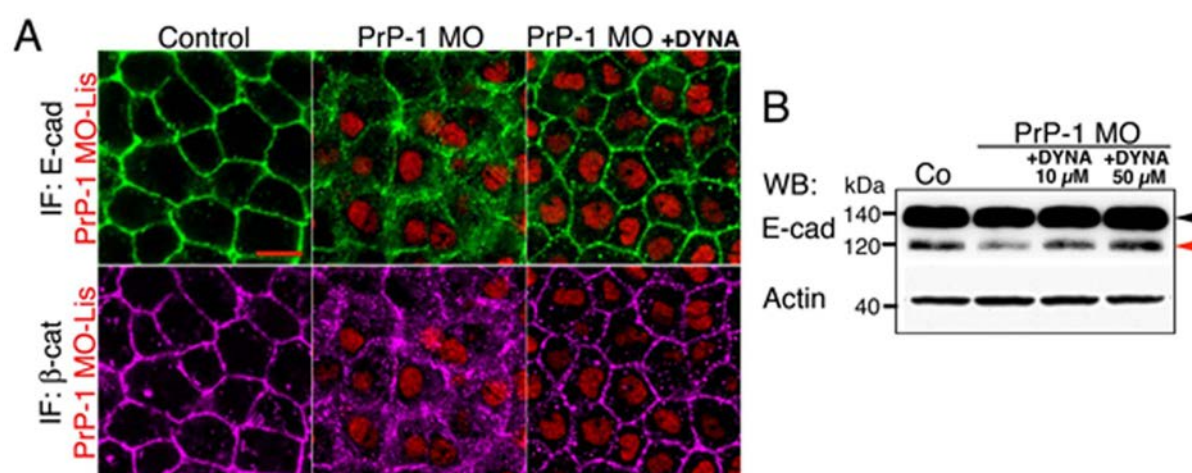


Figure 13 PrP-1 affects the endocytosis of E-cadherin. **A.** Dynasore (=DYNA) treatment (10 μ M) restores the plasma membrane localization of E-cadherin and β -catenin in PrP-1 morphants. Immunofluorescence (IF) of E-cadherin and β -catenin in deep cells of 6 hpf control and PrP-1 knockdown embryos. Red fluorescence signal is from Lissamine-tagged morpholinos (MO). Scale bar indicates 10 μ M. **B.** Western blot (WB) analysis of 6 hpf embryo extracts. Dynasore injection restores the levels of mature E-cadherin (120 kDa, red arrowhead) in PrP-1 morphants; black arrowhead indicates the proteolytically unprocessed E-cadherin precursor form (140 kDa). Actin serves as a loading control.

Interestingly, Dynasore also induced a phenotypic recovery at the morphological level, reducing the proportion of arrested/deformed PrP-1 knockdown embryos by 25 % at 10 μ M ($p < 0.05$) and by 40% at 50 μ M ($p < 0.005$) (Figure 14A and B). Compared to untreated controls, Dynasore-treated PrP-1 morphant embryos exhibited less pronounced tissue irregularities as well as thinner and more cohesive blastoderms, consistent with their increased ability to carry out epiboly beyond 50% (Figure 14A). In contrast, PrP-1 morphants treated with the vehicle substance DMSO did not show improvements in tissue integrity or epibolic progression. This result indicates that, during zebrafish gastrulation, PrP-1 stabilizes AJ components at the plasma membrane by preventing their internalization.

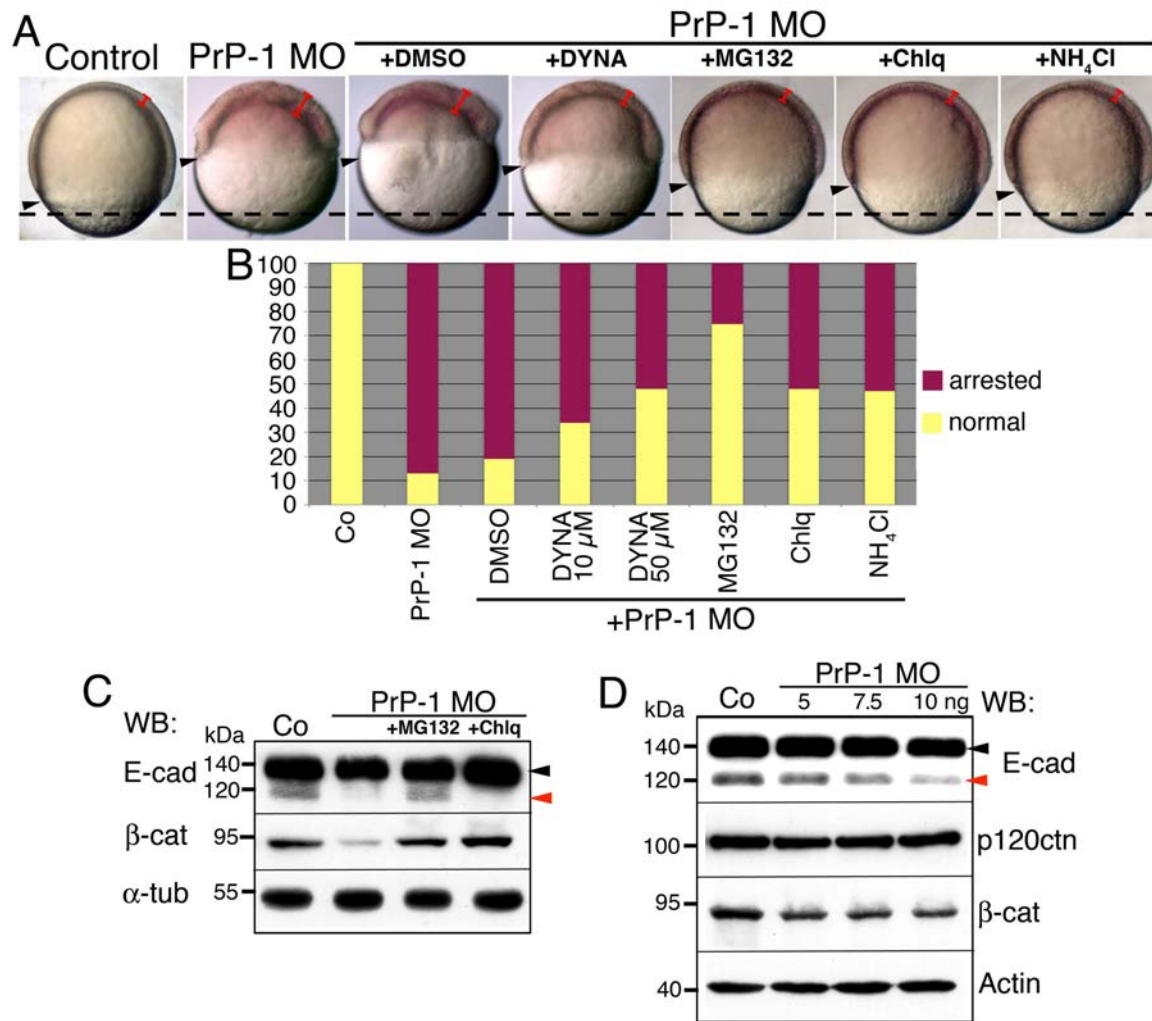


Figure 14 Effect of PrP-1 on the endocytosis and degradation of AJ components **A.** Differences in progression of epiboly and blastoderm morphology of 7.5 hpf embryos. Arrowheads indicate the progression of the blastoderm margin and the dashed line serves for comparison across embryos. Treatment of PrP-1 morphants with inhibitors of endocytosis (DYNA=Dynasore), the proteasome (MG132) or lysosomes (chloroquine [Chlq] and ammonium chloride [NH₄Cl]), but not DMSO, leads to improvements in tissue morphology and epiboly progression. MG132, chloroquine and ammonium chloride were injected at a final concentration of 10 μM, 100 μM and 50 mM, respectively. **B.** Quantification of embryonic phenotypes between 6 and 7.5 hpf. Data shown as mean values of three independent experiments (n=200). **C.** Changes in the levels of E-cadherin and β-catenin upon PrP-1 knockdown and concomitant proteasome or lysosome inhibition, as detected by Western blot (WB) in lysates of 6 hpf embryos (red arrowhead: mature E-cadherin; black arrowhead: E-cadherin precursor). **D.** AJ protein levels detected by Western blot in lysates of 6 hpf embryos injected with different amounts of PrP-1 morpholino; E-cadherin isoforms indicated as in C.

In PrP-1 morphant embryos, the reduction in the levels of mature E-cadherin was concomitant with its increased cytosolic accumulation (Málaga-Trillo et al, 2009), suggesting that upon endocytosis, the protein is directed to degradation. To test this possibility, we treated PrP-1 morphants with MG-132 and chloroquine, well-established inhibitors of proteasomal and lysosomal degradation, respectively. Whereas MG-132 caused a substantial recovery in the levels of mature, 120kDa E-cadherin product, chloroquine

enhanced the levels of its 140 kDa precursor form (Figure 14C). Moreover, treatment with MG-132, chloroquine or a second lysosomal inhibitor, ammonium chloride, led to remarkable improvements in the morphology and epiboly progression of 6 hpf PrP-1 knockdown embryos (Figure 14A). Notably, quantification of embryonic phenotypes between 6 and 7.5 hpf (arrested versus normal) revealed that MG-132, which restores the mature E-cadherin product, had the strongest rescuing effect of all inhibitors tested (71.26% reduction in the proportion of arrested embryos, $p < 0.001$) (Figure 14B). The lysosomal inhibitors were less efficient, causing a 40% reduction in the number of arrested embryos ($p < 0.001$ for both chloroquine and ammonium chloride) (Figure 14B). Altogether, these experiments indicate that in the absence of PrP-1, mature E-cadherin is increasingly endocytosed and degraded by a proteasome-dependent mechanism.

When not bound to E-cadherin at AJs, β -catenin is rapidly degraded in the cytosol unless induced by the canonical Wnt pathway to enter the nucleus and activate the transcription of diverse gene targets (Orsulic et al, 1999). Since β -catenin is largely cytosolic in PrP-1 morphants (Figure 13A), we biochemically examined the stability of this protein pool. Western blot analyses confirmed that the total levels of β -catenin are reduced in these embryos, an effect that can be reverted efficiently by treatment with either MG-132 or chloroquine (Figure 14C). Thus, PrP-1 knockdown triggers the depletion of cytosolic β -catenin via a combination of proteasomal and lysosomal degradation pathways. It was also noteworthy that the association of β -catenin to the plasma membrane could be restored in PrP-1 morphants by treatment with Dynasore, suggesting that its internalization upon PrP-1 knockdown was rather a consequence and not the trigger of E-cadherin endocytosis (Figure 13A). Interestingly, while E-cadherin and β -catenin became increasingly degraded at higher PrP-1 morpholino doses, the levels of p120-catenin remained unaltered (Figure 14D). These data indicate that the degradation of selected AJ components in PrP-1 morphants is specific, and that it does not involve their destabilization by p120-catenin depletion.

5.2 Convergence of SFK and PrP-1 knockdown phenotypes

Our group previously reported that exogenous expression of vertebrate PrPs triggers the formation of weak adhesive contacts between *Drosophila* S2 cells and the recruitment of activated SFKs at cell-cell contact sites (Málaga-Trillo et al, 2009). In that same study, PrP-1 expression was found to be required for the formation of contacts between zebrafish blastocysts and the concomitant localization of the SFK Fyn at these cell contacts. These findings in embryonic cells revealed that PrP can modulate SFK function in diverse physiological scenarios, and that, therefore, this regulatory role of PrP is not restricted to previous observations in cultured neurons (Chen et al, 2003; Mouillet-Richard et al, 2000). The paramount importance of SFKs for early embryonic development is underscored by the

fact that their genetic or chemical inactivation in zebrafish induces strong gastrulation defects ranging from total developmental arrest to impaired morphogenetic cell movements (Jopling & den Hertog, 2005; Sharma et al, 2005; Tsai et al, 2005). Of particular relevance to this thesis is the prominent role of SFKs in the modulation of cadherin-based adhesion, a subject that has been extensively characterized in cultured cells and more recently in mice and *Drosophila* embryos (Calautti et al, 1998; Calautti et al, 2002; Takahashi et al, 1996; Takahashi et al, 2005). The well-established functional connections between PrP and SFKs on one hand, and SFKs and E-cadherin on the other hand, motivated us propose that SFKs mediate the effect of PrP-1 on AJs in the zebrafish embryo (Málaga-Trillo & Sempou, 2009). Three SFKs -Src, Yes and Fyn- are expressed during zebrafish gastrulation and, like PrP-1, they are distributed ubiquitously throughout the embryo (Jopling & den Hertog, 2005). Notably, Fyn and Yes, but not Src, are required for the morphogenetic cell movements that shape the embryonic body plan at this stage of development (Jopling & den Hertog, 2005; Sharma et al, 2005; Tsai et al, 2005). As a first approach, we examined the extent of similarity between Fyn/Yes and PrP-1 loss-of-function phenotypes, reasoning that if the two SFKs acted cooperatively, their individual knockdowns would result in similar phenotypes. In fact, morpholino knockdown of either *Fyn* or *Yes* led to blastoderm thickening/deformation and epibolic arrest in approx. 55-60% of injected embryos, clearly resembling the PrP-1 morphant phenotype (Figures 15A and B). Moreover, the combined *Fyn/Yes* knockdown produced an even stronger effect (82% of injected embryos, Figures 15A and B), indicating that the two kinases act synergistically during epiboly. The protein knockdowns were titrated and verified by Western blot using an anti-Src antibody against the conserved C-terminus of SFKs. We detected two specific bands in the cell extracts of 6 hpf embryos (Figure 15C): one of approximately 60 kDa corresponding in size to kinases Src and Yes, and a lower one of ~50 kDa corresponding to the kinase Fyn (Lemeer et al, 2007). Whereas injection of morpholino against Fyn caused a downregulation of the 50 kDa band as expected, knockdown of Yes reduced the intensity of both the 60 kDa and 50 kDa bands, suggesting that Fyn expression levels are dependent on those of Yes. As anticipated, the Fyn/Yes double knockdown led to the strongest reduction in the intensity of both bands.

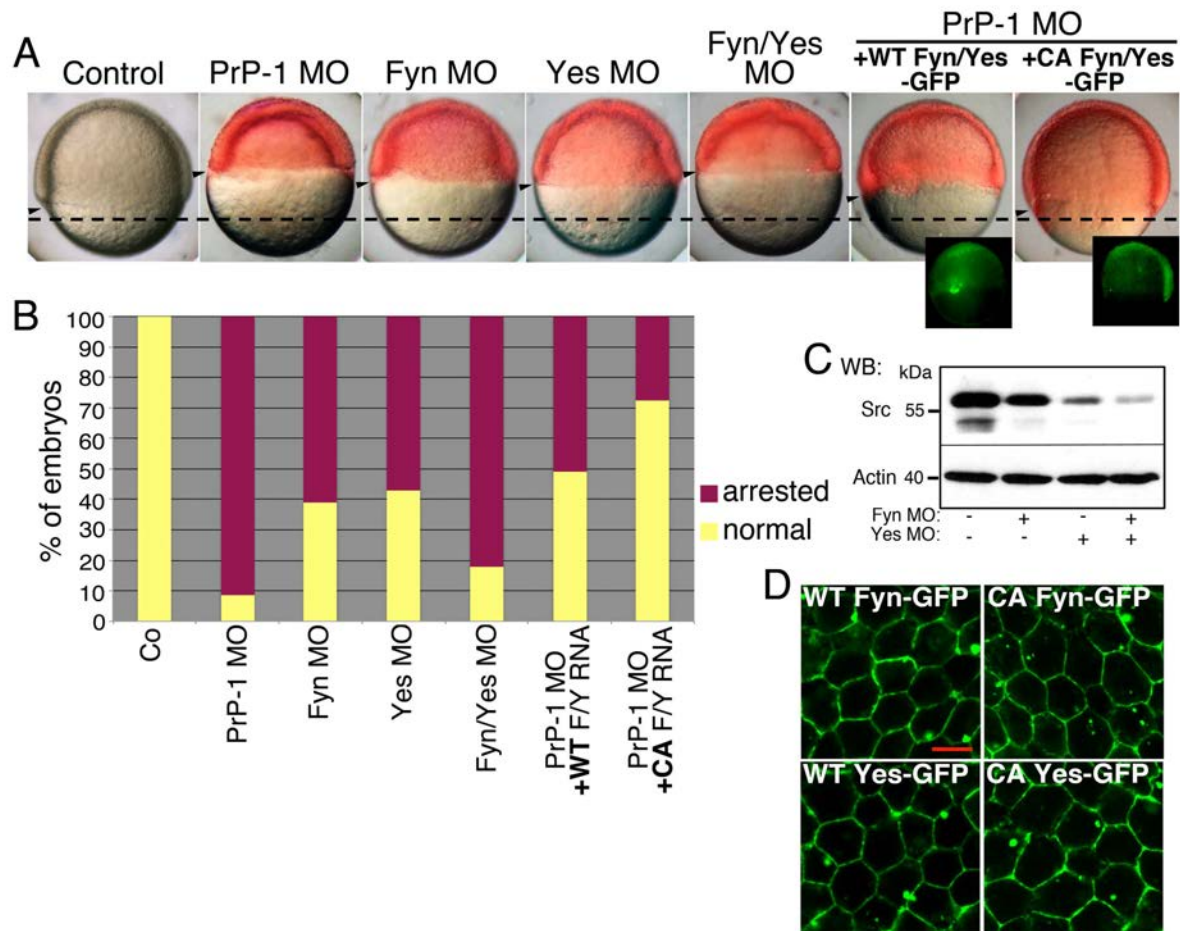


Figure 15 Fyn and Yes act downstream of PrP-1 during epiboly-I. **A.** 7.5 hpf embryos, injected with different morpholinos or co-injected with PrP-1 morpholino and Fyn-/Yes-EGFP mRNAs, encoding wildtype (WT) or constitutively active (CA) forms of the kinases. Transmission images and Lissamine fluorescence of morpholinos (red) are shown merged. Expression of WT or CA Fyn/Yes-EGFP (green) are displayed separately on the lower right. Arrowheads indicate progression of the blastoderm margin and the dashed line serves for comparison. **B.** Quantification of 7.5 hpf embryos with arrested or normal epiboly after injection with different morpholinos or co-injection of PrP-1 morpholino with Fyn-/Yes- EGFP mRNAs. Graph depicts average values of three independent experiments (n=200). **C.** Western blot (WB) analysis of lysates of Fyn and Yes single or double morphants (6 hpf), demonstrating SFK knockdown. **D.** Expression pattern of WT or CA Fyn- and Yes-EGFP in deep cells of 6 hpf PrP-1 morphants. Scale bar indicates 10 μ m.

We then asked whether SFK and PrP-1 morphants share defects in AJ function. In fact, reduced presence at the plasma membrane and intracellular accumulation of E-cadherin and β -catenin were apparent in Fyn and Yes single and double knockdown embryos (Figure 16A). Like in PrP-1 morphants, these defects were evident in deep cells but less pronounced or absent in the outer enveloping layer cells (Figure 16B). Furthermore, Fyn/Yes morphant embryos displayed reduced levels of mature E-cadherin and β -catenin at 6 hpf (WB, Figure 16C). Hence, the morphological and molecular convergence of Fyn/Yes and PrP-1 knockdown phenotypes suggests that these proteins act synergistically to stabilize embryonic AJ components.

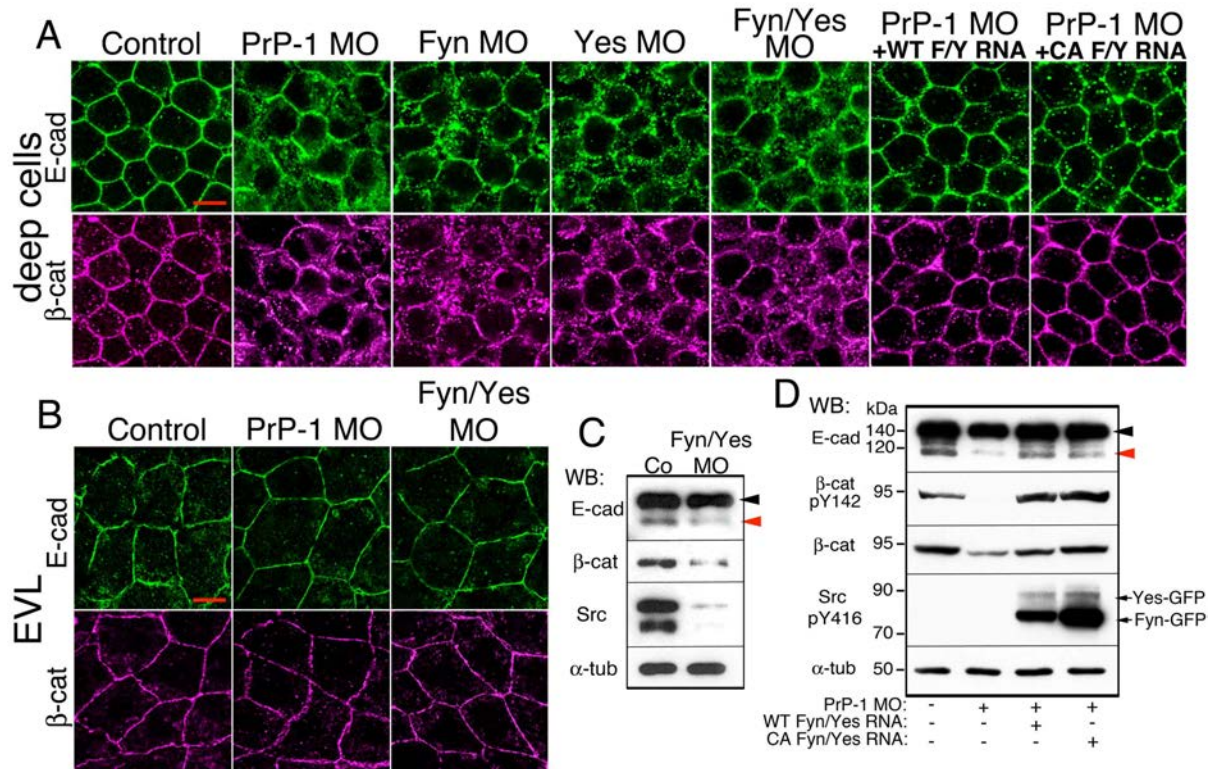


Figure 16 Fyn and Yes act downstream of PrP-1 during epiboly-II. **A and B.** Immunofluorescence of E-cadherin (green) and β -catenin (magenta) in deep cells and the EVL of 6 hpf embryos injected with different morpholinos or co-injected with PrP-1 morpholino and Fyn/Yes-EGFP mRNAs, encoding wildtype (WT) or constitutively active (CA) forms of the kinases. Scale bars indicate 10 μ m. **C.** Levels of AJ proteins detected by Western blot (WB) in extracts of 6 hpf control and Fyn/Yes double knockdown embryos. Red arrowhead: mature E-cadherin; black arrowhead: E-cadherin precursor. **D.** Recovery of the levels of AJ proteins in Fyn/Yes-rescued PrP-1 knockdown embryos (6 hpf), as detected by Western blot. E-cadherin isoforms are indicated as in C.

5.3 Fyn and Yes act downstream of PrP-1 to maintain embryonic AJ stability

Next, we verified whether zebrafish Fyn and Yes are downstream effectors of PrP-1 and could therefore rescue the PrP-1 knockdown phenotype. We tested for this genetic interaction by co-injecting zebrafish Fyn and Yes EGFP-tagged mRNAs into PrP-1 morphants. Since Fyn and Yes act cooperatively during gastrulation, the two mRNAs were injected together at equal amounts. To assess if the rescues were directly related to SFK enzymatic activity, we used wildtype (WT) and constitutively active (CA) forms of Fyn and Yes, the latter exhibiting higher kinase activity due to mutation of a negative regulatory site at Tyr527. Whole-mount immunostaining of 6 hpf embryos showed that both EGFP-tagged SFKs localized at the plasma membrane of deep cells and along cell contacts, as described in other cell types (Bjorge et al, 2000) (Figure 15D). Their rescuing ability was quantified by scoring embryonic phenotypes between 6 and 7.5 hpf (Fig. 15A and B). Co-injection of WT Fyn/Yes mRNAs at 75 pg/embryo significantly reduced the proportion of arrested/deformed morphant embryos (41% reduction, $p < 0.01$). Notably, CA Fyn/Yes mRNAs produced a more efficient rescue of the PrP-1 phenotype (64% reduction; $p < 0.01$) using less mRNA (6

pg/embryo) (Fig. 15A and B). The higher enzymatic activity of the CA constructs was confirmed using an antibody specific for SFKs phosphorylated at Tyr416 (Figure 16D). Phosphorylation at this site is indicative of a stable active conformation of SFKs (Brown & Cooper, 1996). The catalytic activity of exogenous Fyn and Yes was also reflected in increased levels of β -catenin phosphorylation at Tyr142, since active Fyn directly phosphorylates this residue and Yes promotes this activity of Fyn (Piedra et al, 2003). Interestingly, while PrP-1 knockdown caused an almost complete depletion of phospho-Tyr142 β -catenin in Western blots, overexpression of Fyn and Yes in PrP-1 morphants led to its recovery and even boosted its levels beyond those of control embryos (Figure 16D). Furthermore, PrP-1 knockdown embryos phenotypically rescued by Fyn and Yes expression exhibited restored plasma membrane localization and levels of E-cadherin and β -catenin at 6 hpf (Figure 16A and D). Altogether, these data indicate that Fyn and Yes function downstream of PrP-1 to promote AJ function.

5.4 PrP-1 modulates the levels and activation state of SFKs

Having identified Fyn and Yes as downstream effectors of PrP-1, we went on to examine how their function/activity would be regulated by PrP-1. SFKs can be regulated at several levels, including changes in their activation state (mediated by phosphorylation/dephosphorylation), as well as modulation of their cellular levels and subcellular localization (Roskoski, 2004). Western blot analyses of 6 hpf embryos revealed that PrP-1 morphants have reduced total levels of Src/Yes (65 kDa band, 29.77% reduction; $p < 0.05$) and Fyn (50 kDa band, 43.36% reduction; $p < 0.05$) compared to control embryos (Western blot and upper graph in Figure 17A). The reduction became even more pronounced at higher morpholino doses (Figure 17B), indicating that the levels of these SFKs are positively correlated with those of PrP-1. Interestingly, the lysosome inhibitor chloroquine, but not the proteasome blocker MG-132, restored the levels of Src/Yes in PrP-1 morphants, whereas Fyn levels did not respond to either treatment (Figure 17C). The recovery of Src/Yes levels was accompanied by a concomitant increase in phospho Tyr142 β -catenin levels, in agreement with the previously described phosphorylation of this β -catenin residue by SFKs (Figure 17C). Further analyses of whole-mount immunostainings showed that while SFK levels were reduced in 6 hpf morphants, their localization at or near the PM was not affected (Figure 17D; in green). Moreover, like the previously observed defects in AJ localization, the decrease in SFK immunofluorescence was primarily visible in deep cells and not the EVL (Figure 17D). These results show that PrP-1 does not influence the localization but rather the turnover of SFKs, partly by preventing their degradation in lysosomes. The observation that the Fyn levels of PrP-1 morphants were not restored by

degradation inhibitors suggests that PrP-1 affects the function of this kinase via different mechanisms, such as the regulation/modification of its biosynthesis.

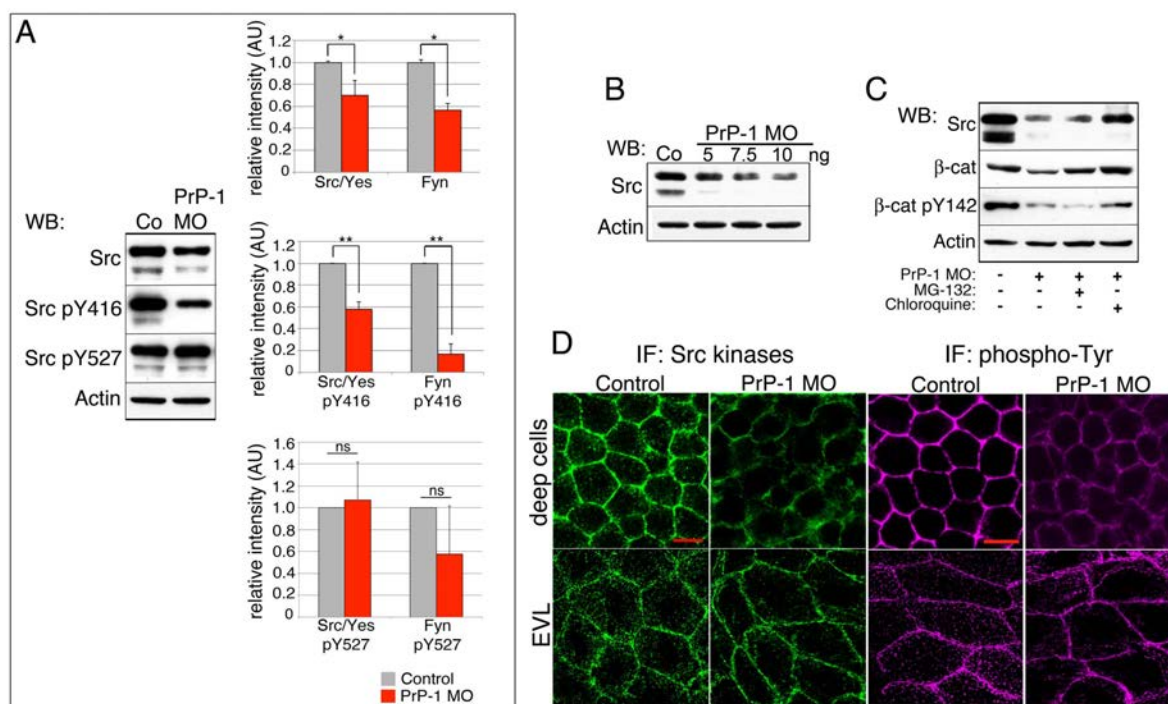


Figure 17 PrP-1 modulates SFK levels and activation. **A.** Detection of SFKs and their phosphorylated forms in 6 hpf embryo lysates by Western blot (WB; left) and densitometric quantification of bands (graphs; right); Values for phospho SFKs were normalized to those of total SFKs. Average values \pm SEM of four independent experiments are shown. Double asterisks (**) indicate $p < 0.01$ and single (*): $p = 0.1-0.05$ in unpaired two-tailed student's t-tests; ns=non significant. **B, C.** Western blot analysis of 6 hpf embryo extracts showing SFK levels after injection with different amounts of PrP-1 morpholino (B) and after treatment with proteasome and lysosome inhibitors (C). **D.** Immunofluorescence (IF) of SFKs (green) and phospho-tyrosine (magenta) in deep cells and the EVL of 6 hpf embryos. Control and PrP-1 knockdown embryos were scanned by the microscope laser using identical settings for comparability. Scale bar indicates 10 μ M.

We next asked whether the reduction of total SFK levels in PrP-1 morphants would correlate with changes in their activation state. SFK activity is directly regulated by phosphorylation of two tyrosine residues, which are highly conserved within the Src family: autophosphorylation of Tyr416 within the activation loop of SFKs renders them catalytically active, whereas C-terminal phosphorylation of Tyr527 inhibits their activity by locking them in a conformation in which autophosphorylation –and thus activation- cannot occur (Roskoski, 2005). We used phospho-specific antibodies against these two regulatory sites to compare the activation status of SFKs in control and morphant embryos via Western blot. These experiments revealed a significant decline in the ratios of activated (phospho Tyr416) vs. total Src/Yes and Fyn (44.28% and 83.29% reduction, respectively; $p < 0.01$) upon PrP-1 knockdown (Western blot and middle graph in Figure 17A). Notably, no significant changes were observed in the ratios of inactive (phospho Tyr527) vs. total Src/Yes and Fyn (Western blot and lower graph in Figure 17A), suggesting that PrP-1 preferentially modulates the turnover

of activated SFKs. Along with the decrease in phospho Tyr416 levels, overall tyrosine phosphorylation was reduced in the deep cells (and not the EVL) of PrP-1 morphants, which is consistent with decreased phosphorylation of multiple SFK substrates (Figure 17D; in magenta). Altogether, these results suggest that PrP-1 regulates SFKs either by modulating their phosphorylation, and/or by affecting the turnover of their activated forms.

5.5 PrP gain-of-function in the zebrafish embryo

Former experiments from our laboratory showed that overexpression of PrPs in the zebrafish embryo produced a clear gain-of-function phenotype associated with increased cell-cell adhesion. Notably, overexpression of EGFP-tagged mouse PrP, zebrafish PrP-1 or zebrafish PrP-2 induced identical phenotypes, characterized by a strong asymmetry of the blastoderm most prominent at 50% epiboly (6 hpf) (Málaga-Trillo et al., 2009 and Figure 18A). Aggregation assays indicated that cells derived from PrP-1 overexpressing embryos, contrary to PrP-1 morphants, have increased Ca²⁺-dependent cell-cell adhesion (see Introduction, paragraph 1.6).

Having identified the pathway by which PrP controls cell adhesion in the zebrafish gastrula, we set out to characterize the PrP overexpression (OE) phenotype more thoroughly. For this, we microinjected mRNAs coding for untagged zebrafish PrP-1 or mouse PrP with a 3F4 epitope (see Methods section) into one-cell stage embryos, and analyzed them at the morphological and molecular levels. As mentioned above, the blastoderm of these embryos forms asymmetrically due to the local accumulation of cells, leading to the unusually thickening of approximately ¼ of its surface (Figure 18A). This abnormal cell “aggregation” phenotype is already visible at 30% epiboly and occurs progressively on the dorsal side of the embryo, where the embryonic organizer (so-called “shield”) is normally formed (Figure 18A; red arrowheads in control embryo). The shield itself is a discrete accumulation of cells, formed at 50% epiboly (6 hpf) at the margin of the blastoderm by a coordinated convergence of cells from different regions of the gastrula. This structure gives rise to the dorsal structures of the embryo and at the same time is the basis for further migratory cell movements that will shape the dorsal/ventral and anterior/posterior axis. It is noteworthy that besides lacking a proper shield, PrP OE embryos die prematurely (before completion of gastrulation), as the massive accumulation of cells in the dorsal blastoderm causes mechanical stress and bursting of the embryo.

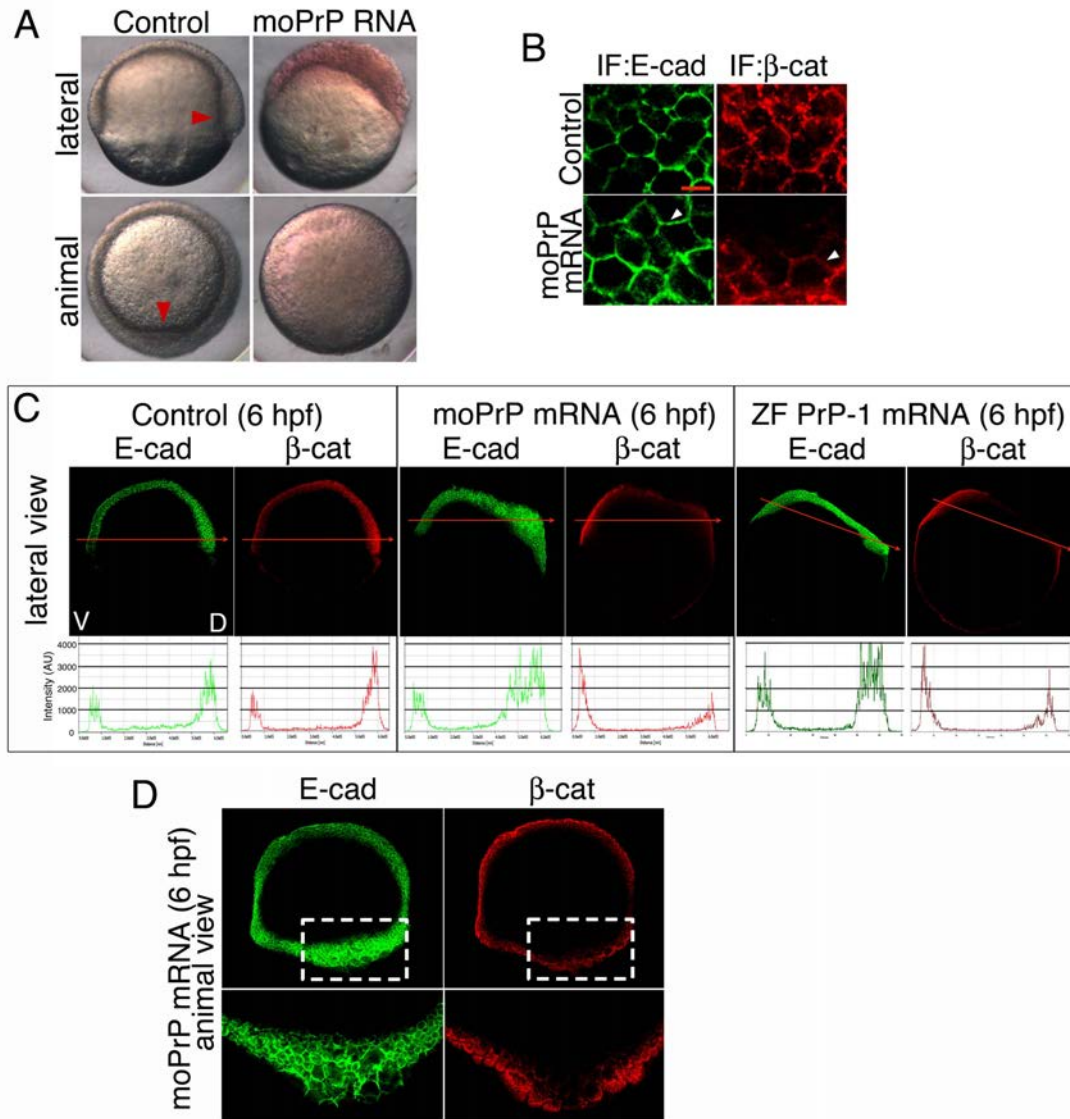


Figure 18 PrP OE embryos undergo asymmetric epiboly and altered distribution of E-cadherin and β -catenin along the dorsoventral axis. **A.** Lateral and animal views of embryos at the shield stage (6 hpf); red arrowheads indicate the position of the shield in control embryos. Mouse PrP OE induces abnormal asymmetric thickening of the blastoderm thus preventing proper shield formation. **B.** E-cadherin and β -catenin immunofluorescence (IF) in the deep cells of 6 hpf control and mouse PrP OE embryos. Arrowheads point at plasma membrane localization. Scale bar indicates 10 μ m. **C.** Whole 6 hpf embryos immunostained as indicated. Gastrula midsections are shown from a lateral or animal perspective. Graphs show fluorescence profiles along the ventral-dorsal axis (indicated by red arrows; V= ventral, D=dorsal); the fluorescence intensity along the red arrows is presented in arbitrary units (AU). **D.** Animal view of the midsection of a 6 hpf mouse PrP OE embryo, immunostained as indicated (up). The rectangular selection is presented at higher magnification (down) to show the aberrant morphology of dorsal deep cells.

To understand the molecular events leading to this phenotype we performed further experiments examining the localization and levels of AJ components, under the assumption that PrP gain-of-function would influence the same downstream targets identified in our PrP-1 loss-of-function experiments. We focused our analysis on the overexpression of mouse PrP and zebrafish PrP-1 because the first allows us to use the zebrafish to study the function of mammalian PrPs, while the latter has direct physiological relevance in the zebrafish blastula/gastrula. Given that PrP-1 knockdown impairs the stability of AJ

components at the plasma membrane, we reasoned that PrP OE would enhance their cell surface expression. In fact, 6 hpf embryos overexpressing mouse PrP showed normal distribution of E-cadherin and β -catenin along the plasma membrane (whole-mount immunostaining, Figure 18B). Consistent with the increased adhesiveness of PrP OE embryonic cells in aggregation assays (Málaga-Trillo et al, 2009), Western blot analyses revealed that mouse PrP OE leads to increased levels of mature E-cadherin in 6 hpf embryos (Figure 19A). Remarkably, unlike E-cadherin, β -catenin levels were reduced upon mouse PrP OE (Figure 19A-6 hpf and B), indicating that excessive levels of E-cadherin are enough to cause an increase in adhesion even when β -catenin is only available at sub-physiological levels. Of note, β -catenin levels could not be recovered upon co-injection of MG-132 or chloroquine (proteasome and lysosome inhibitors, respectively), suggesting that its biosynthesis rather than its degradation might be impaired in these embryos (Figure 19B). Given the asymmetric accumulation of cells in PrP OE gastrulae, we searched for potential alterations in the relative distribution of E-cadherin and β -catenin along embryonic axes. Fluorescence profiles of 6 hpf control embryos revealed a natural ventral to dorsal gradient of both proteins (Figure 18C). In contrast, mouse PrP and PrP-1 OE embryos exhibited increased dorsal E-cadherin accumulation and reduced dorsal β -catenin (Figure 18C). Concomitant with these alterations, dorsal cells appeared deformed and enlarged (Figure 18D). Thus, opposite changes in the levels and tissue distribution of E-cadherin and β -catenin accompany the aberrant morphology of PrP OE embryos.

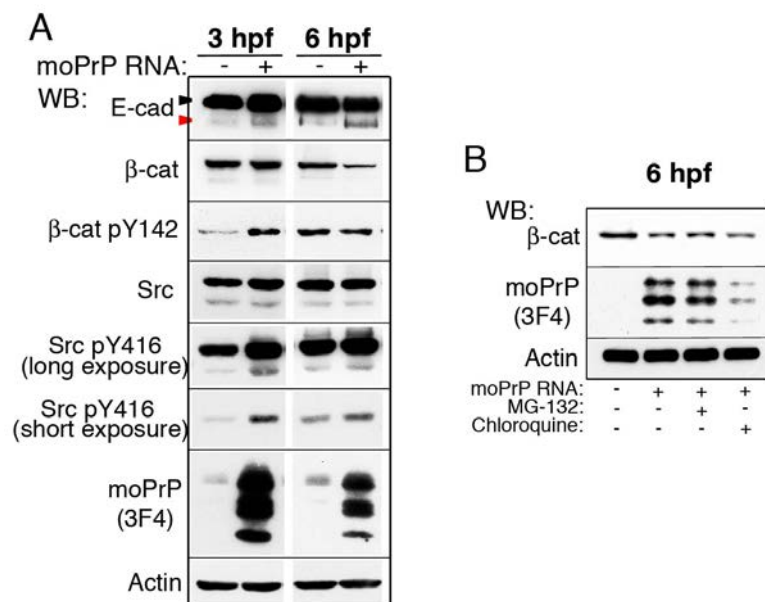


Figure 19 Biochemical changes in embryos expressing mouse PrP. **A.** Western blot (WB) analyses of extracts of 3 and 6 hpf embryos, showing changes in the levels of AJ proteins and SFK activation upon mouse PrP expression. **B.** Detection of β -catenin in lysates of 6 hpf embryos expressing mouse PrP and additionally injected with proteasome (MG132; 10 μ M) and lysosome (chloroquine; 100 μ M) inhibitors. Mouse PrP was detected in A and B with the 3F4 antibody.

The formation of the shield at 66pprox.. 6 hpf marks the appearance of the first visibly asymmetric structure in the zebrafish embryo (Montero et al, 2005). However, the determination of dorsoventral polarity (dorsal specification) begins as early as the 128-cell stage (2.25 hpf), when β -catenin enters the nuclei of a small group of marginal blastomeres to activate the transcription of dorsalizing genes such as *chordin*, *bozozok* or *dickkopf* (Schneider et al, 1996). The local expression of these, in turn, restricts the activity of proteins that induce ventral cell fates (Schier & Talbot, 2005). The lack of shield and reduced levels of dorsal β -catenin in 6 hpf PrP OE embryos suggested to us that PrP OE might disturb dorsal axis formation by depleting nuclear β -catenin at earlier stages. Therefore, we counted cells positive for β -catenin nuclear immunostaining at 3 hpf and found that their average number was ~ 7 in control embryos but only ~ 1.8 and ~ 2.5 in embryos overexpressing mouse PrP or zebrafish PrP-1, respectively (Figure 20A; $p < 0.001$ for both). These data indicate that the early nuclear function of β -catenin in these embryos was compromised as a result of increased PrP activity. Therefore, we went on to investigate the mechanism responsible for this effect.

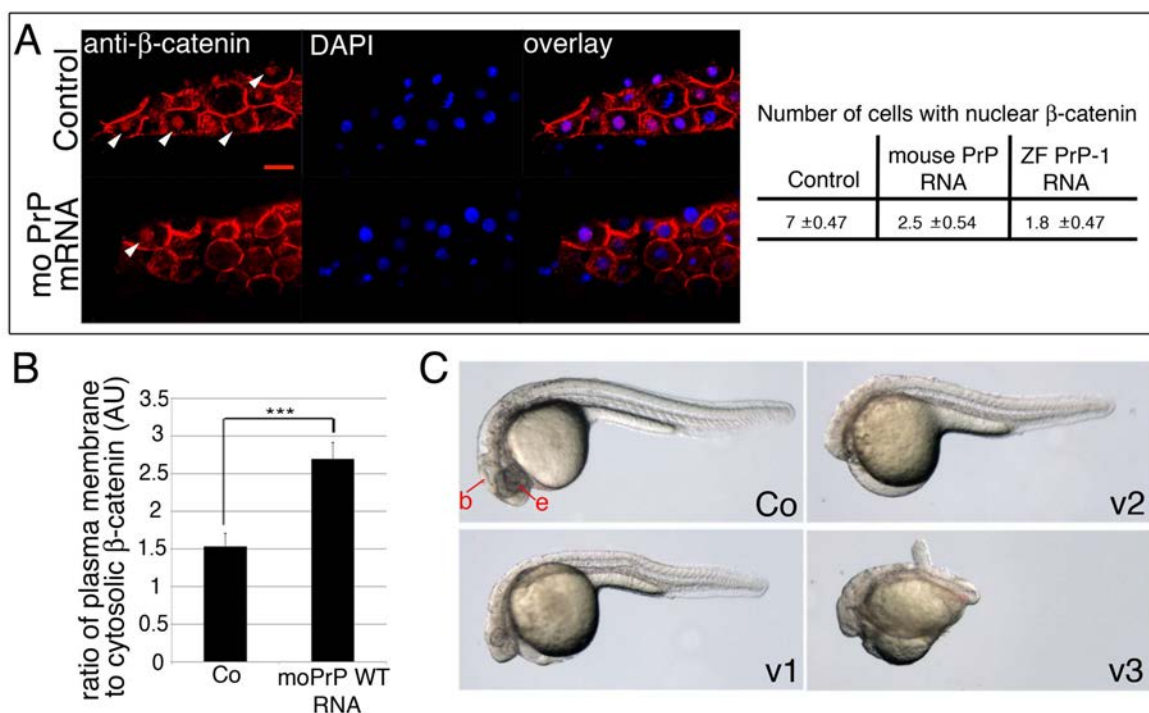


Figure 20 PrP overexpression prevents β -catenin nuclear localization and causes ventralized phenotypes in hypomorph embryos **A.** β -catenin immunofluorescence (red) in marginal blastomeres of 3 hpf embryos. Arrowheads point at nuclear β -catenin. Cell nuclei are counterstained with DAPI. Scale bar indicates $20 \mu\text{m}$. The table shows average numbers of cells positive for nuclear β -catenin per embryo \pm SEM from three independent experiments [$n=5$]. **B.** Ratios of plasma membrane to cytosolic β -catenin, as quantified with ImageJ from immunofluorescence images of dorsal blastomeres of 3 hpf embryos. Mean ratios \pm SEM are from 10 cells/embryo ($n=5$; three independent experiments). Triple asterisks (***) indicate $p < 0.001$ in unpaired two-tailed student's t-tests. **C.** Ventralized phenotypes (v1-3) of 1 dpf (=day post fertilization) embryos after injection with hypomorphic amounts of mouse PrP mRNA; b: brain, e: eye.

In mouse embryonic stem cells, E-cadherin binding can sequester β -catenin at the plasma membrane and prevent its nuclear translocation (Orsulic et al, 1999). We examined if a similar mechanism triggers the early (3 hpf) reduction of nuclear β -catenin upon PrP overexpression. Fittingly, the levels of mature membrane-bound E-cadherin were elevated in 3 hpf PrP OE embryos (Figure 19A), and moreover, fluorescence measurements indicated that the ratio of plasma membrane vs. cytosolic β -catenin was 1.8 times higher in PrP OE than in control cells (Figure 20B; $p < 0.001$). This difference was not due to cytosolic depletion of β -catenin, as control and PrP OE embryos showed comparable levels of this protein at 3 hpf (Figure 19A). Thus, the decay in the total levels of β -catenin seen at 6 hpf takes place subsequently to the reduction in its nuclear localization, not earlier than 3 hpf. These data suggest that a PrP-dependent increase in cell surface E-cadherin retains β -catenin at the plasma membrane, thereby antagonizing its early (nuclear) signaling role.

To further confirm that PrP OE impairs dorsal specification, we injected embryos with lower (halved) amounts of PrP mRNA, allowing them to overcome the early lethality phenotype. Such hypomorphic embryos develop beyond gastrulation and form primary organs. Typically, when nuclear β -catenin is depleted, dorsal and anterior organs are underdeveloped, whereas expression of proteins characteristic for ventral tissues appears expanded (“ventralization”) (Schier & Talbot, 2005). Indeed, mouse PrP-expressing hypomorphic embryos at 1 dpf (day post fertilization) showed defects in dorsal and anterior structures like the brain, eyes and anterior notochord (Figure 20C). The ventralized phenotypes varied in strength, ranging from reduced eyes and brains to completely undifferentiated heads and shortened anterior-posterior axes. These observations support the notion that PrP OE impairs axis formation by indirectly shifting the balance between the adhesive and signaling roles of β -catenin.

Finally, we asked if –like the PrP-1 knockdown phenotype- the PrP OE phenotype is mediated by SFKs. Western blots of 3 hpf embryos revealed that the total SFK levels upon PrP OE were normal but those of activated SFKs were elevated (Figure 19A). The higher SFK activity in these embryos was also evident from the corresponding increase in the levels of phospho Tyr142 β -catenin (Figure 19A). Moreover, blocking SFK activity with the inhibitor PP2, but not its inactive analog PP3, reduced the proportion of 6 hpf PrP OE embryos with abnormal morphology from 83.26% to 49.97% (Figure 21A; $p < 0.01$). Interestingly, SFKs and E-cadherin share a soft gradient-like distribution along the 3 hpf embryo (Figure 21B) that becomes enhanced upon PrP overexpression, suggesting that PrP-dependent overactivation of a pre-existing dorsoventral gradient of SFKs could cause the abnormal dorsal accumulation of E-cadherin at 6 hpf.

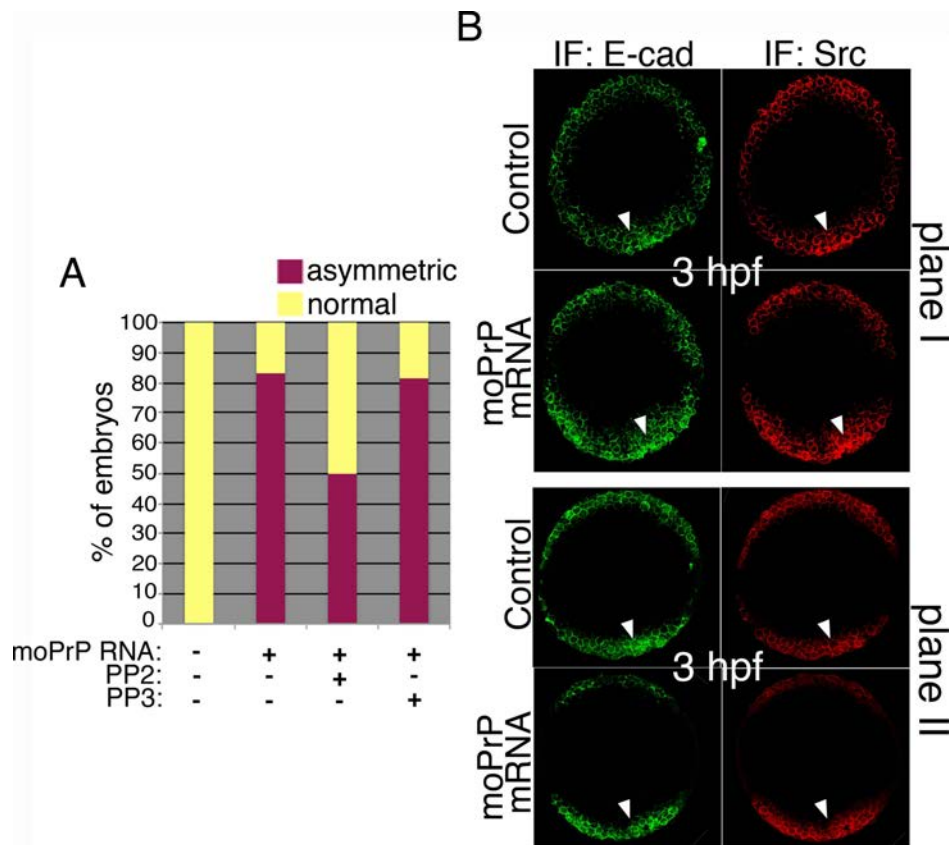


Figure 21 SFKs mediate the PrP OE phenotype. **A.** Quantification of embryos with abnormal dorsoventral asymmetry at 6 hpf after injection with mouse PrP mRNA alone, or mouse PrP mRNA together with SFK inhibitor PP2 or inactive analog PP3 (5 μ M). **B.** Blastula midsections of 3 hpf embryos (two different planes from animal view), immunostained as indicated (IF: immunofluorescence); arrowheads point at areas of increased immunofluorescence.

5.6 PrP expression triggers SFK activation and translocation to cell-cell contacts in human MCF-7 cells

As a next step, we asked whether the above link between fish or mammalian PrPs and SFK activation could be confirmed in a mammalian cell model. For this, we used human mammary cancer cells (MCF-7), which form E-cadherin-dependent cell-cell contacts and are an established cell culture model for the study of AJs. Our aim was to determine whether expression of zebrafish or mouse PrPs would trigger alterations in the activation or localization of SFKs, and if so, whether these would correlate with changes in the levels/localization of AJ components, as observed in zebrafish embryos. In order to visualize exogenous PrP expression, we used EGFP-tagged versions of these proteins (described in detail in the next paragraph and in Figure 23). Plasmids encoding EGFP-mouse PrP, -PrP-1, -PrP-2, or EGFP alone as a control were transfected into MCF-7 cells, which were then analyzed by Western blot or immunofluorescence. All three PrPs, but not EGFP alone, localized at cell-cell contact sites showing subtle differences in their distribution patterns (Figure 22B; also see next paragraph). Western blot analysis confirmed the expression of

the constructs and showed that the expression of zebrafish or mouse PrPs leads to increased levels of phospho Tyr416 SFKs, here detected as a single band of approximately 60 kDa (Figure 22A). Total SFK levels remained largely unaffected by PrP expression, with the exception of zebrafish PrP-1-transfected cells, where a slight increase was evident (Figure 22A).

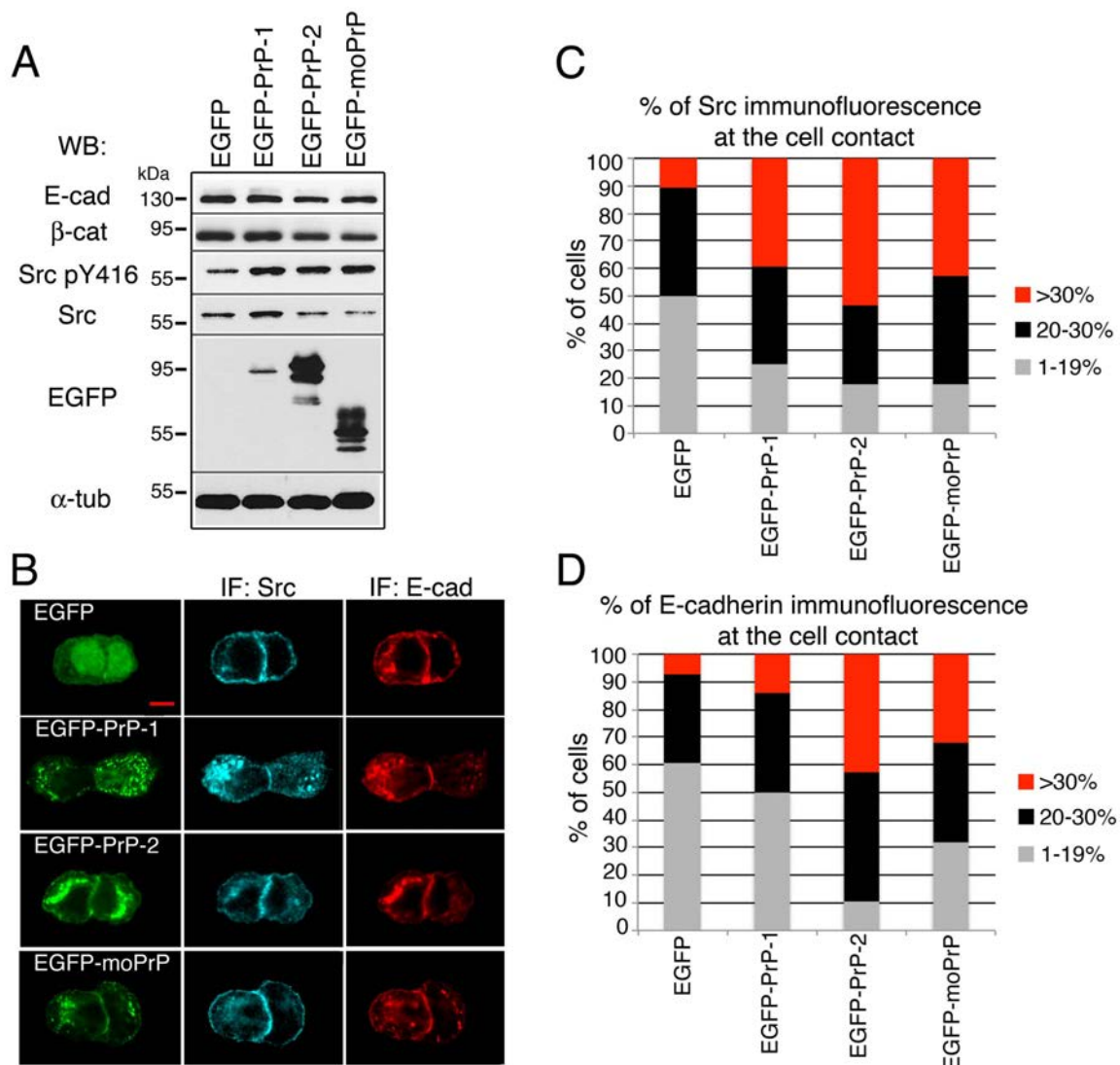


Figure 22 Changes in Src kinase and E-cadherin regulation upon expression of mouse and zebrafish PrPs in MCF-7 cells. **A.** Western blot analysis with lysates of MCF-7 cells expressing EGFP-tagged PrPs. Multiple bands detected by the anti-EGFP antibody represent the un-, mono- and double glycosylated forms of PrP. EGFP-PrP-1 expression levels are too low to discern all isoforms. **B.** Subcellular distribution of EGFP-PrPs, Src and E-cadherin immunofluorescence (IF) in MCF-7 cells. Scale bar = 10 μ M. **C-D.** Quantification of Src and E-cadherin IF at contact sites of MCF-7 cells. Only cell doublets were used for IF quantification with Image J. Graphs display percentages of cells with different percentages of Src/E-cadherin IF at cell contact sites (average values of three experiments for Src; n=30; average values of one experiment for E-cadherin; n=30). Values were normalized to whole cell Src/E-cadherin IF.

We also examined whether the observed PrP-dependent increase in SFK enzymatic activity would be accompanied by changes in their subcellular localization pattern. Since virtually all cells in the zebrafish embryonic tissue make contact with other cells, a putative redistribution

of SFKs from the whole plasma membrane to cell contact sites upon PrP overexpression is difficult to distinguish in this system. Therefore, we addressed this question using MCF-7 cells sharing a single cell-contact. Immunostainings of MCF-7 cell pairs showed that SFKs tend to accumulate at contact sites regardless of whether the cells express PrP-EGFP or only EGFP (Figure 22B). However, when we quantified SFK immunofluorescence at contact sites vs. within the entire cell, it became clear that cells expressing mouse or zebrafish PrPs had a higher percentage of SFKs localized at cell contacts than those expressing only EGFP. Concretely, most control (EGFP-transfected) cells had <19% of SFKs localized at the cell contact site, whereas the majority of PrP-transfected cells had over 30% of their total SFKs positioned at the contact. Hence, the increased SFK activity observed upon zebrafish or mouse PrP expression in MCF-7 cells is accompanied by a partial translocation of SFKs to cell-cell contacts.

The above findings raised the question whether the increased SFK activity triggered by PrP expression would result in or be concomitant with changes in AJ regulation. Western blot analysis showed no consistent changes in the levels of E-cadherin or β -catenin in PrP expressing cells (Figure 22A). However, preliminary quantification of E-cadherin immunofluorescence suggested that its presence at cell contacts is reinforced upon PrP expression. This effect was clearly distinguishable for zebrafish PrP-2 and mouse PrP and less prominent for zebrafish PrP-1 (Figure 22D). Concretely, the number of cells with over 20% total E-cadherin at the cell contact was increased by 11% in PrP-1, 50% in PrP-2 and 29% in mouse PrP expressing cells compared to EGFP-transfected control cells, respectively. However, given that EGFP-PrP-1 expression levels were lower compared to PrP-2 and mouse PrP and taking into account the preliminary nature of the data (only data from one experiment available), further experiments are necessary to confirm this result.

Altogether, our data in zebrafish embryos and MCF-7 cells point at the positive regulation of SFK activity and AJ function by PrP *in vivo* and *in vitro*. In addition, our results in MCF-7 cells demonstrate that besides SFK activity and levels, PrP also supports their localization at cell-cell contacts sites.

5.7 Contribution of PrP domains and glycosylation to PrP localization and regulation of E-cadherin based cell-cell adhesion (Solis et al, 2013)

Although the roles of different PrP domains in the biosynthesis and turnover of the protein are relatively well characterized (see Introduction, paragraph 1.3), little is known about how they modulate cellular functions of PrP. To assess this question, our laboratory generated different PrP mutants and tested their ability to localize at cell-cell contacts and support cell-

cell communication in zebrafish embryos, *Drosophila* S2 and human MCF-7 cells (Solis et al, 2013). While all three models were used to compare the subcellular expression patterns of the mutants, the zebrafish gastrula additionally served to evaluate their functionality *in vivo*, as both zebrafish PrPs and mouse PrP modulate cell-cell adhesion in this system (Málaga-Trillo et al, 2009). Importantly, using two different cell lines allowed us to analyze the behavior of our PrP constructs in cells with different adhesive properties: 1) cells devoid of adhesion molecules but able to form new contacts induced by PrP homophilic interactions on opposing cell membranes (S2 cells), and 2) cells with established E-cadherin-dependent contacts (MCF-7 cells). The mouse and zebrafish PrP mutants used for these experiments included PrP Δ Rep (Rep=repetitive region), Δ Hyd (HD=hydrophobic domain), Δ Glob (Glob=globular domain), Δ Core (lacking the whole protein core from the beginning of the repetitive to the end of the globular domain), GPI⁻ (lacking the GPI anchor attachment signal) and Glyc⁻ (deficient of glycosylation due to point mutations of glycosylation sites) (Figure 23). For visualization purposes, all constructs were tagged with an EGFP moiety positioned downstream of the N-terminal signal peptide and the adjacent polybasic region. The exact positions of the evolutionary conserved domains in PrP-1 and -2 were defined based on fish-to mammal sequence comparisons (Rivera-Milla et al, 2006). Here I will focus on our findings in MCF-7 cells and zebrafish embryos, since they are the ones most relevant to the role of PrP in E-cadherin-mediated cell adhesion. My contribution to this work consisted in conducting and evaluating the mRNA rescue experiments in PrP-1 morphants.

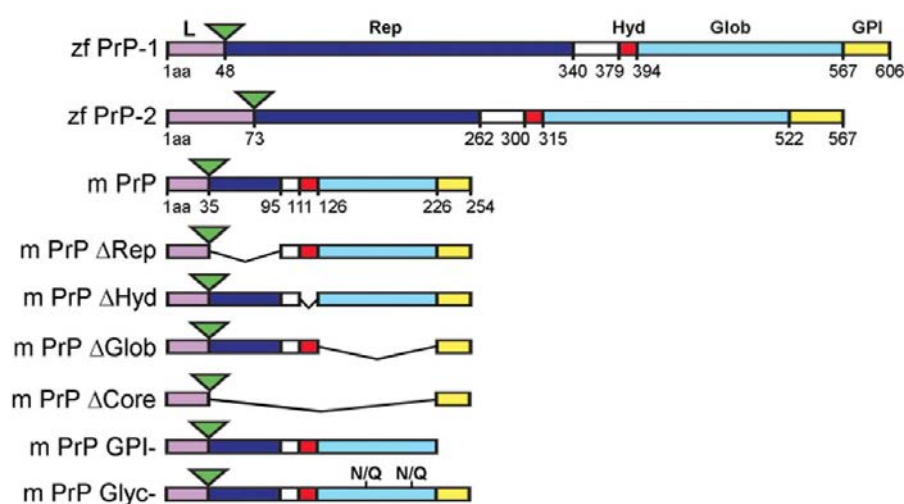


Figure 23 EGFP-tagged PrP constructs used in this study. The structural domains of zebrafish (zf) PrP-1, PrP-2 and mouse (m) PrP are represented as follows: leader peptide containing the polybasic motif (L) in violet, repetitive domain (Rep) in blue, hydrophobic region (Hyd) in red, globular domain (Glob) in light blue and GPI anchored signal (GPI) in yellow. Amino acid (aa) positions of mouse and fish PrP domains are indicated. The EGFP fluorescence tags are depicted as green triangles. Deletion constructs lacking Rep (Δ Rep), Hyd (Δ Hyd), Glob (Δ Glob), Rep+Hyd+Glob (Δ Core), GPI (GPI⁻) and N-glycosylation sites (Glyc⁻) are shown for mouse PrP only. Glycosylation sites in mouse PrP (residues 180 and 196) were mutated from asparagine to glutamine; zebrafish PrP glycosylation mutants carried respective mutations at residues 509 and 514 (PrP-1), and 438 and 443 (PrP-2). PrP domains were defined by evolutionary criteria. From Solis *et al* 2013, *PLoS one* 8: e70327 (modified)

Differential subcellular localization of PrP deletion mutants in MCF-7 cells

Our localization analyses in MCF-7 cells revealed that the mouse PrP and zebrafish PrP-2 constructs localize similarly (Figure 24A; mouse PrP is shown): While the full length/WT proteins accumulated homogeneously along cell-cell contacts, constructs lacking the globular domain, the GPI anchor or glycosylation displayed poor or no localization at these sites. On the other hand, deletion of the repetitive or hydrophobic domain did not alter the normal localization of the proteins. Interestingly, the Δ Core constructs of mouse PrP and PrP-2 (consisting of only the GPI anchor signal) localized normally along cell contacts, indicating that the GPI anchor signal is necessary and sufficient to target the constructs to cell contact sites. The observation that the Δ Glob and Δ Rep localize so differently despite having a functional GPI anchor signal suggests that a complex interplay between PrP domains modifies its positioning at specific sites of the plasma membrane. Unlike mouse PrP or PrP-2, the WT PrP-1 construct was expressed in distinct small clusters along cell-cell contacts (Figure 24B). Surprisingly, the formation of such discrete clusters was completely abrogated upon deletion of the repetitive domain or the whole protein core, resulting in the homogeneous distribution of the protein along cell contacts. The local accumulation of the WT PrP-1 construct in small patches/dots along entire cell contacts indicates that the repetitive domain of PrP-1 -which is up to 1.5-fold and 4.8-fold longer than that of PrP-2 and mouse PrP, respectively- induces the discontinuous localization of the protein. Deletion of the hydrophobic region did not affect the local clustering of PrP-1 at cell contacts, whereas deletion/mutation of the globular, GPI or N-glycosylation sequences strongly reduced it. Altogether, these data suggest that in MCF-7 cells, the hydrophobic domain does not influence the accumulation of PrP at cell contacts, whereas the GPI anchor, N-glycosylation and the globular domain positively contribute to it.

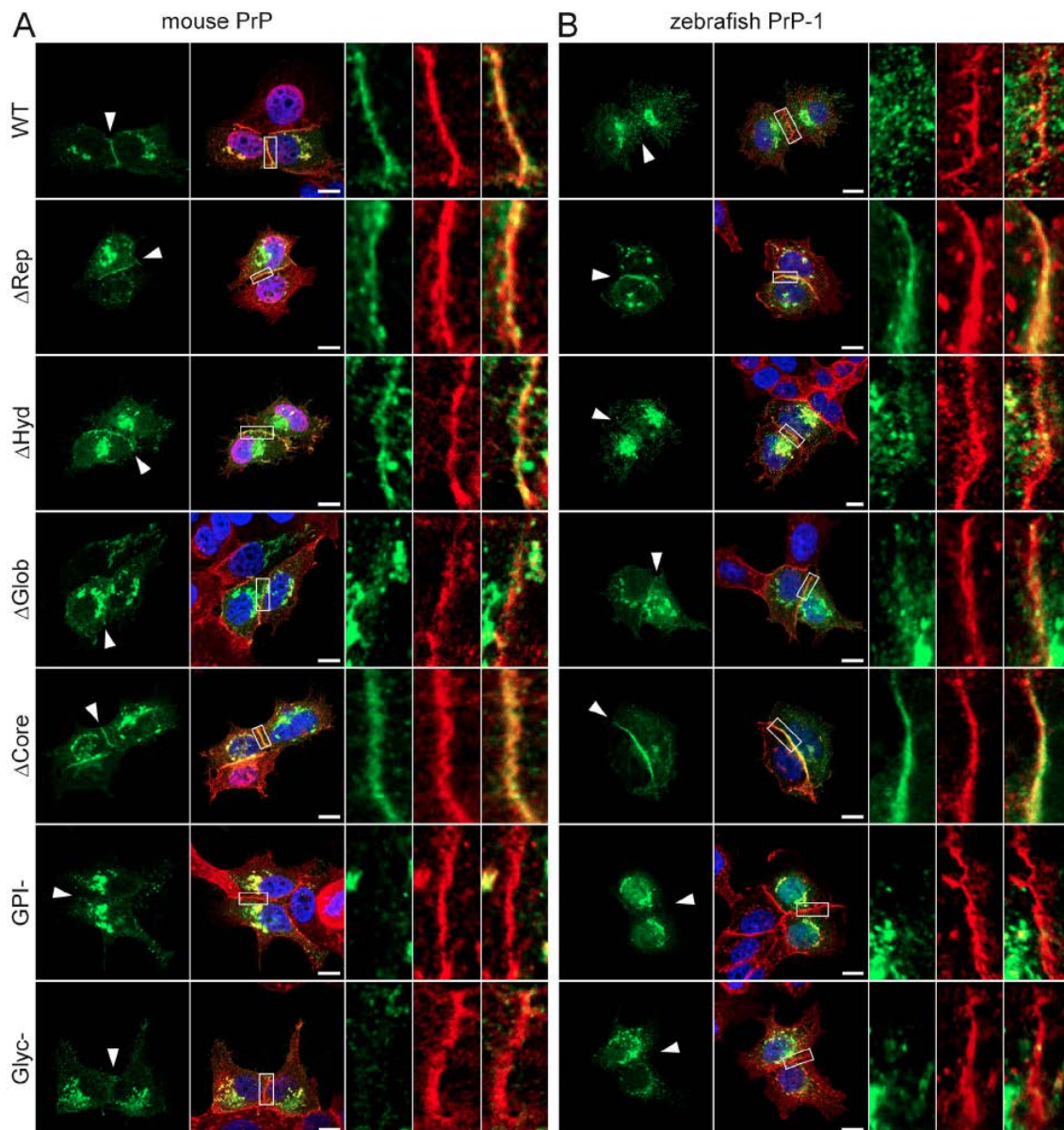


Figure 24 Accumulation of mouse and zebrafish PrP constructs at established MCF-7 cell-cell contacts. Wildtype (WT) and mutant EGFP-tagged constructs of mouse PrP (A) and zebrafish PrP-1 (B) localize differently at E-cadherin-positive cell contact sites (in red). Marked areas on the overlays are enlarged (right) to show detailed views of the contact sites. Cell nuclei are stained with DAPI (blue). Scale bars = 10 mm. From Solis *et al* 2013, *PLoS one* 8: e70327

Differential subcellular localization of PrP deletion mutants in zebrafish embryos

Comparable localization data for these WT and mutant PrP constructs were obtained from our analysis in 6 hpf zebrafish embryos (Solis *et al*, 2013). Although embryonic cells do not form polarized epithelia like MCF-7 cells, their tissue cohesion is also maintained by E-cadherin homophilic interactions. However, since embryonic cells naturally form a continuous tissue, most or all of their surfaces are in contact with adjacent cells, making it difficult to discern if proteins accumulate specifically at cell-cell contact sites or along the entire plasma membrane. Similar to our results in MCF-7 cells, exogenous WT mouse PrP

and PrP-2 were both distributed in a continuous pattern at the plasma membrane of 6 hpf embryonic deep cells (Figure 25A; data for mouse PrP are shown). Moreover, mouse PrP mutants behaved similarly to what we observed in MCF-7 cells (Figure 24). For instance, deletion of the repetitive or the hydrophobic region did not affect its continuous distribution along the plasma membrane (Figure 25B and C), while deletion of the globular domain caused the construct to accumulate in punctate structures at the plasma membrane (Figure 25D). At first glance, this result may suggest that the globular domain is essential for localization of PrP along the entire plasma membrane. However, we excluded this possibility because the mutant lacking the entire protein core (including the globular domain) localized like the WT protein (Figure 25E). Thus, the N-terminal leader peptide and C-terminal GPI anchor are sufficient to ensure continuous surface expression of PrP. Most likely, the repetitive or hydrophobic regions are responsible for the punctate distribution of the Δ Glob mutant, and the presence of the globular domain in the WT construct counteracts this effect. On the other hand, the GPI anchorless and unglycosylated constructs were expressed poorly at the plasma membrane, accumulating instead intracellularly (Figure 25F and G). The localization patterns of these mutants confirm that the GPI anchor is necessary for tethering PrP to the plasma membrane *in vivo*, and further indicate that N-glycosylation plays an important role during trafficking of PrP to cell contact sites and more generally, to the plasma membrane. As in MCF-7 cells, the effects of the various deletions on the localization of PrP-2 were strikingly similar to those observed for mouse PrP. Particularly, removal of the globular domain, GPI anchor and glycosyl residues caused the same distinct effects on PrP-2 localization (not shown).

On the other hand, the localization analysis of PrP-1 constructs revealed interesting differences and similarities to mouse PrP and zebrafish PrP-2. Unlike these, and similar to our observations in MCF-7 cells, WT PrP-1 displayed a discontinuous patchy distribution along the plasma membrane (Figure 25H). Deletion of the repetitive domain had the same effect on PrP-1 localization seen in MCF-7 cells, as the corresponding construct was expressed continuously along the plasma membrane (Figure 25I). These data further support the notion that the extensive repetitive domain of PrP-1 is required for its local accumulation in patches at the plasma membrane. Deletion of the PrP-1 hydrophobic region or the globular domain had the same effect as seen with mouse PrP and zebrafish PrP-2 constructs: lack of the hydrophobic region did not alter PrP-1's patchy localization (Figure 25J), whereas absence of the globular domain induced punctate accumulation of the protein at the plasma membrane (Figure 25K). Moreover, the latter effect was observed only when the repetitive domain was present (Δ Glob mutant) but not when the entire protein core was deleted (Δ Core mutant, Figure 25L). Together with the MCF-7 data, these results strongly suggest that the repetitive and globular domains exert opposing effects on the patterned

distribution of PrP within contact sites. Finally, as seen with mouse PrP and zebrafish PrP-2 constructs, lack of GPI anchoring or N-glycosylation also caused PrP-1 to localize poorly at the plasma membrane and remain intracellularly (Figure 25M and N). Extensive intracellular accumulation was observed particularly for the GPI anchorless mutant (Figure 25M).

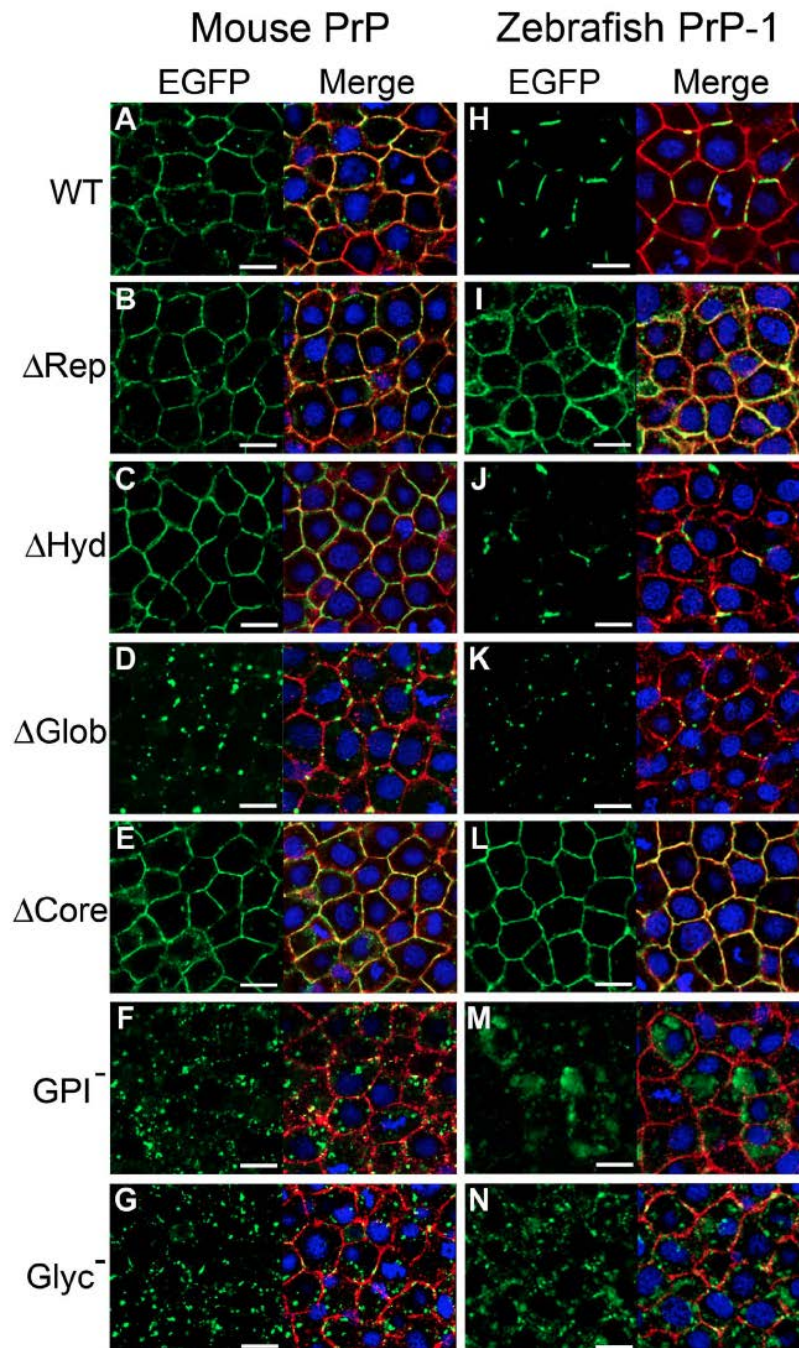


Figure 25 Localization of EGFP-tagged zebrafish PrP-1 constructs in the deep cells of early zebrafish embryos (6hpf). mRNAs encoding wildtype (WT) or mutant mouse PrP or zebrafish PrP-1 constructs were microinjected at the one-cell stage. Plasma membranes were double-counterstained using antibodies against phospho Tyr 416 Src and β -catenin (merged in red). Cell nuclei were stained with DAPI (blue). Scale bars = 10 μ m. From Solis *et al* 2013, *PLoS one* 8: e70327

Functional tests through rescue assays

To investigate the functional importance of PrP domains and posttranslational modifications, we tested the ability of our PrP constructs to rescue the PrP-1 embryonic knockdown phenotype. mRNAs coding for WT or mutant PrP-1 were co-injected together with PrP-1 morpholinos and the numbers of embryos with normal or arrested epiboly were scored at 6 hpf (50% epiboly). It is important to note that the morpholinos used do not block the expression of our synthetic mRNAs, since these do not contain the PrP-1 morpholino target sequence, located within the 5' UTR of the respective cellular mRNA. Unlike WT PrP-1 (77.15% rescued embryos; $p < 0.001$), the mutant constructs had a significantly reduced ability to revert the knockdown phenotype (Figure 26A). This reduction was more pronounced for the Δ Glob construct (no significant rescue) than for the Δ Rep construct (35.67% rescued embryos; $p < 0.001$). Similarly, mutation of the N-glycosylation sites led to a considerable decrease in rescuing activity (28.24% rescued embryos; $p < 0.001$), possibly due to the poor cell surface expression of the construct (Figure 26A).

In addition, we tested the ability of these constructs to specifically rescue the defect in E-cadherin-mediated cell adhesion. In line with the morphological evaluation, whole-mount immunostainings of 6 hpf embryos showed that WT PrP-1 mRNA could restore the normal surface localization of E-cadherin in PrP-1 knockdown embryos, whereas the Δ Rep, Δ Glob and Glyc⁻ mutants all largely failed to do so (Figure 26B). Interestingly, while deletions of the repetitive or globular domains had opposite effects on PrP-1 localization (continuous vs. punctate distributions at the plasma membrane, respectively), both of them negatively affected PrP-1 function in epiboly. Hence, the ability of PrP-1 to stabilize E-cadherin at cell contacts correlates with a specific pattern of expression at the plasma membrane, which appears to be dictated by the interplay between the repetitive and globular domains. Similarly, the largely intracellular localization of the N-glycosylation mutant correlates with its failure to restore E-cadherin at cell-cell contacts. Besides facilitating proper PrP-1 localization, however, these domains/modifications may also contribute to PrP-1 function by mediating interactions with other proteins, a possibility that was not addressed specifically in this study.

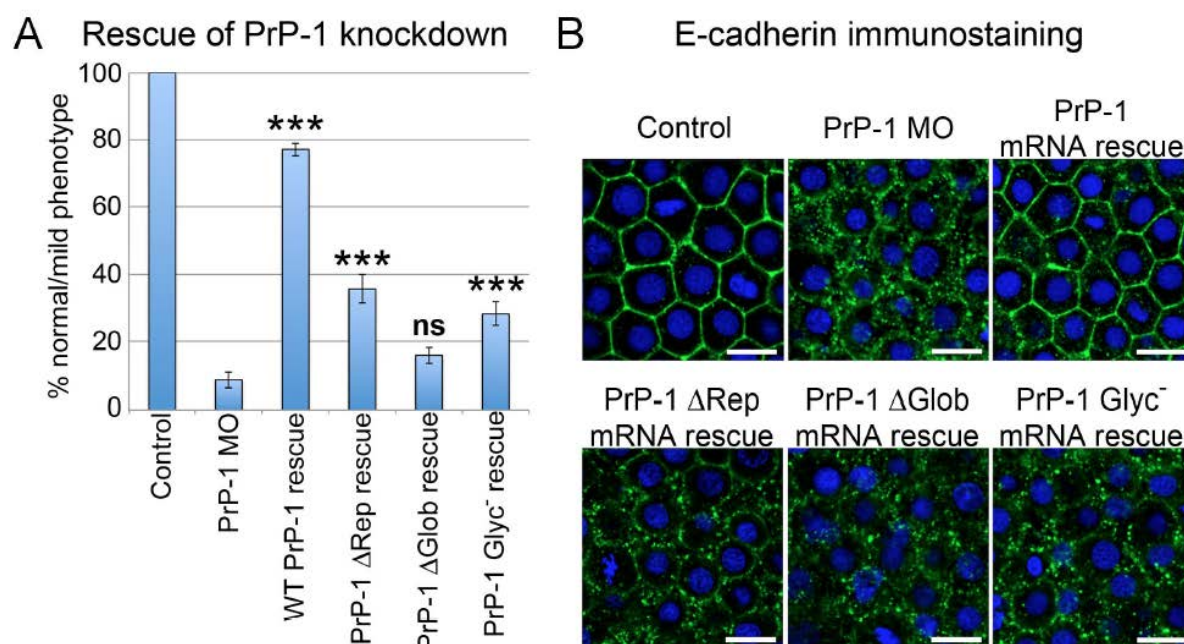


Figure 26 Rescue of PrP-1 knockdown embryos by mutant PrP-1 constructs. PrP-1 morphant embryos were microinjected with mRNAs encoding EGFP-tagged PrP-1 constructs, and their rescue activity was evaluated morphologically and molecularly. **A.** Quantitative differences in normal morphology between control, PrP-1 morphant embryos, and PrP-1 knockdown embryos expressing WT, Δ Rep, Δ Glob and Glyc⁻ PrP-1 constructs. Data are given as the proportion of embryos showing normal-to-mild gastrulation phenotypes at 6 hpf. Three independent experiments were analyzed (n=30). Triple asterisks (***) indicate statistically significant rescues at $p < 0.001$; one-way ANOVA test; error bars represent SEM. **B.** E-cadherin immunofluorescence in deep cells of 6 hpf embryos. Rescue is indicated by the recovery of E-cadherin plasma membrane localization. Scale bar=10 μ m. From Solis *et al* 2013, *PLoS one* 8: e70327

Functional tests through overexpression assays

To further assess the physiological relevance of these changes *in vivo*, we took advantage of the PrP gain-of-function phenotype, characterized by asymmetric epiboly at 6 hpf (Figure 27A), and asked how the mutations introduced in our constructs would affect this activity of PrPs. As a functional readout, we quantified the number of embryos showing OE phenotypes upon expression of each construct (Figure 27B-D). Interestingly, analogous deletions in mouse or zebrafish PrPs produced similar changes in their activity (Figure 27B-D). For instance, compared to WT constructs, all three mutants lacking the hydrophobic stretch retained significant activity (92%, 100% and 77% for mouse PrP, zebrafish PrP-2 and zebrafish PrP-1, respectively), whereas deletion of the globular or repetitive domains significantly reduced the ability of these mutants to cause the embryonic OE phenotype. Moreover, the activity of the globular domain mutants was consistently lower than that of mutants lacking the repetitive domain (31% vs 49% for mouse PrP, 17% vs 45% for zebrafish PrP-2 and 9% vs 24% for zebrafish PrP-1). On the other hand, mutants lacking the entire protein core were only minimally able to elicit OE phenotypes (14%, 10% and 6% activity for mouse PrP, zebrafish PrP-2 and zebrafish PrP-1, respectively). Notably, the levels of activity of unglycosylated PrPs were comparable to those of the Δ Glob mutants (37%, 24% and 21% for mouse PrP, zebrafish PrP-2 and zebrafish PrP-1 mutants,

respectively). Since PrP N-glycosylation sites are located within the globular domain, this result further indicates that sugar residues are key functional elements of this domain. Finally, GPI anchorless mutants showed residual levels of activity larger than those of Δ Core mutants (50%, 27% and 18% for mouse PrP, zebrafish PrP-2 and zebrafish PrP-1, respectively), suggesting that they carry out functional interactions (possibly with endogenous PrP-1) despite not being tethered to the plasma membrane.

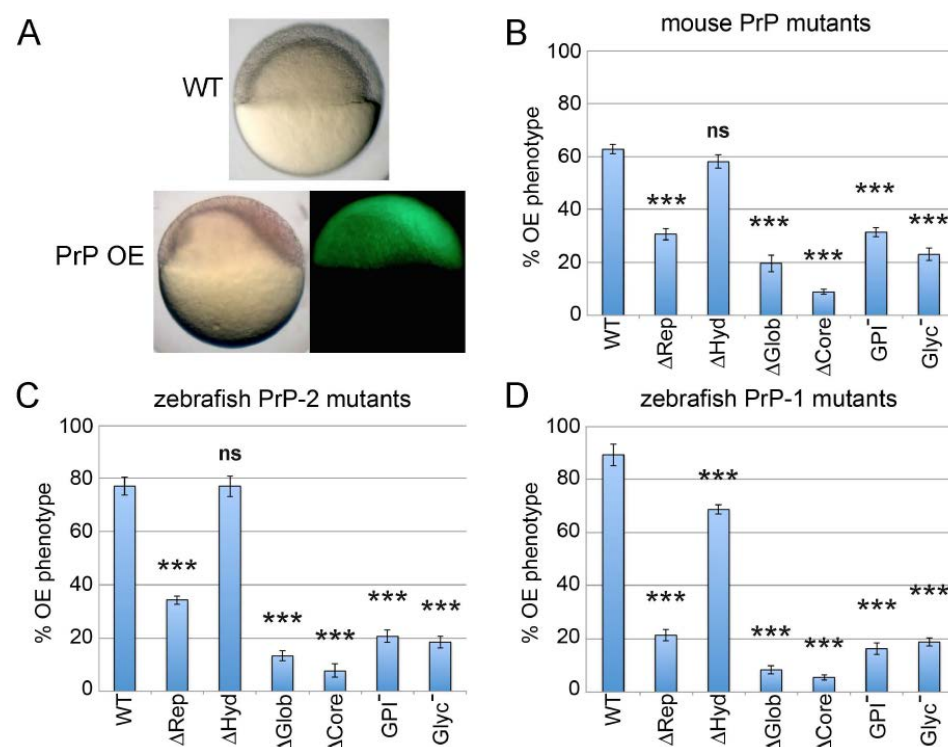


Figure 27 Overexpression (OE) of mouse and zebrafish PrP constructs in early zebrafish embryos. Embryos were microinjected with mRNAs encoding mouse or zebrafish EGFP-tagged PrP constructs. **A.** PrP gain-of-function phenotype characterized by asymmetric epiboly at 6 hpf (WT: wildtype/control embryo). **B–D.** Quantification of 6 hpf embryos exhibiting normal vs. asymmetric epiboly upon expression of different PrP constructs. Three independent experiments were analyzed (average $n=30$ embryos). Triple asterisks (***) indicate statistically significant reduction in activity at $p<0.001$; one-way ANOVA test; error bars represent SEM.

5.8 Functionality of neurotoxic mouse PrP mutants in zebrafish embryos

Earlier work in our lab showed that mouse PrP can partially revert the zebrafish PrP-1 knockdown phenotype (Málaga-Trillo et al, 2009). This experiment demonstrated that mammalian and fish PrPs share the ability to control zebrafish embryonic cell adhesion. Therefore, we decided to use the zebrafish gastrula as an experimental paradigm to assess the functionality of mammalian PrP mutants with established connections to neuronal disease, neurotoxicity and neuronal survival. This issue is important because most of these mutants are well characterized in terms of their tendency to misfold or cause disease, yet little is known about whether or how their pathogenic properties are related to alterations in

the physiological role of PrP. To address these pathophysiological issues, we expressed an array of different mouse PrP mutants in zebrafish embryos and analyzed their behavior relative to WT mouse PrP, in terms of a) their subcellular distribution, b) their ability to rescue the PrP-1 knockdown phenotype, and c) their ability to induce a gain-of-function phenotype. The following mouse PrP constructs were selected (Figure 28):

- A mutant carrying a short deletion in its N-terminal polybasic domain: PrP $\Delta 23-31$.
- A mutant lacking almost the entire hydrophobic region and 6 N-terminally adjacent residues (central region=CR): PrP $\Delta CR=\Delta 105-125$.
- A mutant carrying both the PrP $\Delta 23-31$ and $\Delta CR=\Delta 105-125$ deletions: PrP $\Delta 23-31/\Delta CR$.
- Mutants carrying large N-terminal deletions: PrP F35 ($\Delta 32-134$), PrP C3 ($\Delta 23-134$), PrP C1 fragment ($\Delta 23-111$).
- A mutant carrying an insertion of nine octapeptide repeats upstream of the five naturally existing ones, PrP PG14.

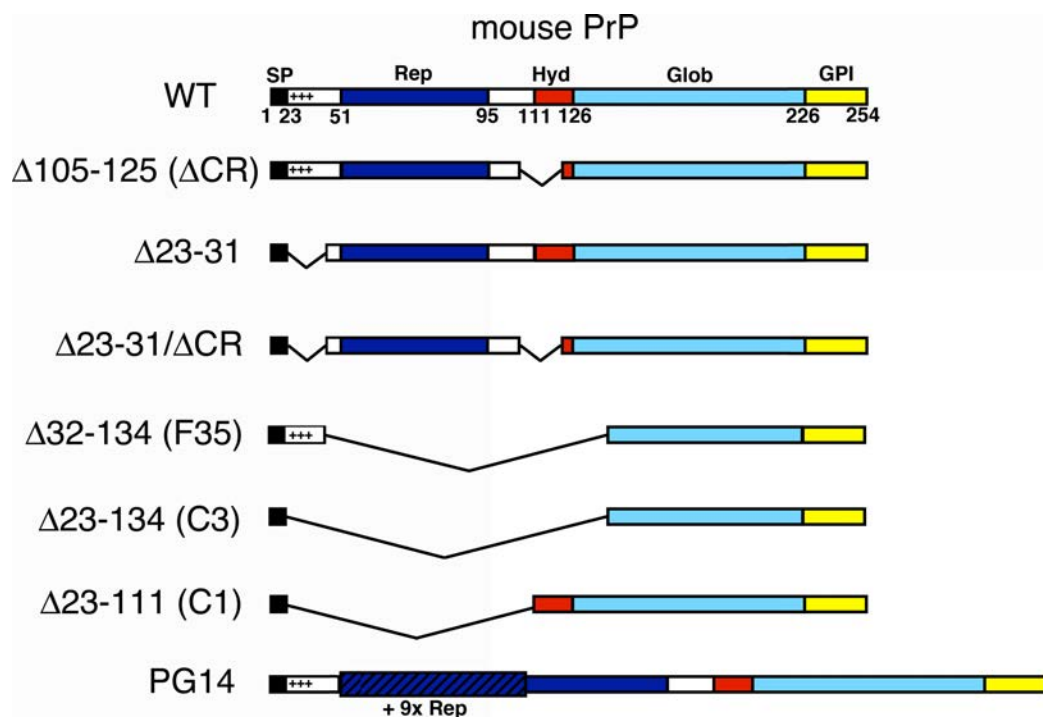


Figure 28 Mouse PrP mutants affecting neurotoxic and neuroprotective properties of PrP. The structural domains of mouse PrP are represented as follows: signal peptide (SP) in black, repetitive domain (Rep) in blue, hydrophobic region (Hyd) in red, globular domain (Glob) in light blue and GPI anchor signal (GPI) in yellow. Plus symbols indicate the N-terminal positively charged region. Numbers indicate amino acid positions.

Two of these PrP mutants - Δ CR and F35, both lacking the central region- cause neurodegeneration when expressed as transgenes in mice with a PrP^{0/0} (knockout) background, even though they do not misfold or form aggregates (Li et al, 2007; Shmerling et al, 1998). Interestingly, PrP Δ CR appears to exert its toxicity in neurons by inducing large, spontaneous ionic currents. This effect has been hypothesized to result from its ability to either form pores in the plasma membrane or to influence the activity of endogenous ion channels (Solomon et al, 2010a). Regardless of the precise mechanism involved, this increased ion permeability sensitizes neurons to glutamate-evoked Ca²⁺ influx and causes excitotoxic stress (Biasini et al, 2013). Notably, PrP Δ CR-induced ion inflow is not restricted to neurons, since a number of non-neuronal cell types expressing the construct (including human HEK and *Drosophila* Sf9 cells) experience similar ionic currents and become hypersensitive to cationic drugs like Zeocin or G418 (Massignan et al, 2009; Solomon et al, 2010a). Moreover, G113V, a neurodegeneration-associated point mutation in the central region of human PrP also triggers ionic currents *in vitro* (Solomon et al, 2010a). Based on these findings, the thesis was put forward that deletion of the central region somehow replicates the misfolding event that occurs during PrP^C to PrP^{Sc} conversion (Biasini et al, 2013). This scenario is valid considering that the central region undergoes major conformational change when PrP^{Sc} is formed (Holscher et al, 1998; Muramoto et al, 1996; Norstrom & Mastrianni, 2005). Hence, elucidating the molecular events involved in PrP toxicity might help us understand the mechanistic basis of prion-induced neurodegeneration.

The PrP Δ 23-31 mutant, which lacks the PrP N-terminal polybasic stretch, is very informative despite not being pathogenic. Interestingly, this mutant is -unlike WT PrP- unable to rescue the toxicity induced by PrP Δ CR or PrP F35. Moreover, deleting residues 23-31 in PrP Δ CR (Δ 105-125) or PrP F35 (Δ 32-134) curbs their toxicity. (also see Introduction, paragraph 1.6) (Solomon et al, 2011; Turnbaugh et al, 2011). These double mutants are referred to as Δ 23-31/ Δ CR and C3 (Δ 23-134), respectively. Altogether, the studies on the PrP Δ 23-31 mutant indicate that these residues control a basic activity of PrP responsible for its neurotoxic and neuroprotective roles. Interestingly, this short N-terminal polybasic stretch also modulates general cellular properties of PrP, like its endocytosis or its interaction with extracellular glycosaminoglycans (GAGs) (Pan et al, 2002; Shyng et al, 1995a; Shyng et al, 1995b; Sunyach et al, 2003). More recently, it was demonstrated that mice expressing a PrP Δ 23-31 transgene instead of WT PrP are unable to efficiently propagate prions and show only mild illness when infected with PrP^{Sc}. This effect, in turn, correlates with reduced binding of PrP^{Sc} to PrP Δ 23-31 (Turnbaugh et al, 2012). Therefore, residues 23-31 control not only the biological activity of PrP but also its tendency to misfold and convert.

A further PrP construct used in this study is C1 ($\Delta 23-111$), a fragment that is generated naturally from the constitutive proteolytic cleavage of PrP between residues 111 and 112 in brain and other tissues (Chen et al, 1995; Harris et al, 1993b; Vincent et al, 2000). C1 represents the C-terminal membrane-anchored product of the cleavage and, unlike F35, does not cause neurodegeneration in mice with a PrP^{0/0} background (Westergard et al, 2011a). This is likely due to its intact hydrophobic domain, the lack of which has been suggested to be the cause of toxicity triggered by PrP Δ CR and F35 (Westergard et al, 2011b). Like PrP $\Delta 23-31$, the C1 fragment is not a suitable substrate for PrP^{Sc} replication, since PrP null mice expressing a PrP C1 transgene do not become ill when infected with prions (Westergard et al, 2011a). Additionally, when expressed together with WT PrP, the C1 fragment has the ability to antagonize PrP^{Sc} formation in prion-infected mice (Westergard et al, 2011a).

The PrP PG14 construct used in this study is the mouse homologue of a natural mutant causing familial prion disease in humans. It contains an N-terminal insertion of 9 octarepeats, which causes PrP to misfold into so-called PrP^{Spon} (Spon=spontaneously formed) and aggregate, triggering neurodegeneration in transgenic mice (Chiesa et al, 1998). PrP^{Spon} is highly neurotoxic and shares several biochemical properties with PrP^{Sc}, it is however structurally different from it and is not infectious (Biasini et al, 2008; Chiesa et al, 2003).

Localization of mouse PrP mutants in zebrafish embryos

As it can be appreciated from the above overview, these mouse PrP mutants cover diverse aspects of PrP pathobiology. It was an important goal of my thesis to find out whether they could be used to test the hypothesis that neurotoxicity in prion-related disorders involves alterations in PrP function. We began by examining the subcellular distribution of these PrP mutants in zebrafish gastrulae, as this would allow us to control for potential dysfunction caused by abnormal trafficking or plasma membrane attachment. To this aim, we microinjected the corresponding synthetic mRNAs into one-cell stage embryos, fixed these at 6 hpf, and stained them with an antibody against mouse PrP (6H4). The plasma membrane was visualized by counterstaining the embryos for β -catenin. Whole-mount confocal analysis revealed that all PrP deletion constructs localized predominantly at the plasma membrane of deep cells. The typical continuous distribution of WT PrP along cell contacts was observed for all deletion mutants (Figure 29A-E), except for two -F35 ($\Delta 32-134$) and C3 ($\Delta 23-134$) (Figure 29F and G)- which exhibited a tendency to accumulate in patches of variable size. Remarkably, the discontinuous plasma membrane localization of F35 and C3 was accompanied by a similar effect on the distribution of β -catenin (Figure 29F and G). This stood in contrast to the even localization of β -catenin along the cell contacts of

control embryos or embryos expressing WT mouse PrP (Figure 29A). However, the abnormal β -catenin patches observed upon expression of PrP F35 or C3 did not overlap with those formed by F35 or C3 PrP themselves (arrows in Figure 29F and G).

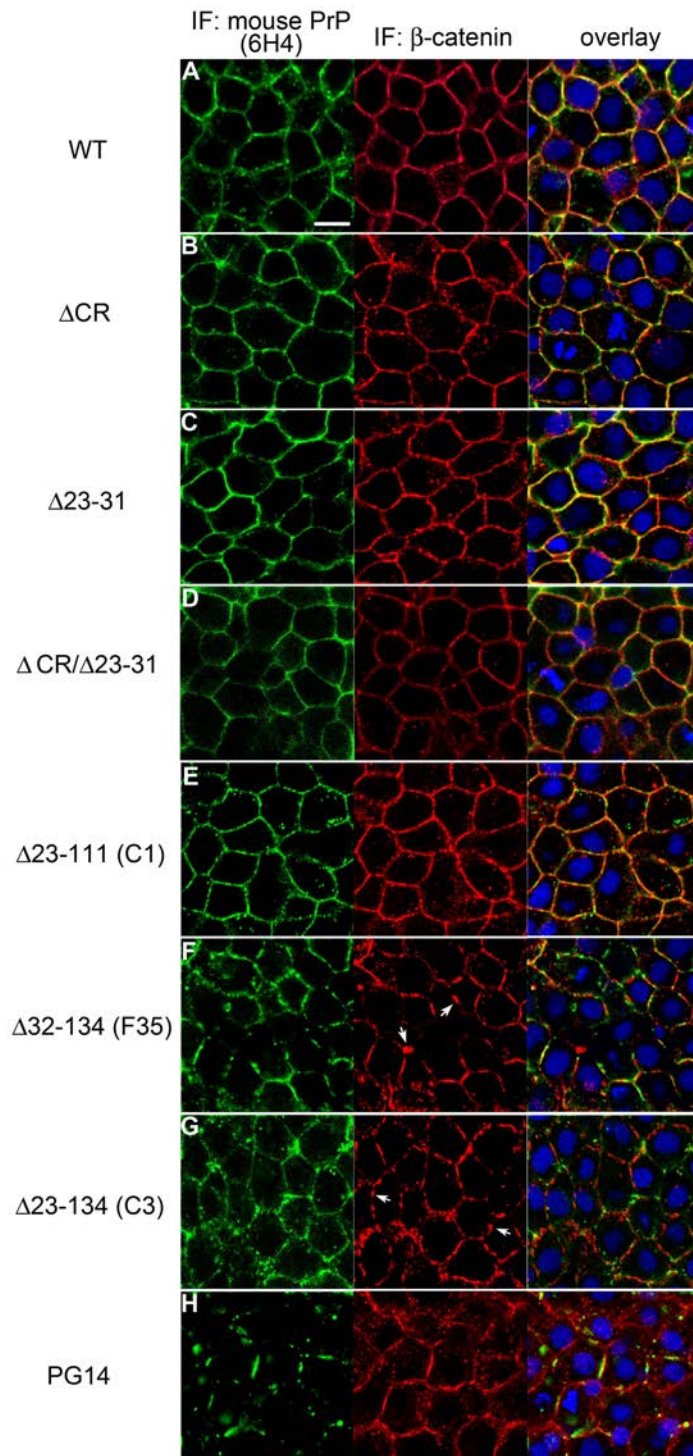


Figure 29 Localization of mouse PrP mutants in deep cells of 6 hpf embryos. IF: immunofluorescence. Mouse PrP constructs were detected with the anti-PrP 6H4 antibody and the plasma membrane was counterstained against β -catenin. Cell nuclei were stained with DAPI. Scale bar indicates 10 μ M.

Functional tests through rescue assays

We next examined the functionality of some of these mutants in the zebrafish gastrula. We focused this analysis on a subgroup of constructs consisting of Δ CR, Δ 23-31 and the double mutant Δ 23-31/ Δ CR PrP. After having verified that these localize correctly at the plasma membrane of embryonic deep cells (Figure 29), we titrated the amounts of the microinjected mRNAs to achieve comparable expression levels of all constructs (Figure 30A). The functional properties of the mutants were examined by testing their ability to revert the PrP-1 knockdown phenotype. For this, we co-injected the corresponding mRNAs together with PrP-1 morpholinos into fertilized eggs and scored embryonic phenotypes at 6 hpf. Notably, Δ CR rescued PrP-1 morphants as efficiently as WT PrP, whereas Δ 23-31 showed a ~74% reduction in rescue activity relative to WT PrP ($p < 0.01$). In addition, the mutant carrying both deletions (Δ CR/ Δ 23-31) behaved like the Δ 23-31 single mutant (Figure 30B).

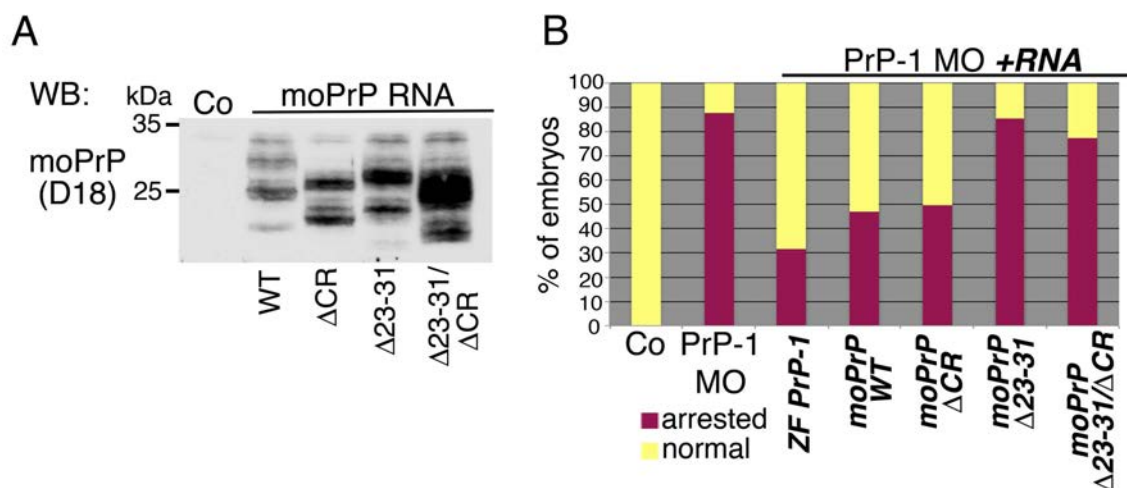


Figure 30 The N-terminal polybasic region is required for mouse PrP rescuing activity in zebrafish embryos. **A**. Detection of different mouse PrP (moPrP) constructs by Western blot (WB) in lysates of 6 hpf embryos using the D18 anti-PrP antibody. **B**. Quantification of 6 hpf embryos with normal or arrested epiboly after injection with PrP-1 morpholinos together with mRNAs encoding WT or mutant PrPs (ZF=zebrafish).

Functional tests through overexpression assays

Because both PrP-1 knockdown and PrP overexpression cause dramatic morphological effects, we reasoned that the accuracy of the above quantification may have been affected by the complexity of the combined phenotypes. To circumvent this problem, we confirmed these results in a simpler experimental setup, by testing the ability of the mutants to cause an overexpression phenotype. In these assays, WT and Δ CR constructs induced high and comparable proportions of embryos with asymmetric epiboly (~95%), whereas deletion of residues 23-31 reduced this effect by ~50% ($p < 0.001$ for Δ 23-31 and Δ 23-31/ Δ CR) (Figure 31A and B). Consistent with their ability to cause this phenotype, WT and Δ CR PrP showed decreased numbers of cells with nuclear β -catenin localization at 3 hpf (~2.5 and ~3.7 cells vs. 7 cells/embryo in control embryos), whereas β -catenin nuclear translocation was normal

in $\Delta 23-31$ and $\Delta 23-31/\Delta CR$ PrP OE embryos (~ 7.8 and ~ 7.7 cells/embryo with nuclear β -catenin, respectively) (Figure 31C). Therefore, the ability of mouse PrP to produce or revert zebrafish gastrulation phenotypes is modulated by residues 23-31 and not by the central region.

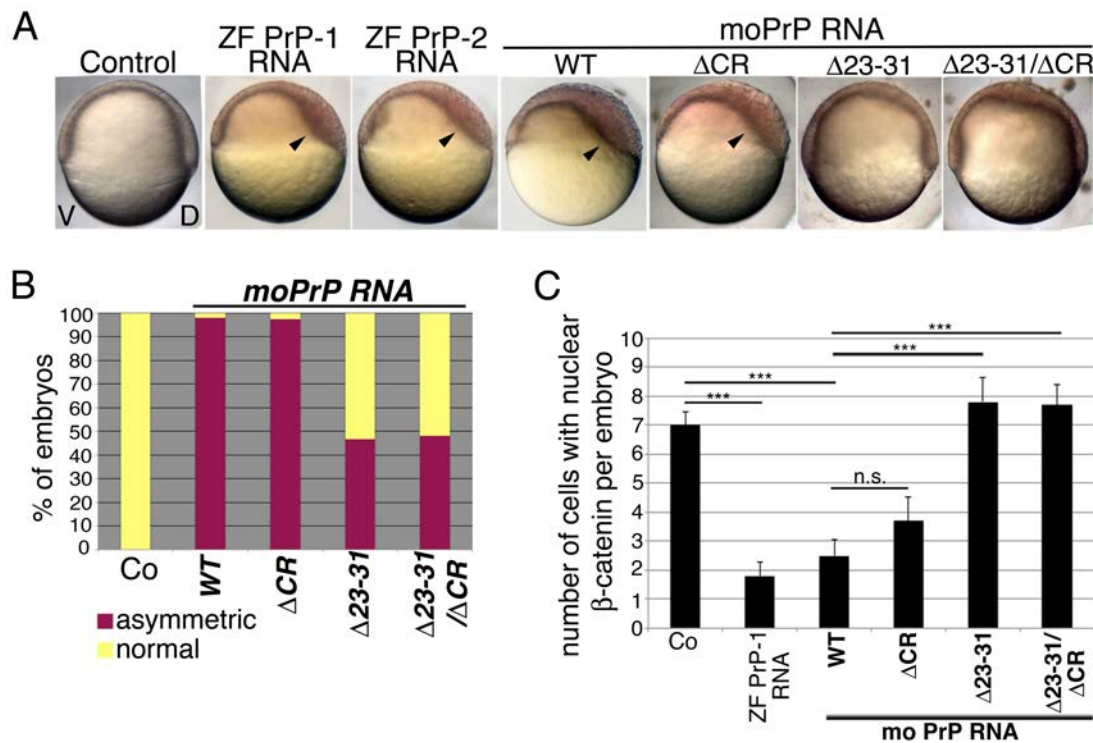


Figure 31 The ability of PrP to cause an OE phenotype depends on its N-terminal polybasic domain. **A.** Phenotypes of 6 hpf embryos after injection with RNAs encoding different PrP constructs (ZF=zebrafish; moPrP=mouse PrP). Arrowheads indicate the typical asymmetry of the PrP OE phenotype. V: ventral, D: dorsal. **B.** Quantification of embryos with normal vs. asymmetric epiboly at 6 hpf after injection with RNAs encoding different PrP constructs. **C.** Quantification of cells positive for β -catenin immunofluorescence in 3 hpf embryos, after injection with PrP RNAs. Triple asterisks (***) indicate $p < 0.001$ in unpaired two-tailed student's t-tests; ns=non significant.

Zebrafish ΔCR PrPs act cytotoxically in a drug-based cell assay

In mice, expression of PrP ΔCR in the absence of endogenous PrP (knockout background) leads to spontaneous neurodegeneration and neonatal lethality (Li et al, 2007). Importantly, in zebrafish embryos monitored up to 1 dpf, expression of mouse PrP ΔCR did not appear to cause added toxicity or lethality, irrespective of the presence or absence of endogenous PrP-1 (OE vs. rescue experiments, see paragraph above). This implied that, as in mice, either PrP ΔCR is not lethal at early embryonic stages of gastrulation or that the zebrafish altogether lacks the cellular components required for ΔCR toxicity to unfold. To find out whether the ability of the central region to control PrP-induced neurotoxicity is evolutionarily conserved, we generated ΔCR versions of zebrafish PrP-1 and -2 and tested them in an assay previously developed to evaluate ΔCR toxicity in cultured cells. In the so-called drug-

based cell assay (DBCA), expression of PrP Δ CR causes cultured HEK cells to become abnormally permeable to cytotoxic cationic drugs and undergo non-apoptotic cell death (Christensen et al, 2010; Massignan et al, 2009). Common examples of such drugs are Zeocin and G418, which are routinely used for the selection of stably transfected cells. Since HEK cells normally do not express PrP at detectable levels, endogenous (WT) PrP is not expected to block the toxic effect. We tested the potential of zebrafish Δ CR PrPs to cause drug-induced cell death by expressing them and their WT counterparts in HEK293 cells and incubating the cells overnight with 0.5 mg/ml Zeocin. Cell viability was then assessed by measuring the percentage of cells able to metabolize (3-(4,5-dimethylthiazol-2-yl)-2,5-diphenyltetrazolium bromide (MTT), a tetrazolium dye that can act as a substrate for mitochondrial oxidoreductase enzymes. In healthy cells, the latter reduce naturally yellow MTT to a purple formazan product, whose OD can be measured at a wavelength of 550-600 nm. Mouse PrP WT and Δ CR constructs were used in this assay as negative and positive controls for toxicity, respectively. Western blot analysis of HEK cell lysates with antibodies against zebrafish PrP-1 and/or -2, or mouse PrP indicated that all PrP Δ CR constructs were expressed at comparable levels to their WT equivalents (Figure 32A-C). Notably, upon incubation with Zeocin, cells expressing either zebrafish or mouse Δ CR PrPs showed significantly reduced MTT metabolic activity than those expressing WT PrPs (Figure 32D; 20%, 40% and 45% reduction for PrP-1-, PrP-2- and mouse PrP-expressing cells; $p < 0.05$, $p = 0.01$, and $p = 0.01$, respectively). Given that PrP Δ CR has not been reported to affect cell proliferation, these data strongly suggest that –like mouse PrP Δ CR - zebrafish Δ CR PrPs behave cytotoxicity in the DBCA. From these experiments we concluded that the role of the central region as suppressor of cytotoxicity is conserved from fish to mammals but not deployed during early zebrafish development.

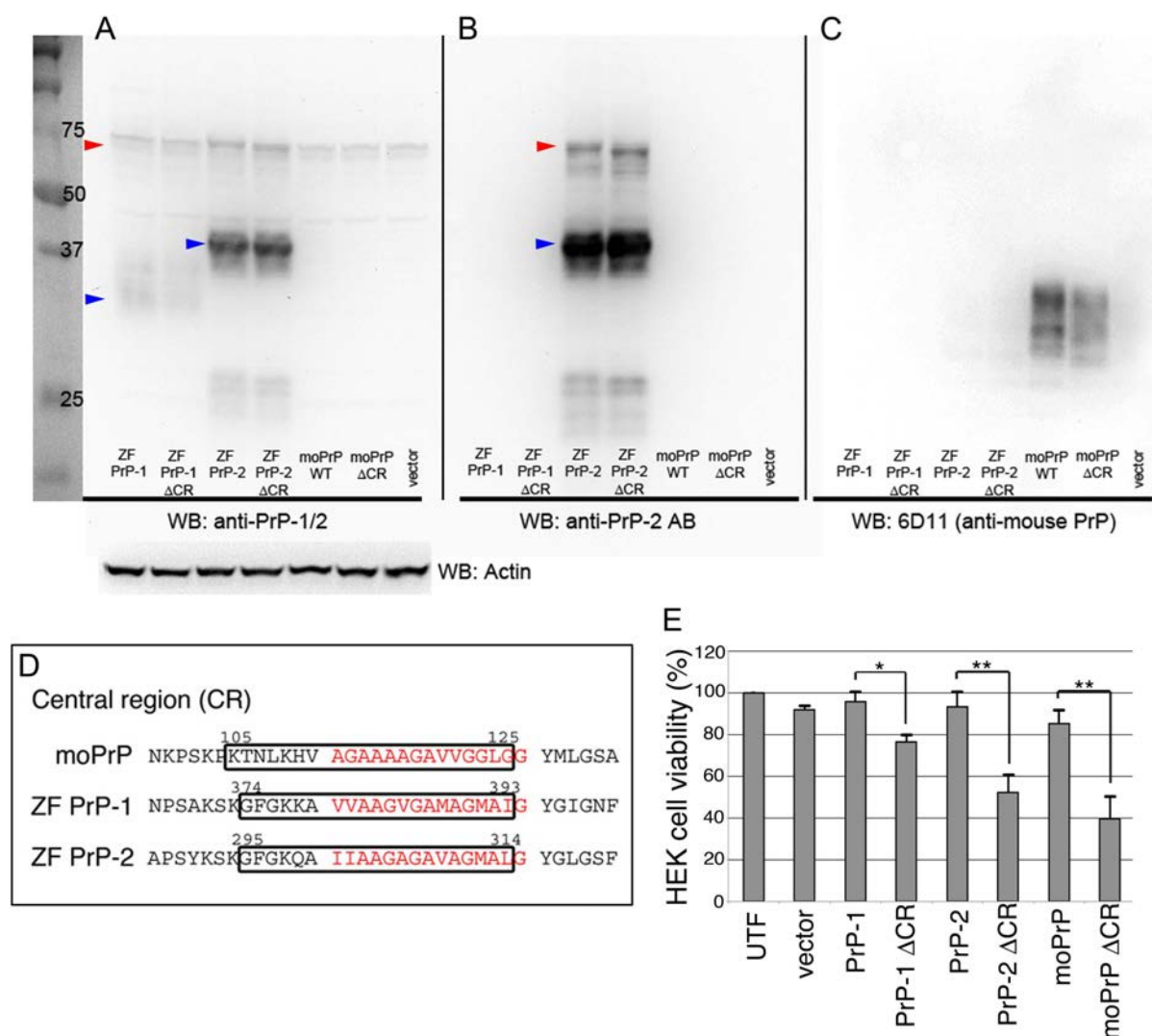


Figure 32 Expression of zebrafish Δ CR PrP constructs causes reduced viability of HEK293 cells. A-C. Western blot analysis of HEK cell lysates and detection of zebrafish (ZF) and mouse (mo) PrPs (WT and Δ CR forms). **A.** Detection of zebrafish PrP-1 and PrP-2 constructs with a polyclonal antibody originally designed against the globular domain of PrP-1. The full-length proteins (red arrowheads at 70 kDa) are weakly detected; bands of lower molecular weight (blue arrowheads; ~30 kDa for PrP-1 and ~40 kDa for PrP-2) likely correspond to cleavage products. **B.** Detection of zebrafish PrP-2 constructs with a polyclonal antibody designed against the globular domain of PrP-2; arrowheads as in (A). **C.** Detection of mouse PrP constructs with the 6D11 antibody. **D.** The central regions of mouse and zebrafish PrPs (marked in boxes). Numbers indicate amino acid positions. Residues of the hydrophobic domain are shown in red. The central regions of zebrafish PrPs were defined by sequence comparison with mouse PrP. **E.** Drug-based cell assay (DBCA) in HEK cells expressing mouse or zebrafish PrPs (WT vs. Δ CR) and incubated with Zeocin. Data are presented as the percentage of OD_{570nm} (Zeocin-treated)/ OD_{570nm} (untreated). UTF=untransfected. Triple asterisks (***) indicate $p < 0.001$, double (**): $p < 0.01$ and single (*): $p = 0.1-0.05$ in unpaired two-tailed student's t-tests; ns=non significant.

5.9 Treatment of zebrafish embryonic cells with $A\beta_{1-42}$ oligomers activates the PrP-1/SFK pathway affecting AJ protein levels

It was recently demonstrated that PrP can act as a receptor for neurotoxic $A\beta_{1-42}$ oligomers, thereby mediating the impairment in synaptic function and long-term potentiation (memory)

typically observed during Alzheimer's disease (AD) (Lauren et al, 2009). Such oligomers are composed of fibrillogenic $A\beta_{1-42}$ peptides, which in turn, are generated by proteolytic cleavage of an endogenous protein, the amyloid precursor protein (APP). During AD progression, $A\beta_{1-42}$ peptides become secreted and aggregate on the surface of neurons, forming amyloid plaques and triggering neurotoxicity (Price et al, 1995). Notably, several studies point at oligomeric species of $A\beta$ ($A\beta_o$) rather than the larger amyloid plaques as the actual cause of neuronal damage in AD (Lambert et al, 1998; Lesne et al, 2006; Walsh et al, 2002). Accumulating evidence indicates that $A\beta_o$ bind to cell surface PrP, leading to cell death, reduced synaptic plasticity and synaptic loss, as well as axon degeneration of serotonergic neurons and spatial memory loss in transgenic mice models (Barry et al, 2011; Freir et al, 2011; Gimbel et al, 2010; Jeong et al, 2010; Resenberger et al, 2011). Interestingly, at least two of the neurotoxic effects resulting from the $A\beta_o$ -PrP interaction - glutamate excitotoxicity and dendritic spine loss- are mediated by activated Fyn, which phosphorylates and transiently stabilizes NMDA receptors at neuronal cell surfaces (Um et al, 2012). Given the wide range of neurological responses/defects triggered by $A\beta$ as well as the variety of Fyn phosphorylation substrates, we reasoned that the $A\beta$ -PrP dependent activation of Fyn is likely to affect other proteins important for neuronal homeostasis besides the NMDA receptor. Because of the known functional redundancy among SFKs, we also tested whether SFK members other than Fyn would mediate signals triggered by $A\beta$ and PrP.

Our PrP gain- and loss-of-function experiments in zebrafish embryos identified AJ components as downstream effectors of the PrP-SFK pathway. Therefore, we asked whether E-cadherin and β -catenin could also be potential regulatory targets of the $A\beta_o$ -PrP pathway. To answer this question, we treated embryos with $A\beta_o$ and used Western blot to assess putative changes in the levels and/or activation of SFKs and AJ proteins. As a negative control, we used monomeric $A\beta$ ($A\beta_m$), which unlike $A\beta_o$, does not induce pathogenic PrP-dependent signaling (Um et al, 2012). For these experiments, embryos were dissociated mechanically at 4 hpf and the dissociated cells were left to re-aggregate for 1 h in suspension in the presence of $A\beta_o$ or $A\beta_m$. The purpose of the cell dissociation procedure was to facilitate access of the oligomers to embryonic cell surfaces. To verify the role of PrP in $A\beta_o$ -mediated signaling, we performed these tests both in the presence and absence of PrP-1 (control and PrP-1 knockdown embryos). In agreement with the findings in mammalian cells, oligo- but not monomeric $A\beta$ led to SFK activation, as indicated by increased phosphorylation of Src/Yes and Fyn at Tyr416 in cells of control embryos (4-fold and 10-fold increase respectively; $p < 0.001$) (Figure 33C and D). Importantly, the levels of total SFKs were not affected by exposure to $A\beta_o$ (Figure 33E). Consistent with the increased SFK activation, changes upon $A\beta_o$ treatment were also observed in the downstream targets

of the PrP/SFK pathway: an elevation in levels of mature E-cadherin and β -catenin by 2.5- and 2-fold, respectively ($p < 0.001$ for both proteins) (Figure 33A and B). These effects were dependent on the presence of PrP-1, since they could not be observed in cells derived from PrP-1 morphants. Intriguingly, $A\beta_m$ also caused a PrP-1 dependent increase in mature E-cadherin levels ($p < 0.001$) (Figure 33A), without however activating the upstream SFK pathway or the levels of downstream β -catenin (Figure 33B-D). These results suggest that $A\beta_o$ modulates the levels of AJ components via the PrP-1/SFK pathway, whereas $A\beta_m$ influences E-cadherin via an unrelated mechanism. From these experiments, it can be generally concluded that $A\beta$ oligomers replicate a PrP-1 gain-of-function, boosting the levels of active SFKs and AJ proteins.

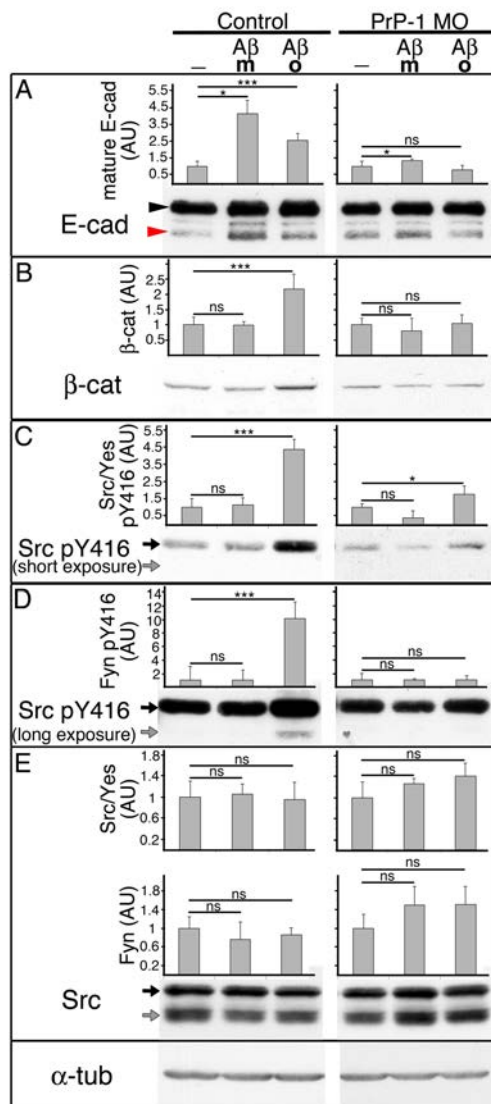


Figure 33. Biochemical changes in 6 hpf embryonic cells treated with 500 nM oligo- or monomeric $A\beta$ peptide. Western blots and densitometric analyses of bands. Graphs display average band intensities \pm SEM from three independent experiments in arbitrary units (AU). $A\beta_m$ =monomeric $A\beta_{1-42}$; $A\beta_o$ =oligomeric $A\beta_{1-42}$. Red and black arrowheads indicate the mature and precursor forms of E-cadherin, respectively. Arrows point at distinct SFKs bands (black: Src/Yes; grey: Fyn). Triple asterisks (***) indicate $p < 0.001$, double (**): $p < 0.01$ and single (*): $p = 0.1-0.05$ in unpaired two-tailed student's t-tests; ns=non significant.

6 Discussion

In this doctoral thesis I describe the use of the zebrafish embryo to address basic questions in prion biology. On one hand, we employed loss-and gain-of-function approaches to identify the molecular mechanisms by which PrP controls embryonic cell signaling and adhesion. On the other hand, we carried out *in vivo* mutational analyses to study the functional contributions of PrP's protein domains and posttranslational modifications, as well as to scrutinize the connection between PrP's functional and pathogenic properties. Finally, we examined the functional implications of the A β -PrP interaction as a means to shed light on the common cellular events underlying prion and Alzheimer's diseases.

Being so far the only model organism in which PrP depletion causes specific and lethal phenotypes *in vivo*, the zebrafish embryo provides a unique opportunity to dissect PrP-dependent molecular pathways with physiological and pathological relevance. Elucidating the natural signaling partners of PrP is a precondition to understand which cellular pathways are deregulated upon misfolding of PrP^C to PrP^{Sc}. It is important to note that most of my work was performed in embryonic, largely undifferentiated cells. However, the molecules we identified as downstream effectors of PrP -like SFKs, cadherins and catenins- are also expressed in neuronal tissues and play central roles in neuronal homeostasis and growth. These functional connections will be highlighted at several points throughout the Discussion.

6.1 Regulation of AJ stability by PrP-1

Using pharmacological inhibitors against endocytosis and degradation, we established that upon PrP-1 knockdown, mature plasma membrane-bound E-cadherin is endocytosed via a clathrin-dependent mechanism, and targeted for depletion by the proteasome. Concretely, treatment of PrP-1 morphants with either an inhibitor of clathrin-dependent endocytosis (Dynasore) or the proteasome (MG132) restored E-cadherin cell surface localization, recovered its levels and led to large improvements in the morphology of PrP-1 knockdown embryos and their ability to perform epiboly. These results agree with former studies in oncogene-transformed cells, in which targeting of E-cadherin to endocytic and proteasomal degradation pathways correlated with reduced cell adhesiveness and increased metastatic behavior (Davis et al, 2003; Yang et al, 2006). Interestingly, lysosome inhibition with chloroquine did not restore mature E-cadherin levels but led to abnormally high levels of its larger precursor form and the surprising restoration of epiboly in a significant portion of PrP-1 morphants. Indeed, the E-cadherin precursor has been shown to be degraded differentially

from the mature form via the lysosomal pathway (Lin et al, 2008). Even though lysosomal inhibition did not rescue morphant embryos as effectively as the proteasome blocker, these results suggest that the E-cadherin precursor would, at least in our system, be able to compensate for the function of its mature counterpart. This stands in contrast to its inability to trigger the aggregation of mouse fibroblasts (Ozawa & Kemler, 1990) and suggests that the E-cadherin precursor has adhesive properties under physiological conditions. Alternatively, the zebrafish and mammalian E-cadherin precursors may differ in their adhesive properties due to species-specific posttranslational processing (e.g. glycosylation). Although multiple mechanisms have been shown to influence the endocytic trafficking of E-cadherin, it remains to be clarified which ones are physiologically relevant. Targeting of E-cadherin for degradation in either lysosomes or the proteasome requires the ubiquitination of the protein at the cell surface by E3 ligases such as Hakai or Mdm2 and their clathrin-dependent internalization into early endosomes (Fujita et al, 2002; Yang et al, 2006). Whereas ubiquitination by Hakai leads to depletion of the protein in lysosomes, Mdm2-mediated degradation is proteasome-dependent and thus more related to our findings. Nevertheless, it should be taken into account that E3 ligases constitute a large protein family, and that it remains to be determined which ones are expressed and active during early zebrafish development. Moreover, little is known about the mechanisms that cause specific ubiquitin ligases to interact with E-cadherin and target it for degradation. For instance, whereas binding of Hakai is stimulated by Tyr phosphorylation of E-cadherin but outcompeted by binding of p120 to E-cadherin, it is unknown whether similar mechanisms control Mdm2 activity. However, because E-cadherin turnover is determined by the cellular levels of p120 (Davis et al, 2003), and because these remained unaltered in PrP-1 morphants, the observed endocytosis and degradation of E-cadherin upon PrP-1 knockdown is likely to proceed via a p120-independent pathway.

In cultured cells, the adhesive function of E-cadherin has often been shown to depend on its association with β -catenin, which ensures its anchorage to the actin cytoskeleton via additional downstream proteins (Chitaev & Troyanovsky, 1998; Nagafuchi et al, 1994; Ozawa et al, 1990). *In vivo*, the regulation of E-cadherin function is more complex because β -catenin depletion does not reproduce the strong adhesion-related defects caused by lack of E-cadherin; similar results have been obtained across various model organisms including mice (Hynes, 1996), *Xenopus* (Levine et al, 1994), zebrafish and *Drosophila* (Song & Xie, 2002) embryos. For instance, depletion of β -catenin by gene knockout in mice (Hynes, 1996), morpholino knockdown or antibody inactivation in zebrafish and *Xenopus* (Bellipanni et al, 2006; Heasman et al, 2000; McCrea et al, 1993) or mutational inactivation of the β -catenin gene in *Drosophila melanogaster* (Peifer et al, 1991), leads mostly to defects in body axis formation due to the impairment of β -catenin (nuclear) signaling function. Surprisingly,

no defects in cell adhesion are evident in these animals despite the strong *in vitro* mechanistic evidence showing that β -catenin indirectly mediates E-cadherin anchorage to actin. While the lack of β -catenin adhesion phenotypes challenges the view that this molecule is an essential component of AJs, other lines of evidence indirectly further support this notion. One example of data favoring the *in vivo* adhesive role of β -catenin is the finding that E-cadherin-mediated adhesion was restored by boosting the levels of cytosolic β -catenin in zebrafish embryos lacking 2-O-sulfotransferase, which modifies sugar chains on cell surface GAGs (glycosaminoglycans) (Cadwalader et al, 2012). A possible explanation for the lack of β -catenin adhesive phenotypes *in vivo* may be that when this protein is depleted *in vivo*, related proteins like plakoglobin become upregulated to compensate for its adhesive function (Haegel et al, 1995).

In PrP-1 knockdown embryos, β -catenin behaved similarly to E-cadherin, both proteins undergoing reduction of their cellular levels due to degradation upon their dissociation from the plasma membrane. This raised the question whether the two AJ molecules (E-cadherin and β -catenin) are simultaneously affected by the loss of PrP-1, or whether one of them is the primary regulatory target of PrP-1 in AJs, thus influencing the stability of its binding partner at the plasma membrane. Since β -catenin depletion alone is not enough to compromise E-cadherin-based adhesion *in vivo*, we reasoned that, most likely, E-cadherin itself is the direct downstream target of PrP-1 signaling. Of note, we could not observe any co-localization of E-cadherin and β -catenin in cytosolic vesicles, proximal or distal to the plasma membrane, in the presence or absence of PrP-1. We interpreted this observation by suggesting that the two proteins are not internalized together as a complex but rather become removed differentially/sequentially from the plasma membrane. Although little is known about the regulation of β -catenin internalization, it is well established that E-cadherin undergoes endocytosis via clathrin-coated pits (Le et al, 1999). Because treatment of PrP-1 morphants with Dynasore restored the localization of both proteins at the plasma membrane, we concluded that the association of β -catenin with the plasma membrane was most likely disrupted as a consequence of the destabilization of cell surface E-cadherin.

6.2 Fyn and Yes act downstream of PrP-1 during gastrulation

Developmental studies have demonstrated that several ubiquitously-expressed Src family kinase members are essential for morphogenetic cell movements during zebrafish gastrulation. For instance, it was shown that blocking all SFK activity with the protein tyrosine kinase inhibitor PP2 causes lethal epibolic arrest (Tsai et al, 2005). Similar zebrafish gastrulation phenotypes were produced by injection of morpholinos against Yes, or mRNAs encoding a Fyn dominant negative construct (Sharma et al, 2005). Interestingly, the failure

of PP2-treated or Yes knockdown embryos to carry out epiboly is strongly reminiscent of our PrP-1 morphant phenotype, as in all these cases the migration of embryonic cells is impaired and the blastoderms appear deformed (Tsai et al, 2005). In related experiments, den Hertog and colleagues were able to circumvent the lethality of early SFK knockdown by using lower amounts of Yes morpholino (5 ng, vs. 12.5 ng per embryo used by Tsai et al) (Jopling & den Hertog, 2005). Interestingly, double Fyn/Yes knockdown embryos generated using such low morpholino doses were able to complete epiboly but showed defects in convergence-extension movements at later stages of gastrulation. These results suggest that, from these two types of gastrulation movements, convergence-extension is more sensitive to SFK downregulation than epiboly. On the other hand, single knockdowns of Fyn or Yes, or the combined knockdown of Fyn/Src or Yes/Src did not produce noticeable gastrulation phenotypes (Jopling & den Hertog, 2005). It was concluded that Src is most likely dispensable for gastrulation, and that Fyn and Yes are required synergistically. Although these studies addressed the function of Fyn and Yes during zebrafish gastrulation, they did not specifically examine the influence of these kinases on cell-cell adhesion. During my thesis work, we injected morpholino amounts halfway between those used in the aforementioned studies (8 ng per embryo), and showed that the combined knockdown of Fyn and Yes phenocopies that of PrP-1 with regard to the control of epiboly and AJ function. Thus, Fyn and/or Yes knockdowns caused developmental arrest at 50% epiboly, characterized by reduced plasma membrane localization and diminished cellular levels of E-cadherin and β -catenin. Besides supporting our hypothesis that Fyn, Yes and PrP-1 act along the same pathway that regulates cell adhesion during gastrulation, our findings reveal the concrete mechanisms by which SFKs contribute to embryogenesis in the zebrafish. Our conclusions are also likely to provide mechanistic explanations to previous observations made in SFK-depleted *Xenopus* and mice embryos (Denoyelle et al, 2001a; Klinghoffer et al, 1999; Stein et al, 1994).

The role of SFKs as key downstream signaling partners of PrP-1 in the positive regulation of AJs was confirmed here by rescue experiments, in which exogenous Fyn/Yes expression in PrP-1 morphants restored AJ protein levels and localization, causing remarkable phenotypic recovery. Naturally elevated activity levels of Fyn and Yes throughout gastrulation stages (Sharma et al, 2005; Tsai et al, 2005) as well as the increased rescuing capacity of CA Fyn and Yes compared to their WT equivalents (this study), underscores the importance of SFK enzymatic activity for cell adhesion and gastrulation cell movements. Oppositely, the inability of PrP-1 morphants to perform epiboly correlated with sub-physiological levels of active SFKs.

Two key aspects of SFK biology relevant to this thesis are their functional redundancy and pleiotropy. Our characterization of both Fyn and Yes as downstream signaling molecules of PrP-1 further supports the notion of functional SFK redundancy during embryonic development, as previously suggested by work in frog and mice embryos (Denoyelle et al, 2001b; Weinstein & Hemmati-Brivanlou, 2001). For instance, single knockouts of *fyn*, *yes* or *src* caused mild developmental phenotypes in mice but double (*src/fyn* or *src/yes*) and triple knockouts were embryonic lethal (Klinghoffer et al, 1999; Stein et al, 1994). Aside from these similarities across model organisms, some interesting differences are also evident: Although Fyn/Yes depletion is lethal for zebrafish embryos, *fyn/yes* knockout mice undergo kidney degeneration but remain viable (Stein et al, 1994). Furthermore, Src is essential for epiboly in *Xenopus* but not in zebrafish (Denoyelle et al, 2001b; Jopling & den Hertog, 2005). This functional divergence of SFKs is attributed to their evolutionary diversification after gene/genome duplication (Gu & Gu, 2003). The combinatorial and interchangeable nature of SFK function as well as the diversity of their cellular substrates (Courtneidge, 2002) emerge as issues of key relevance to prion biology, as they provide an adequate explanation for the differences observed between PrP loss-of-function phenotypes of fish and mammals (see Introduction, paragraphs 1.5 and 1.6).

6.3 SFK-mediated changes in cell-cell adhesion

Our identification of Fyn and Yes as positive regulators of AJs in the zebrafish embryo provides new insights into how SFKs control cell-cell adhesion under physiological conditions. It is important to note that nearly all the widely accepted evidence stating that SFK activity disrupts AJ function was gathered in experiments using oncogene-transformed cells (see Introduction, paragraph 1.7). In contrast, work from our laboratory and other *in vivo* studies challenge this view. Concretely, depletion of SFK levels/activity in the zebrafish embryo -either by Fyn/Yes knockdown or indirectly by downregulation of PrP-1- led to abnormal AJ protein levels and localization, whereas elevated SFK activity in PrP OE embryos correlated with increased adhesiveness of embryonic cells (this study and aggregation assays from Málaga-Trillo et al, 2009). Accordingly, in *Drosophila*, SFK member DSrc42A promotes the localization of DE-cadherin at the cell surface during embryonic morphogenesis (Takahashi et al, 2005) and at contact sites between eye photoreceptor cells (Takahashi et al, 1996). Also in mice, Fyn and Src positively regulate the maintenance of keratinocyte cell-cell adhesion (Calautti et al, 1998). Notably, even in cancer cells SFK activity does not always correlate with diminished cell adhesion. For instance, inhibition of physiological Src activation levels in MCF-7 cells by expression of dominant negative Src or PP2-treatment was shown to perturb E-cadherin localization at cell contacts (McLachlan et al, 2007). Similarly, our present work with MCF-7 cells argues for a positive correlation

between SFK activity and the presence of E-cadherin at cell contact sites. Altogether, the functional data collected in different cells and organisms lead to the paradoxical conclusion that the influence of SFKs on E-cadherin cell adhesion is positive in some cases and negative in others. These seemingly contradictory findings in different models can be best explained by a “bimodal” model, in which SFK activity promotes cell adhesion at low, physiological levels but suppress it at high, oncogenic levels. This hypothesis was derived from the observation that endogenous activation levels of Src or low levels of exogenously expressed CA Src in MCF-7 cells support/enhance E-cadherin contact formation, while high CA Src expression levels weaken adhesion (McLachlan et al, 2007). The results presented in my dissertation further support the physiological “arm” of the bimodal model by showing that Fyn and Yes promote E-cadherin cell adhesion during embryonic development.

A key question that emerges from these findings is how exactly SFKs control E-cadherin adhesive function. As described in paragraph 1.7 of the Introduction, the function of E-cadherin and β -catenin can be regulated via various mechanisms, from which phosphorylation and endocytosis/degradation are the most relevant to my work. Through biochemical analyses in PrP-1 morphants and PrP OE embryos, we confirmed a positive correlation between E-cadherin adhesion, SFK activity and the levels of β -catenin phosphorylation at Tyr142. Fittingly, this residue was previously identified as a direct substrate of Fyn and an indirect target of Yes activity (Piedra et al, 2003). However, in contrast to our findings, this phosphorylation event disrupts β -catenin binding to α -catenin in cell-free systems, suggesting that it would destabilize AJs by decoupling them from actin (Aberle et al, 1996; Pokutta & Weis, 2000). That increased β -catenin phosphorylation at Tyr142 does not impact negatively on embryonic cell adhesion was particularly evident in our PrP OE experiments with zebrafish: despite exhibiting abnormally high levels of Tyr142-phosphorylated β -catenin, these embryos accumulated E-cadherin and β -catenin at the plasma membrane, and their cells were more adhesive than those of control embryos (this study and Málaga-Trillo et al, 2009). A similar phenomenon was observed in mouse keratinocytes, in which elevated β -catenin phosphorylation concurred with increased cell-cell adhesion, required for their differentiation (Calautti et al, 1998). Accordingly, keratinocytes of *fyn/src* deficient mice showed significantly reduced levels of β -catenin phosphorylation and could not properly adhere to each other, causing structural defects in the skin (Calautti et al, 1998). Taken together, these data indicate that, *in vivo*, SFK-induced phosphorylation of β -catenin is not the dominant event controlling AJ assembly but rather a minor modulator of AJ stability, or perhaps, part of a mechanism that regulates an AJ-independent function of β -catenin. These scenarios would also be in line with our hypothesis that E-cadherin -and not β -catenin- is the decisive factor that destabilizes AJs in the absence of PrP-1.

If the above is true, how could SFKs influence E-cadherin localization at the plasma membrane in a β -catenin independent manner? In MDCK cells, expression of v-Src -a virally encoded, constitutively active form of Src- has been suggested to directly phosphorylate E-cadherin, inducing the ubiquitination of the latter at the plasma membrane and its subsequent endocytosis and degradation (Fujita 2002). However, like most other studies performed in oncogene-transformed cells, this one also supports the notion of Src being a negative regulator of E-cadherin-based adhesion. In order to conciliate these and our findings, it will be necessary to determine if such direct regulation of E-cadherin via tyrosine phosphorylation follows the bimodal model and thus has a positive regulatory counterpart under physiological conditions.

Another important route by which SFKs influence E-cadherin adhesion complexes is via the regulation of the actin cytoskeleton (see introduction, paragraph 1.7). In fact, our group reported abnormalities in the distribution of F-actin along the plasma membrane of PrP-1 knockdown zebrafish embryos (Málaga-Trillo et al, 2009). This observation and the finding that exogenous PrP expression triggers actin recruitment to S2 cell-cell contacts strongly suggest a positive influence of PrP on cortical actin (Málaga-Trillo et al, 2009). Interestingly, Cortactin -a known substrate of Src-, becomes localized to cell contacts upon E-cadherin homophilic binding, where it stabilizes AJs by promoting actin assembly (Helwani et al, 2004; Wu & Parsons, 1993; Wu et al, 1991). When phosphorylated by Src, Cortactin triggers actin polymerization by recruiting the actin-nucleating Arp2/3 complex to cortical actin (Tehrani et al, 2007; Uruno et al, 2001; Weaver et al, 2002; Weaver et al, 2001). In addition, Cortactin binds and stabilizes nascent actin filament branches produced by Arp2/3 (Weaver et al, 2001). Remarkably, Cortactin has also been reported to interact with dynamin2 as a component of clathrin-coated pits and influence endocytosis, a process also proposed to depend on Src activity (Cao et al, 2003). Thus, it would be interesting to examine whether altered Cortactin phosphorylation contributes to the zebrafish PrP-1 knockdown phenotype by affecting actin dynamics or the endocytosis of AJ components. Further evidence for a link between PrP-1 and actin dynamics is provided by the finding that zebrafish Fyn and Yes are upstream regulators of the small GTPase RhoA, a known modulator of actin polymerization (Heasman & Ridley, 2008; Jopling & den Hertog, 2005). Although the embryonic requirement of the Fyn/Yes/RhoA pathway was studied in the context of convergence and extension cell movements, which take place after the onset of our PrP-1 phenotype, it is conceivable that earlier stages of epiboly are equally affected by this signaling cascade.

6.4 Regulation of SFKs by PrP

Both the PrP gain- and loss-of-function experiments described in this thesis indicate a positive correlation between the activities of PrP and SFKs. This conclusion is in agreement with earlier studies aimed at elucidating the pathophysiological properties of PrP. For instance, PrP^{Sc}-infected mouse brains or cultured N2a cells were found to have elevated levels of total and activated SFKs, including Src, Yes, Fyn and Lck (Nixon, 2005). In *C. elegans*, Fyn was identified as the mediator of neuronal dysfunction triggered by the PrP octarepeat insertional mutant PG14 (Bizat et al, 2010). Several, more recent reports revolve around the role of Fyn as a transducer of neurotoxic signals triggered by the binding of A β to PrP during Alzheimer's disease (Larson et al, 2012; Lauren et al, 2009; Um et al, 2012). In cultured neuronal cells and under non-pathological conditions, antibody-mediated crosslinking of PrP was also found to result in Fyn activation, although the physiological relevance of these experiments was not evident (Mouillet-Richard et al, 2000). A later study found that the interaction between PrP and the neural cell adhesion molecule NCAM leads to Fyn activation in the context of neurite outgrowth (Santuccione et al, 2005). In the early zebrafish embryo, we showed that PrP-1 is required to maintain the levels of total and activated SFKs, an effect partly achieved by preventing their lysosomal degradation. Upon PrP-1 knockdown, total SFK levels were reduced, levels of phospho Tyr416 (active) SFKs underwent an even stronger downregulation, whereas those of phospho Tyr527 (inactivated) SFKs were not significantly altered. The latter indicates that, in the absence of PrP-1, SFKs are not placed into a closed conformation by phosphorylation at Tyr527, but remain in an unrestrained state that allows their activation by autophosphorylation at Tyr416 (Harrison, 2003). It also suggests that PrP-mediated regulation of SFKs is likely not occur via kinases or phosphatases which catalyze the (de-)phosphorylation of Tyr527, such as Csk or PTP1B (Nada et al, 1991; Okada & Nakagawa, 1989). Therefore, three mechanistic scenarios can be envisaged to explain the reduced SFK activity in embryos lacking PrP-1: a) SFKs undergo active dephosphorylation at Tyr416 (deactivation) and become degraded, b) their activation by autophosphorylation cannot be sustained and this leads to their degradation, or c) active phosphorylated SFKs are specifically targeted for depletion upon PrP-1 knockdown. Tyr416 is an auto-phosphorylation site and, as such, no kinases besides SFKs themselves are known to affect its phosphorylation state (Roskoski, 2005). However, decreases in auto-phosphorylation were shown to take place in cell-free systems when the availability of artificial SFK substrates was increased, suggesting that a similar saturation mechanism could limit activation levels *in vivo* (Sun et al, 2002). The possibility that activated SFKs might specifically be targeted for depletion upon PrP-1 knockdown is suggested by the finding that these are preferentially degraded by lysosomes (Kim et al, 2004). Indeed, this mechanism would explain why we observed the recovery of SFK levels

in PrP-1 morphants upon lysosomal but not proteasomal inhibition. In a related scenario, it was recently shown that the degradation of activated SFKs can switch from proteasomal to autophagic/lysosomal when a key upstream stimulus, such as focal adhesion kinase (FAK) signaling, is absent (Sandilands et al, 2012). Similarly, the loss of PrP-1 could direct activated SFKs to a lysosomal degradation pathway.

The notion of a positive functional link between PrP and SFK activity is also supported by our studies in embryos and MCF-7 cells overexpressing PrP. However, although the levels of phospho Tyr416 SFKs were clearly elevated in both systems upon expression of zebrafish or mouse PrPs, those of total SFKs remained unaltered (mouse PrP and zebrafish PrP-2) or were only slightly increased (zebrafish PrP-1). These results suggest that, unlike in the PrP-1 knockdown paradigm, alterations in SFK activation levels induced by PrP overexpression are not concomitant to changes in the turnover/degradation of these kinases. Alternatively, it could imply that PrP-1 -but not PrP-2 or mouse PrP- has the unique ability to influence SFKs in a dual manner (total cellular levels and activation levels).

How exactly does PrP control SFK function? Could this regulation involve an activation via direct physical interaction? This seems unlikely because although PrP co-immunoprecipitates with Src (Morel et al, 2004) and triggers Fyn activation (Mouillet-Richard et al, 2000), it has no known kinase or phosphatase activities. Moreover, even though PrP and SFKs may be part of a common protein complex, it is not clear whether the GPI anchor of PrP can extend through the plasma membrane and interact directly with cytoplasmic SFKs. However, since PrP associates with various transmembrane proteins at the cell surface, including EGFR and NCAM, it could indirectly signal to intracellular SFKs via these putative *cis*-interacting partners (Llorens et al, 2013; Schmitt-Ulms et al, 2001). Interestingly, PrP-mediated activation of Fyn has been linked to clustering of PrP at the cell surface and its subsequent translocation from lipid rafts into caveolin-rich membrane domains (Toni et al, 2006). This serves as another indication that PrP may require an interaction partner –such as caveolin itself or a protein localized in these domains- that is capable of inducing SFK activation.

6.5 PrP overexpression: adhesion vs. β -catenin signaling

At the beginning of this work, the developmental defects caused by PrP overexpression in zebrafish embryos had not been as thoroughly characterized as those induced by PrP-1 knockdown. Our working hypothesis was that PrP gain- and loss-of-function phenotypes should be explained by opposing alterations in the same molecular network. Therefore, after studying PrP-1 morphant gastrulae to dissect the signaling pathway downstream of PrP-1, I

went on to determine whether related molecular events contribute to the PrP OE phenotype. Our experiments show that PrP OE impairs zebrafish gastrulation and body axis formation via two distinct cellular mechanisms.

The first and, most likely, direct effect caused by PrP OE is the exacerbation of E-cadherin-mediated cell adhesion in the deep cell layers of the zebrafish gastrula. As indicated by their increased aggregation potential (Málaga-Trillo et al, 2009) and their elevated levels of mature E-cadherin, cells derived from PrP OE embryos are more adhesive than those of control embryos. Enhanced cell adhesion caused by abnormally high cell surface levels of E-cadherin is likely to impair morphogenesis (radial intercalation, convergence extension) by impinging on the rapid turnover of cell-contacts and thus the dynamic migratory movements of cells. Interestingly, in zebrafish embryos deficient of Prostaglandin E2, increased E-cadherin-mediated cell adhesion also leads to epibolic arrest and the local aggregation of cells (“cell-clumping”), similar to what we observed on the dorsal side of PrP OE embryos. Since E-cadherin was increasingly endocytosed and depleted in the absence of PrP-1, it is reasonable to assume that the opposite effect, namely its reduced endocytosis upon PrP OE, is responsible for its stabilization at the cell surface and the increased levels of its mature form. Therefore, the aberrantly stretched and enlarged morphology of dorsal blastomeres in PrP OE embryos is possibly the result of disruptive mechanical forces caused by enhanced cell adhesion. Consistent with this interpretation, the endocytosis and constitutive turnover of E-cadherin have been shown to be as critical for gastrulation cell movements as the continuous maintenance of a basic amount of the protein at the cell-surface (Ulrich et al, 2005).

Our data revealed that during blastula and gastrula stages, SFKs and E-cadherin are co-distributed in a ventral-to-dorsal gradient, the dorsal side of the embryo exhibiting the highest levels of both proteins. While the existence of an early embryonic SFK gradient had not been reported previously, a related distribution pattern has been observed for E-cadherin (Babb & Marrs, 2004). However, in that study, E-cadherin was found evenly distributed throughout blastula stages, and its dorsal accumulation only became noticeable as epiboly progressed. Because the detection of such early gradient requires detailed analysis of high-resolution confocal images, this discrepancy may result from technical differences. In any event, the characteristically strong asymmetry of PrP OE embryos correlates with an enhanced version of this SFK/E-cadherin double gradient. The PrP-dependent accumulation of SFKs and E-cadherin appears more prominent in dorsal cells probably because these proteins are already more abundant dorsally under control conditions. Therefore, although PrP upregulates E-cadherin and SFK throughout the entire embryo, the increased adhesion

defect caused by PrP OE becomes more marked dorsally, leading to asymmetric cell-clumping and deformation of the blastoderm.

The second major embryonic defect induced by PrP OE concerns the control of axis specification by nuclear β -catenin signaling. In PrP OE embryos, the enhanced cell surface localization of E-cadherin and β -catenin correlate with the reduced translocation of β -catenin into dorsal nuclei at mid-blastula stages (3 hpf). These observations strongly agree with the reported ability of E-cadherin to sequester β -catenin at the plasma membrane in various cultured cell types (Orsulic et al, 1999). A similar phenomenon was demonstrated in *Xenopus* and *Drosophila* embryos, in which the abnormal upregulation of E-cadherin function antagonizes nuclear β -catenin signaling during axis specification and segment patterning, respectively (Fagotto et al, 1996; Heasman et al, 1994; Sanson et al, 1996). Although no specific antibodies are available to distinguish between the two zebrafish β -catenins (β -catenin-1 and -2), our data suggest that PrP modifies the function of at least β -catenin-2, as only this duplicate has dorsalizing activity (Bellipanni et al, 2006; Kelly et al, 2000). Remarkably, the total levels of β -catenin are not upregulated along with those of E-cadherin in PrP OE embryos. In fact, while its levels were unaffected in 3 hpf PrP OE embryos, they were clearly reduced at 6 hpf in the dorsal blastoderm, which derives from cells with reduced nuclear translocation of β -catenin. Because β -catenin can promote its own transcription (Bandapalli et al, 2009), our data suggest that its reduction in the dorsal nuclei of 3 hpf PrP OE embryos impairs its local biosynthesis. Also consistent with such a hypothesis is our finding that β -catenin levels in 6 hpf PrP OE embryos cannot be recovered by treatment with degradation inhibitors, unlike in PrP-1 morphants. Of note, the reduced levels of β -catenin in 6 hpf PrP OE embryos contrast with their increased E-cadherin levels and enhanced cell adhesion, indicating that the adhesive function of β -catenin is not critically required to maintain cell-cell adhesion in the gastrula. This observation also supports our conclusion that the impaired cell adhesion observed in PrP-1 morphants is primarily caused by the downregulation of E-cadherin and not by the internalization and degradation of β -catenin.

Nuclear β -catenin signaling is normally activated by the canonical Wnt pathway. This entails the binding of soluble Wnt to its cell surface receptor, an event that ultimately inhibits the degradation of intracellular β -catenin leading to its stabilization and subsequent translocation into dorsal nuclei (Wodarz & Nusse, 1998). Notably, this process affects only the cytosolic pool of β -catenin and does not implicate the β -catenin fraction engaged in AJs at the plasma membrane (Nelson and Nusse, 2004). In our experiments, we found that PrP OE induces the sequestration of β -catenin at the plasma membrane, thus preventing its physiological accumulation in the cytosol and its subsequent nuclear localization. This suggests that

overexpressed PrP antagonizes Wnt function by reducing the availability of cytosolic β -catenin that can be translocated to the nucleus. It remains to be clarified whether such a potential interplay between PrP and Wnt signaling takes place under physiological conditions. However, this scenario seems unlikely in light of our finding that upon its internalization in PrP-1 morphants, β -catenin does not form stable cytosolic pools but instead becomes targeted for degradation. Thus, there are no direct indications for increased Wnt signaling upon PrP-1 knockdown, and PrP most likely interferes with this pathway only when its levels/activity are abnormally enhanced. This notion is further supported by the observation that mutants of the zebrafish dorsalizing gene Wnt8 exhibit a dorsoventral phenotype which is related but different to the one of PrP OE embryos, with no defects in cell adhesion (Lekven et al, 2001). Remarkably, the Wnt pathway is crucial for neuronal development (Zhang et al, 2009), whereas the activity of several of its components, including β -catenin, is compromised in the brains of AD patients (De Ferrari & Inestrosa, 2000). Since AD and prion disorders are causally linked by PrP, it would be interesting to examine whether the Wnt pathway is deregulated during prion disease.

6.6 Roles of different PrP domains in PrP localization and function

Glycosylation and GPI-anchorage

Determining the physiological significance of PrP requires thorough understanding of how its structural elements contribute to its activity and subcellular distribution. Part of my doctoral work addressed this subject by using specific functional readouts in MCF-7 cells and zebrafish embryos. In several cell types, including human cultured enterocytes, HeLa, and neuroblastoma N2a cells, surface expression of PrP is particularly prominent at contact sites and basolateral membranes (Málaga-Trillo et al, 2009; Morel et al, 2004; Sarnataro et al, 2002). This type of accumulation has been previously observed by our group in N2a cells not only for mouse, but also for zebrafish, frog and chicken PrPs (Málaga-Trillo et al, 2009 and unpublished data). Our current analysis in MCF-7 cells and zebrafish embryos revealed that the most dramatic defects in the localization of PrP are caused by lack of the GPI anchor or mutation of the N-glycosylation sites within the globular domain, since the corresponding mutants altogether fail to reach the plasma membrane. This result agrees with previous studies showing that targeted sorting of PrP is determined by a molecular signal encoded within the GPI anchor, and further modulated by N-linked glycans (Chesebro et al, 2005a; Puig et al, 2011). It also correlates with the strongly reduced ability of these constructs to influence zebrafish gastrulation. Being a secreted molecule, it is evident that GPI-anchorless PrP cannot be stabilized at the plasma membrane or accumulate at cell-cell contacts (Chesebro et al, 2005b). In contrast, the reasons behind the impaired cell-surface localization of PrP glycosylation mutants are more complex and difficult to interpret. For

instance, the fact that our PrP glycosylation mutants exhibit defective localization in MCF-7 and zebrafish embryos is consistent with related studies in other mammalian cells (Cancellotti et al, 2005; Korth et al, 2000; Lehmann & Harris, 1997; Puig et al, 2011; Rogers et al, 1990), altogether leading to the straightforward conclusion that glycosylation is essential for the delivery of PrP to the plasma membrane. However, we found that the same glycosylation mutants are correctly localized at the plasma membrane of *Drosophila* S2 cells (Solis et al, 2013). This is in line with a previous report showing that WT hamster PrP is correctly targeted to the surface of S2 cells despite being incompletely glycosylated (Raeber et al, 1995). Moreover, treatment of CHO and human neuroblastoma cells with tunicamycin efficiently blocks PrP glycosylation but does not influence its trafficking (Lehmann & Harris, 1997; Petersen et al, 1996). Together with more detailed mutational analyses (Neuendorf et al, 2004), these studies strongly suggest that the specific mutations introduced into the consensus sequence Asn-X-Thr -and not the lack of glycosylation *per se*- result in deficient PrP trafficking in vertebrate cells. The reason for this is unclear, as is the normal trafficking of these mutants in *Drosophila* cells. Because N-linked glycans are important to ensure proper folding, stability and quality control of glycoproteins in the ER (Vagin et al, 2009), these observations may be explained by differences in biosynthetic processing and folding of proteins between vertebrate and invertebrate cells.

Hydrophobic domain

Unlike our data on the GPI anchor and the glycosylation sites within the globular domain, our experiments with hydrophobic domain mutants (PrP Δ HD) indicate that this central stretch does not influence PrP's subcellular localization. Zebrafish and mouse PrPs lacking the hydrophobic domain localized -similar to WT PrPs- at cell contacts in MCF-7 cells, zebrafish embryos (this dissertation) and S2 cells (Solis et al, 2013). The WT-like localization pattern of the Δ HD PrP mutants (Δ 112-126 for mouse PrP) is thus comparable to the one observed for the mouse PrP Δ CR mutant (Δ 105-125) in zebrafish embryos and other cell types (Christensen & Harris, 2009). Another previous report suggested a role for residues 113-133 in the basolateral sorting of mouse PrP in MDCK cells (Uelhoff et al, 2005), in apparent conflict with our data. However, because the deletion used in that study extends C-terminally beyond ours, it is possible that residues 127-133 are responsible for the effect missing in our constructs. Importantly, the WT-like distribution of the PrP Δ HD mutant is in line with our finding that the hydrophobic domain does not affect key functional properties of PrP such as its ability to influence zebrafish gastrulation, form contacts sites and trigger intracellular signals in S2 cells (Solis et al, 2013).

Repetitive and globular domains

Unlike the hydrophobic region, we showed that the repetitive and globular domains act as

important determinants of PrP localization at cell contacts. Key insights on the role of the repetitive domain were provided by zebrafish PrP-1, which –unlike mouse PrP or zebrafish PrP-2- exhibits a naturally patched/dotted distribution along contact sites of MCF-7 and zebrafish embryonic cells. In both these systems, deletion of the repetitive domain induced the loss of PrP-1's discontinuous pattern and its homogeneous presence along the entire cell contact. This suggests that this region either promotes the protein's local accumulation at discrete locations or facilitates its exclusion from other, complementary subregions of the cell contact. The former scenario is in line with earlier studies ascribing self-aggregation properties to the repetitive region (Parham et al, 2001; Tank et al, 2007). Interestingly, although deleting the repetitive domain did not affect the *per se* sorting/transport of PrP to contact sites in MCF-7 and zebrafish embryonic cells, it did impair its accumulation at S2 cell contacts (Solis et al, 2013). This likely reflects the differential regulation of cell contact formation in these experimental models: while formation of S2 cell contacts requires the establishment of PrP *trans*-interactions, mediated -at least partly by the repetitive domain- MCF-7 and embryonic cell contacts are independently maintained by E-cadherin homophilic interactions.

Contrary to the repetitive region, deletion of the globular domain in all three PrPs (mouse PrP, zebrafish PrP-1 and -2) did not prevent them from reaching the plasma membrane but produced instead a punctate, discontinuous distribution of the proteins at cell contacts of MCF-7 cells and the embryo. This finding suggests that the globular domain promotes the continuous localization of PrP at contact sites, thereby counteracting the clustering effect of the repetitive region. Conceivably, this may be achieved via the stabilization of PrP homophilic *trans*-interactions along larger regions of the contact site. The fact that WT PrP-1 normally localizes in punctae/patches would suggest that its repetitive region has a stronger clustering activity than that of mouse PrP or PrP-2. In fact, PrP-1 contains larger and more complex repeats than mouse PrP or PrP-2, owing to multiple expansion cycles of this domain during evolution (Cotto et al, 2005; Rivera-Milla et al, 2006). Thus, its globular domain would not be sufficient to ensure a continuous localization pattern. It remains to be established whether the local clusters of PrP-1 at cell contacts define signaling subregions of the plasma membrane, or whether they result from the specific recruitment of PrP-1 to preformed specialized sites. Interestingly, a similar localization pattern has been described for zebrafish Frizzled 7 (Fz7), and shown to modulate the persistence of cell contacts in the gastrula (Witzel et al, 2006). In that study, non-canonical Wnt11 was found to induce the local accumulation of its receptor Fz7 at “adhesive subdomains” within contact sites, thus modulating the endocytosis of the co-localized, atypical cadherin Flamingo. Similar cell contact subdomains were reported in HeLa cells and *Xenopus* animal caps, where canonical Wnt induces the local aggregation of LRP6-signalosomes at cell contacts to stabilize β -

catenin (Bilic et al, 2007). Hence, it would be interesting to examine whether PrP-2 and mouse PrP -like PrP-1- reside in or induce the formation of such distinct regions within cell contacts, which we may not have been discernible in this study due to the limitations of current microscopy techniques.

Aside from their clear effects on PrP localization, the repetitive and globular domains contribute significantly to PrP function during gastrulation, since the corresponding mutant constructs display a strongly reduced ability to cause an OE phenotype or rescue PrP-1 morphants. Because the presence of copper-binding histidines is not conserved in the repetitive regions of zebrafish PrPs, it is unlikely that these mediate PrP function by inducing copper-dependent endocytosis (Pauly & Harris, 1998). Instead, our results indicate that the repetitive and globular domains support PrP function either by determining its exact position in subregions of the plasma membrane -via opposing effects on local clustering- or by mediating interactions of PrP with itself or other proteins on the surface of neighboring cells. The importance of the repetitive domain for PrP homophilic *trans* interactions is underscored by the lack of contact formation in S2 cells expressing the PrP Δ Rep mutants (Solis et al, 2013). Accordingly, both the repetitive and globular regions have been reported to mediate PrP/PrP interactions in a yeast two-hybrid system (Hundt et al, 2003).

Physiological vs. pathological functions of PrP domains

Taken together, the present work identifies the GPI-anchor, N-glycosylation and the repetitive and globular domains as the elements determining PrP localization and function. The lack of an apparent function of the hydrophobic domain during zebrafish gastrulation may seem contradictory to the important neuroprotective role attributed to it by other studies (Biasini et al, 2013; Li et al, 2007). This discrepancy may reflect variations in the molecular set-up of different experimental models and will be discussed in connection to our analysis of the PrP Δ CR mutant in the following section of the Discussion. On the other hand, the dramatic functional impact of mutations/deletions affecting the GPI-anchor or the N-glycosylation sites corresponds to the important roles of these elements in prion pathogenesis. Concretely, the mutation of N-glycosylation sites was shown to confer PrP with prion-like properties (Lehmann & Harris, 1997), whereas mice expressing GPI-anchorless PrP replicated prions but did not become ill (Chesebro et al, 2005b). Our most intriguing finding is perhaps the crucial role of the globular domain in zebrafish gastrulation/cell adhesion, since no functional properties had been attributed to this region of PrP until now, aside from its pathogenic role as a template for PrP^{Sc} replication (Moroncini et al, 2004; Morrissey & Shakhnovich, 1999; Norstrom & Mastrianni, 2006; Solfrosi et al, 2007). Interestingly, the repetitive domain also contributed largely to PrP's ability to control embryonic cell adhesion. Consistently, the important role of this domain is inferred by its

ability to trigger neuronal disease when expressed in expanded versions in PG14 and other PrP mutants (Bizat et al, 2010; Chiesa et al, 1998).

6.7 Functionality of mouse PrP mutants with a known impact on neuronal survival

Various alterations in the primary sequence of PrP -due to substitutions, insertions or deletions- have been shown to influence neuronal viability and susceptibility to prion disease. Due to the lack of functional *in vivo* readouts for PrP, it had not been feasible to assess whether or how such mutations impinge on its physiological role. To address this question, we examined several such PrP mutants for their subcellular localization and their ability to influence gastrulation in zebrafish embryos.

Subcellular localization in zebrafish embryos

Our expression analysis in embryonic deep cells revealed that mouse PrPs carrying a nine octarepeat insertion (PG14) or large N-terminal deletions (F35 (Δ 32-134) and C3 (Δ 23-134)) differ from WT PrP in their subcellular distribution patterns. For instance, while WT PrP localized evenly along the plasma membrane/cell contacts, the PG14 mutant exhibited a strong tendency to cluster in large patches both in the cytosol and at the cell surface. Such expansions of the octarepeat region are known to trigger the multimerization and/or aggregation of PrP (Biasini et al, 2008; Medrano et al, 2008) and in some cell types, they can induce partial retention of the protein in the ER (Ivanova et al, 2001). In addition, they have been reported to interfere with the dynamics of PrP homophilic copper-dependent interactions, mediated by the repetitive domain (Leliveld et al, 2006). Interestingly, PrP mutants with expanded repetitive domains can cause familial neurodegenerative disorders by spontaneously converting to PrP^{Sc}-like in cases of familial CJD and Gerstmann-Sträussler-Scheinker syndrome- or without forming PrP^{Sc}-like in the case of PG14 (Biasini et al, 2008; Chiesa et al, 1998; Owen et al, 1992). It is however unknown, which of their cellular/molecular properties contribute to either of these pathogenic events. Remarkably, a PrP mutant with an eight octarepeat insertion (PG13) was shown to cause neuronal dysfunction in *C. elegans*, which could be blocked by depleting a Fyn-related kinase (Bizat et al, 2010). Our observation that Fyn acts downstream of PrP under physiological conditions suggests that octarepeat insertions may cause the kinase to acquire an abnormal gain-of-function activity. The reported impact of these repeat expansions on neuronal physiology is also in line with our identification of the repetitive domain as necessary for the roles of PrP in gastrulation and S2 cell contact formation. Remarkably, the expression pattern of PrP PG14 in patches at the plasma membrane of deep cells strongly resembles the localization of WT zebrafish PrP-1. This finding further supports the notion that the

extended repeat region of PrP-1 drives its natural clustering in subregions at cell contacts sites.

The F35 and C3 PrP mutants were not as strongly clustered as PG14, but also displayed a discontinuous/patchy pattern at the plasma membrane of deep cells, triggering a similar but not overlapping distribution of β -catenin. Being N-terminal deletion mutants, F35 and C3 were expected to exhibit a continuous localization, similar to our mouse PrP Δ Rep mutant. However, their discontinuous distribution partly resembled that of Δ Glob, our deletion mutant lacking the entire globular domain. This is somewhat counterintuitive because our functional analysis of PrP domains concluded that the accumulation of PrP in membrane patches is primarily induced by the repetitive domain (residues 36-95 in mouse PrP), and that the globular domain (residues 127-226 in mouse PrP) counteracts this effect by promoting its continuous localization along the plasma membrane (Solis et al, 2013). Since F35 and C3 lack the entire repetitive domain, it can be concluded that their partial accumulation in patches is due to other factors. For instance, it should be noted that these deletions extend C-terminally into residue 134, and therefore the constructs also lack the entire hydrophobic domain and the first 7 amino acids of the globular domain. This suggests that the lack of globular residues 128-134 in F35 and C3 might induce a mild clustering effect independently of the repetitive domain, a scenario that can be addressed in the future using new reporter constructs. Previous studies in mice have also demonstrated that PrP F35 is expressed on the cell surface, without however visualizing its exact localization pattern at the plasma membrane (Shmerling et al, 1998). Thus, it would be interesting to examine whether the pathogenic properties of this mutant are somehow linked to its aberrant plasma membrane distribution. It also remains to be clarified, whether the abnormal concentration of β -catenin in patches upon expression of F35 or C3 PrP is a consequence of the abnormal localization of these PrPs and/or their possible loss-of-function. Our finding that overexpression of WT PrP leads to sequestration of β -catenin at the plasma membrane suggests that N-terminally deleted PrPs with reduced functionality (due to lack of the repetitive domain) may be less efficient at causing this effect, resulting in an uneven β -catenin distribution along the plasma membrane.

In contrast to the aforementioned mutants, mouse PrP constructs missing the N-terminal polybasic stretch (residues 23-31) or the central region (residues 105-125) displayed a subcellular distribution comparable to that of WT PrP. Accordingly, and although these mutations have a great impact on the neuroprotective properties of PrP in mice models (see Results, paragraph 5.8), they are known to localize normally at the plasma membrane (Christensen & Harris, 2009; Turnbaugh et al, 2011). In fact, PrP lacking N-terminal polybasic residues has been shown to be more stably expressed on the cell-surface than

WT PrP due to its defective clathrin-mediated endocytosis (Shyng et al, 1995b; Sunyach et al, 2003). Finally, the WT-like distribution of PrP Δ CR along cell contacts of embryonic deep cells matches the pattern observed for our mutant PrPs lacking the hydrophobic domain, further confirming that this region of PrP does not influence its cellular trafficking or positioning within the plasma membrane.

The N-terminal polybasic residues 23-31 but not the central region affect PrP's function during zebrafish gastrulation

According to our mRNA rescue and overexpression analyses in embryos, the ability of PrP to modulate gastrulation strongly relies on an intact N-terminal polybasic region, which also controls neuronal survival and neurotoxicity in transgenic mice (Solomon et al, 2011; Turnbaugh et al, 2011). This raises the question whether such dissimilar activities of PrP could have a common regulatory mechanism. The 23-31 equivalent regions of mouse and zebrafish PrPs are considerably divergent in amino acid sequence but share a positive charge that may be the key to a common function. In fact, N-terminal polybasic regions can greatly enhance the plasma membrane association of many proteins via electrostatic interactions with membrane lipids (Crouthamel et al, 2008). As demonstrated for G α subunits, the ensuing lateral segregation within plasma membrane sub-regions has a profound effect on the molecule's signaling properties (Crouthamel et al, 2008). Along these lines, the polybasic N-terminus of PrP has been proposed to allow the insertion of PrP into the plasma membrane (Turnbaugh et al, 2011). Thus, the 23-31 region of PrP could indirectly facilitate its interaction with distinct partner molecules located at special microdomains of the plasma membrane. At the same time, this region has been found to be crucial for PrP's endocytosis via clathrin-coated pits (Sunyach et al, 2003). This constitutes another basic mechanism by which the small polybasic stretch could influence several activities of PrP in neurons or the gastrula. Relevant to this would be to examine whether PrP endocytosis is in some way essential for the activation of downstream signaling events.

Unlike the N-terminal polybasic stretch, our analyses do not suggest a significant contribution of the central region of PrP to its function during gastrulation. Accordingly, PrP Δ CR localizes similar to WT PrP at the plasma membrane of embryonic deep cells. These results match our observations on the related zebrafish and mouse Δ HHD mutants, which were also properly localized and fully supported cell-cell adhesion in *Drosophila* S2, human MCF-7 cells and zebrafish embryos (Solis et al, 2013). At the same time, no Δ CR-associated lethality was evident in up to one day old zebrafish embryos, even though we confirmed via the DBCA in mammalian cells that zebrafish Δ CR PrPs harbor the same cytotoxic potential as mouse PrP Δ CR. The WT-like function of PrP Δ CR and its negligible effect on cell viability in zebrafish embryos may at first glance contradict the strong neurotoxic phenotype caused

by this molecule in transgenic mice (Li et al, 2007). However, in the latter animals, Δ CR-triggered toxicity manifests itself only one week after birth and is restricted to neurons. Thus, similar to mouse embryos, early zebrafish gastrulae are refractory to Δ CR-induced toxicity possibly because they lack additional co-factors that only appear at later developmental stages in restricted cell types like neurons. Such a factor could be a molecule whose binding to PrP's central region modulates a neurotoxic/neuroprotective signal. Hence, rather than having an activity of its own, the central region is likely to encode an evolutionary conserved binding site for a molecule that modifies PrP function. The observation that PrP Δ CR induces spontaneous ionic currents in cultured cells prompted the thesis that it either forms ion channels at the plasma membrane or that it regulates the activity of canonical endogenous channels (Biasini et al, 2012; Solomon et al, 2010a). Notably, SFKs can regulate ligand- and voltage-gated ion channel activity in the CNS via tyrosine phosphorylation, thereby influencing neuronal excitability and synaptic plasticity (Ebner-Bennatan et al, 2012). Thus, it will be interesting to examine whether a pathway that links PrP to ion channels via SFKs contributes to Δ CR toxicity in particular, and PrP-induced neurodegeneration in general.

6.8 Neurotoxic A β oligomers induce changes in SFK activation and AJ protein levels in a PrP-1-dependent way

The fact that some of the best known neurodegenerative diseases involve protein misfolding and aggregation lent support to the notion that these conditions could be explained by common molecular mechanisms. During the progress of my doctoral research, the Strittmatter laboratory achieved a breakthrough in this direction by linking Alzheimer's and prion pathologies to a common signaling pathway mediated by PrP (Lauren et al, 2009; Um et al, 2012). This work produced two key findings: a) that PrP acts as a receptor for A β oligomers on the surface of mammalian neurons and b) that the PrP-A β interaction triggers Fyn activation and mediates synaptic damage.

Notably, our experiments in early zebrafish embryonic cells reproduce the activation of Fyn by A β oligomers. In addition, we show that A β treatment activates not only Fyn but also other SFKs like Yes and Src. The fact that this effect was dependent on the expression of zebrafish PrP-1 is remarkable and suggests that A β -binding is an evolutionarily conserved property of vertebrate PrPs. Interestingly, the two major A β -binding sites of mammalian PrPs (Chen et al, 2010; Lauren et al, 2009) and the corresponding protein motifs in zebrafish PrPs are not conserved in their linear sequence but rather in their content of positively charged amino acids. This strongly suggests that binding of PrP to A β is based on electrostatic charge rather than amino acid sequence recognition.

The ability of A β to induce the PrP-dependent activation of SFKs in fish embryonic cells and mammalian neurons illustrates the relevance of PrP-mediated signaling across a wide range of physiological scenarios. Importantly, our work allowed us to compare PrP function in such dissimilar experimental setups and uncover interesting mechanistic similarities. For instance, in both cases SFK activation enhances the cell surface localization of key protein complexes: adherens junction components (zebrafish blastocysts), and the NMDA receptor (mammalian neurons) (Um et al, 2012). Each of these macromolecular assemblies contains transmembrane proteins (E-cadherin and NR2B, respectively) whose endocytic trafficking is negatively modulated by SFKs (Ishiyama et al, 2010; Prybylowski et al, 2005; Roche et al, 2001). Thus, by exerting its control over SFK activity, PrP emerges as a pleiotropic regulator of cell surface expression for proteins involved in diverse forms of cell-cell communication. Accordingly, the combined findings by us and the Strittmatter group demonstrate that A β oligomers can hijack and (over)activate the PrP/SFK pathway, leading to two very different and detrimental physiological outcomes: increased E-cadherin-mediated cell adhesion in the early gastrula, and elevated glutamate-induced excitotoxicity in adult neurons (Um et al, 2012). These A β -induced effects clearly mimic a PrP gain-of-function, making our zebrafish PrP overexpression phenotype especially relevant to the study of prion and Alzheimer's pathogenesis.

Besides directing the cohesion and remodeling of early embryonic tissues, cadherins play key roles during neuronal development and function, particularly in the establishment and maintenance of synapses (Arikkath, 2010). Consequently, a further corollary of our findings is that A β -mediated synaptic dysfunction might not be solely due to impaired ion-channel activity but also to defects in neuronal cell adhesion. Testing this notion in fish and mammalian neurons will likely shed light on the complexity and universality of the cellular pathways contributing to neurodegeneration.

Finally, it is noteworthy that in our experiments, A β induced the PrP-dependent upregulation of E-cadherin regardless of its oligomerization state. Because the analogous effect on SFK activation required A β oligomerization, this result suggests that monomeric A β peptides can also trigger E-cadherin upregulation via PrP but in an SFK-independent manner. Since PrP and E-cadherin do not appear to interact physically (Morel et al, 2004), our data raise the possibility that A β monomers achieve their effect on E-cadherin via the PrP-dependent activation of a different signaling pathway. This would be consistent with the ability of PrP to modulate multiple signaling pathways (Linden et al, 2008). However, given the virtual lack of information regarding the stoichiometry of the A β -PrP interaction, detailed structural studies will be needed to confirm this scenario.

7 Conclusions and Outlook

In this thesis I describe how we used the zebrafish embryo to understand basic, evolutionary conserved roles of PrP in cell-cell communication. Concretely, my doctoral research allowed us to place PrP upstream of a signaling cascade, which relies on SFK activity to modulate the function of cell surface adhesion complexes by controlling their endocytosis and degradation. Most importantly, we thoroughly analyzed how these pathways are affected in both PrP loss- and gain-of-function situations, taking into account that either or both of these two conditions may be relevant to pathogenic events during prion diseases.

Several important insights have been gained from these analyses. For instance, that SFK activation is not an event triggered by PrP only during pathogenesis, but that it in fact mediates at least one physiological cellular function of PrP, namely cell adhesion. Moreover, although previous studies have highlighted Fyn as an activation target of PrP (Mouillet-Richard et al, 2000; Um et al, 2012), here we show that at least one more SFK family member, Src or Yes (or both), is activated in a PrP-dependent manner, either during normal embryonic development or upon treatment of embryonic cells with A β oligomers. Because of its diverse and numerous phosphorylation substrates, Fyn alone can account for several molecular alterations in neuronal physiology (Lee et al, 2004; Um et al, 2012). Our work on embryonic cell signaling and adhesion further suggests that a simultaneous deregulation of multiple SFKs by the same upstream PrP signal would impact additional protein networks important for neuronal homeostasis. Thus, it will be interesting to examine the possibility of a wider palette of neuronal pathways being influenced by SFKs other than Fyn in a PrP-dependent manner. Our study also sheds light on the redundancy of SFK functions under physiological conditions, which may explain the substantial differences between the PrP loss-of-function phenotypes of zebrafish and mice. A systematic double knockout analysis of PrP and different SFK genes in mice, along with the corresponding proteomic studies, will be instrumental in uncovering precisely which array of SFKs and SFK targets is regulated by PrP in mammalian neurons.

In addition, my research specifically addressed how altered levels of cellular PrP impact the equilibrium between plasma membrane and cytosolic pools of AJ proteins. Although neurons do not express E-cadherin, they do form AJs containing its neuronal analogue N-cadherin, β -catenin and proteins with links to the actin cytoskeleton (Knudsen et al, 1995). Interestingly, like their epithelial cousins, neuronal AJs are also regulated via mechanisms

that rely on SFK-mediated phosphorylation and targeted endocytosis (Nelson, 2008). Given these similarities, it becomes an obvious perspective to assess the influence of PrP depletion, overexpression or conversion on the stability of neuronal cadherin/catenin complexes. In fact, ongoing efforts in our lab are aimed at understanding how zebrafish PrP-2 (which contributes to neuronal development and differentiation) may interfere with the regulation of such neuronal adhesive structures. Another interesting finding of my work is that, depending on its levels, PrP can affect not only the adhesive but also the nuclear signaling role of β -catenin. Given the prominent role of β -catenin in the Wnt signaling pathway, our findings raise the intriguing possibility that this signaling cascade may undergo deregulation in neurons infected with prions or exposed to Alzheimer's A β oligomers.

Furthermore, by exploring the role of PrP on SFK-regulated cell adhesion under several conditions (PrP loss- and gain-of function, exposure to A β oligomers), we have been able to draw parallels between the normal function of PrP addressed in our work and its previously reported activity during pathogenesis. For example, an increase in SFK activity appears to be a common consequence of PrP overexpression in the embryo, A β oligomer binding to PrP (Um et al, 2012) and PrP^{Sc} infection (Nixon, 2005), suggesting that the latter two pathogenic events over-stimulate a physiological function of PrP. If the activity of PrP at the plasma membrane is a prerequisite for the onset of neurodegeneration in prion diseases, as implied by mice studies (Chesebro et al, 2005b; Mallucci et al, 2003), it will be important to understand more concretely which regions within PrP's primary sequence modulate its localization and functionality. In this context, our analysis has identified the repetitive and globular domains (as larger regions within the core of the protein) as well as the N-terminal polybasic stretch as important determinants of PrP's ability to influence zebrafish gastrulation. Further steps need to be taken in order to map the smallest, functionally relevant PrP domains/motifs and develop compounds that can bind to these and modulate PrP function. Finally, since PrP activity can be assayed phenotypically and in a quantitative manner in the zebrafish embryo, this model organism constitutes an ideal experimental system for the initial screening of such substances before their assessment as therapeutic drugs in established prion or AD mouse models.

8 References

Aberle H, Schwartz H, Hoschuetzky H, Kemler R (1996) Single amino acid substitutions in proteins of the armadillo gene family abolish their binding to alpha-catenin. *The Journal of biological chemistry* **271**: 1520-1526

Arikkath J (2010) N-cadherin: stabilizing synapses. *The Journal of cell biology* **189**: 397-398

Babb SG, Marrs JA (2004) E-cadherin regulates cell movements and tissue formation in early zebrafish embryos. *Dev Dyn* **230**: 263-277

Balsamo J, Leung T, Ernst H, Zanin MK, Hoffman S, Lilien J (1996) Regulated binding of PTP1B-like phosphatase to N-cadherin: control of cadherin-mediated adhesion by dephosphorylation of beta-catenin. *The Journal of cell biology* **134**: 801-813

Bandapalli OR, Dihlmann S, Helwa R, Macher-Goeppinger S, Weitz J, Schirmacher P, Brand K (2009) Transcriptional activation of the beta-catenin gene at the invasion front of colorectal liver metastases. *The Journal of pathology* **218**: 370-379

Barry AE, Klyubin I, Mc Donald JM, Mably AJ, Farrell MA, Scott M, Walsh DM, Rowan MJ (2011) Alzheimer's disease brain-derived amyloid-beta-mediated inhibition of LTP in vivo is prevented by immunotargeting cellular prion protein. *The Journal of neuroscience : the official journal of the Society for Neuroscience* **31**: 7259-7263

Bellipanni G, Varga M, Maegawa S, Imai Y, Kelly C, Myers AP, Chu F, Talbot WS, Weinberg ES (2006) Essential and opposing roles of zebrafish beta-catenins in the formation of dorsal axial structures and neurectoderm. *Development (Cambridge, England)* **133**: 1299-1309

Bendheim PE, Brown HR, Rudelli RD, Scala LJ, Goller NL, Wen GY, Kascsak RJ, Cashman NR, Bolton DC (1992) Nearly ubiquitous tissue

distribution of the scrapie agent precursor protein. *Neurology* **42**: 149-156

Benetti F, Legname G (2009) De novo mammalian prion synthesis. *Prion* **3**: 213-219

Biasini E, Medrano AZ, Thellung S, Chiesa R, Harris DA (2008) Multiple biochemical similarities between infectious and non-infectious aggregates of a prion protein carrying an octapeptide insertion. *J Neurochem* **104**: 1293-1308

Biasini E, Turnbaugh JA, Unterberger U, Harris DA (2012) Prion protein at the crossroads of physiology and disease. *Trends in neurosciences* **35**: 92-103

Biasini E, Unterberger U, Solomon IH, Massignan T, Senatore A, Bian H, Voigtlaender T, Bowman FP, Bonetto V, Chiesa R, Luebke J, Toselli P, Harris DA (2013) A mutant prion protein sensitizes neurons to glutamate-induced excitotoxicity. *The Journal of neuroscience : the official journal of the Society for Neuroscience* **33**: 2408-2418

Bilic J, Huang YL, Davidson G, Zimmermann T, Cruciat CM, Bienz M, Niehrs C (2007) Wnt induces LRP6 signalosomes and promotes dishevelled-dependent LRP6 phosphorylation. *Science* **316**: 1619-1622

Bizat N, Peyrin JM, Haik S, Cochois V, Beaudry P, Laplanche JL, Neri C (2010) Neuron dysfunction is induced by prion protein with an insertional mutation via a Fyn kinase and reversed by sirtuin activation in *Caenorhabditis elegans*. *J Neurosci* **30**: 5394-5403

Bjorge JD, Jakymiw A, Fujita DJ (2000) Selected glimpses into the activation and function of Src kinase. *Oncogene* **19**: 5620-5635

Bolos V, Peinado H, Perez-Moreno MA, Fraga MF, Esteller M, Cano A (2003) The transcription factor Slug represses E-cadherin expression and induces epithelial to mesenchymal transitions: a comparison with Snail and E47 repressors. *Journal of cell science* **116**: 499-511

Bolton DC, Bendheim PE (1988) A modified host protein model of scrapie. *Ciba Found Symp* **135**: 164-181

Bolton DC, Bendheim PE, Marmorstein AD, Potempska A (1987) Isolation and structural studies of the intact scrapie agent protein. *Arch Biochem Biophys* **258**: 579-590

Bolton DC, McKinley MP, Prusiner SB (1982) Identification of a protein that purifies with the scrapie prion. *Science* **218**: 1309-1311

Bosque PJ, Ryou C, Telling G, Peretz D, Legname G, DeArmond SJ, Prusiner SB (2002) Prions in skeletal muscle. *Proc Natl Acad Sci U S A* **99**: 3812-3817

Brandner S, Isenmann S, Raeber A, Fischer M, Sailer A, Kobayashi Y, Marino S, Weissmann C, Aguzzi A (1996) Normal host prion protein necessary for scrapie-induced neurotoxicity. *Nature* **379**: 339-343

Bremer J, Baumann F, Tiberi C, Wessig C, Fischer H, Schwarz P, Steele AD, Toyka KV, Nave KA, Weis J, Aguzzi A (2010) Axonal prion protein is required for peripheral myelin maintenance. *Nat Neurosci* **13**: 310-318

Brown MT, Cooper JA (1996) Regulation, substrates and functions of src. *Biochimica et biophysica acta* **1287**: 121-149

Bruce ME, Will RG, Ironside JW, McConnell I, Drummond D, Suttie A, McCardle L, Chree A, Hope J, Birkett C, Cousens S, Fraser H, Bostock CJ (1997) Transmissions to mice indicate that 'new variant' CJD is caused by the BSE agent. *Nature* **389**: 498-501

Bueler H, Aguzzi A, Sailer A, Greiner RA, Autenried P, Aguet M, Weissmann C (1993) Mice devoid of PrP are resistant to scrapie. *Cell* **73**: 1339-1347

Cadwalader EL, Condic ML, Yost HJ (2012) 2-O-sulfotransferase regulates Wnt signaling, cell adhesion and cell cycle during zebrafish epiboly. *Development* **139**: 1296-1305

Calautti E, Cabodi S, Stein P, Hatzfeld M, Kedersha N, Paolo Dotto G (1998) Tyrosine phosphorylation and src family kinases control keratinocyte cell-cell adhesion. *Journal of Cell Biology* **141**: 1449

Calautti E, Grossi M, Mammucari C, Aoyama Y, Pirro M, Ono Y, Li J, Dotto G (2002) Fyn tyrosine kinase is a downstream mediator of Rho/PRK2 function in keratinocyte cell-cell adhesion. *The Journal of Cell Biology* **156**: 137

Calzolari L, Lysek DA, Perez DR, Guntert P, Wuthrich K (2005) Prion protein NMR structures of chickens, turtles, and frogs. *Proc Natl Acad Sci U S A* **102**: 651-655

Cancellotti E, Wiseman F, Tuzi NL, Baybutt H, Monaghan P, Aitchison L, Simpson J, Manson JC (2005) Altered glycosylated PrP proteins can have different neuronal trafficking in brain but do not acquire scrapie-like properties. *The Journal of biological chemistry* **280**: 42909-42918

Cao H, Orth JD, Chen J, Weller SG, Heuser JE, McNiven MA (2003) Cortactin is a component of clathrin-coated pits and participates in receptor-mediated endocytosis. *Molecular and cellular biology* **23**: 2162-2170

Cashman NR, Loertscher R, Nalbantoglu J, Shaw I, Kascsak RJ, Bolton DC, Bendheim PE (1990) Cellular isoform of the scrapie agent protein participates in lymphocyte activation. *Cell* **61**: 185-192

Caughey BW, Dong A, Bhat KS, Ernst D, Hayes SF, Caughey WS (1991) Secondary structure analysis of the scrapie-associated protein PrP 27-30 in water by infrared spectroscopy. *Biochemistry* **30**: 7672-7680

Chen S, Mange A, Dong L, Lehmann S, Schachner M (2003) Prion protein as trans-interacting partner for neurons is involved in neurite outgrowth and neuronal survival. *Mol Cell Neurosci* **22**: 227-233

Chen S, Yadav SP, Surewicz WK (2010) Interaction between human prion protein and amyloid-beta (A β) oligomers: role OF N-terminal residues. *The Journal of biological chemistry* **285**: 26377-26383

Chen SG, Teplow DB, Parchi P, Teller JK, Gambetti P, Autilio-Gambetti L (1995) Truncated forms of the human prion protein in normal brain and in prion diseases. *The Journal of biological chemistry* **270**: 19173-19180

Cheng CW, Wu PE, Yu JC, Huang CS, Yue CT, Wu CW, Shen CY (2001) Mechanisms of inactivation of E-cadherin in breast carcinoma: modification of the two-hit hypothesis of tumor suppressor gene. *Oncogene* **20**: 3814-3823

Chesebro B, Race R, Kercher L (2005a) Scrapie pathogenesis in brain and retina: effects of prion protein expression in neurons and astrocytes. *J Neurovirol* **11**: 476-480

Chesebro B, Trifilo M, Race R, Meade-White K, Teng C, LaCasse R, Raymond L, Favara C, Baron G, Priola S, Caughey B, Masliah E, Oldstone M (2005b) Anchorless prion protein results in infectious amyloid disease without clinical scrapie. *Science* **308**: 1435-1439

Chiarini LB, Freitas AR, Zanata SM, Brentani RR, Martins VR, Linden R (2002) Cellular prion protein transduces neuroprotective signals. *Embo J* **21**: 3317-3326

Chiesa R, Piccardo P, Ghetti B, Harris DA (1998) Neurological illness in transgenic mice expressing a prion protein with an insertional mutation. *Neuron* **21**: 1339-1351

Chiesa R, Piccardo P, Quaglio E, Drisaldi B, Si-Hoe SL, Takao M, Ghetti B, Harris DA (2003) Molecular distinction between pathogenic and infectious properties of the prion protein. *J Virol* **77**: 7611-7622

ChitaeV NA, Troyanovsky SM (1998) Adhesive but not lateral E-cadherin complexes require calcium and catenins for their formation. *The Journal of cell biology* **142**: 837-846

Christensen HM, Dikranian K, Li A, Baysac KC, Walls KC, Olney JW, Roth KA, Harris DA (2010) A highly toxic cellular prion protein induces a novel,

nonapoptotic form of neuronal death. *The American journal of pathology* **176**: 2695-2706

Christensen HM, Harris DA (2009) A deleted prion protein that is neurotoxic in vivo is localized normally in cultured cells. *J Neurochem* **108**: 44-56

Clavaguera F, Bolmont T, Crowther RA, Abramowski D, Frank S, Probst A, Fraser G, Stalder AK, Beibel M, Staufenbiel M, Jucker M, Goedert M, Tolnay M (2009) Transmission and spreading of tauopathy in transgenic mouse brain. *Nature cell biology* **11**: 909-913

Collinge J (1997) Human prion diseases and bovine spongiform encephalopathy (BSE). *Hum Mol Genet* **6**: 1699-1705

Collinge J, Whittington MA, Sidle KC, Smith CJ, Palmer MS, Clarke AR, Jefferys JG (1994) Prion protein is necessary for normal synaptic function. *Nature* **370**: 295-297

Cotto E, Andre M, Forgue J, Fleury HJ, Babin PJ (2005) Molecular characterization, phylogenetic relationships, and developmental expression patterns of prion genes in zebrafish (*Danio rerio*). *Febs J* **272**: 500-513

Courtneidge SA (2002) Role of Src in signal transduction pathways. The Jubilee Lecture. *Biochemical Society transactions* **30**: 11-17

Crouthamel M, Thiyagarajan MM, Evanko DS, Wedegaertner PB (2008) N-terminal polybasic motifs are required for plasma membrane localization of Galpha(s) and Galpha(q). *Cell Signal* **20**: 1900-1910

Davis MA, Ireton RC, Reynolds AB (2003) A core function for p120-catenin in cadherin turnover. *The Journal of Cell Biology* **163**: 525-534

De Ferrari GV, Inestrosa NC (2000) Wnt signaling function in Alzheimer's disease. *Brain research Brain research reviews* **33**: 1-12

DeArmond SJ, Mobley WC, DeMott DL, Barry RA, Beckstead JH, Prusiner SB (1987) Changes in the localization of brain prion proteins during scrapie infection. *Neurology* **37**: 1271-1280

Denoyelle M, Valles AM, Lentz D, Thiery JP, Boyer B (2001a) Mesoderm-independent regulation of gastrulation movements by the src tyrosine kinase in *Xenopus* embryo. *Differentiation; research in biological diversity* **69**: 38-48

Denoyelle M, Valles AM, Lentz D, Thiery JP, Boyer B (2001b) Mesoderm-independent regulation of gastrulation movements by the src tyrosine kinase in *Xenopus* embryo. *Differentiation* **69**: 38-48

Devanathan V, Jakovcevski I, Santuccione A, Li S, Lee HJ, Peles E, Leshchyns'ka I, Sytnyk V, Schachner M (2010) Cellular form of prion protein inhibits Reelin-mediated shedding of Caspr from the neuronal cell surface to potentiate Caspr-mediated inhibition of neurite outgrowth. *The Journal of neuroscience : the official journal of the Society for Neuroscience* **30**: 9292-9305

Drees F, Pokutta S, Yamada S, Nelson WJ, Weis WI (2005) Alpha-catenin is a molecular switch that binds E-cadherin-beta-catenin and regulates actin-filament assembly. *Cell* **123**: 903-915

Ebner-Bennatan S, Patrich E, Peretz A, Kornilov P, Tiran Z, Elson A, Attali B (2012) Multifaceted modulation of K⁺ channels by protein-tyrosine phosphatase epsilon tunes neuronal excitability. *J Biol Chem* **287**: 27614-27628

Ewing CM, Ru N, Morton RA, Robinson JC, Wheelock MJ, Johnson KR, Barrett JC, Isaacs WB (1995) Chromosome 5 suppresses tumorigenicity of PC3 prostate cancer cells: correlation with re-expression of alpha-catenin and restoration of E-cadherin function. *Cancer research* **55**: 4813-4817

Fagotto F, Funayama N, Gluck U, Gumbiner BM (1996) Binding to cadherins antagonizes the signaling activity of beta-catenin during axis formation in *Xenopus*. *The Journal of Cell Biology* **132**: 1105-1114

-
- Ford MJ, Burton LJ, Morris RJ, Hall SM (2002) Selective expression of prion protein in peripheral tissues of the adult mouse. *Neuroscience* **113**: 177-192
- Freir DB, Nicoll AJ, Klyubin I, Panico S, Mc Donald JM, Risse E, Asante EA, Farrow MA, Sessions RB, Saibil HR, Clarke AR, Rowan MJ, Walsh DM, Collinge J (2011) Interaction between prion protein and toxic amyloid beta assemblies can be therapeutically targeted at multiple sites. *Nat Commun* **2**: 336
- Fujita Y, Krause G, Scheffner M, Zechner D, Leddy HEM, Behrens J, Sommer T, Birchmeier W (2002) Hakai, a c-Cbl-like protein, ubiquitinates and induces endocytosis of the E-cadherin complex. *Nature cell biology* **4**: 222-231
- Fukata M, Nakagawa M, Kuroda S, Kaibuchi K (1999) Cell adhesion and Rho small GTPases. *Journal of cell science* **112 (Pt 24)**: 4491-4500
- Gimbel DA, Nygaard HB, Coffey EE, Gunther EC, Lauren J, Gimbel ZA, Strittmatter SM (2010) Memory impairment in transgenic Alzheimer mice requires cellular prion protein. *The Journal of neuroscience : the official journal of the Society for Neuroscience* **30**: 6367-6374
- Glatzel M, Abela E, Maissen M, Aguzzi A (2003) Extraneural pathologic prion protein in sporadic Creutzfeldt-Jakob disease. *The New England journal of medicine* **349**: 1812-1820
- Gorodinsky A, Harris DA (1995) Glycolipid-anchored proteins in neuroblastoma cells form detergent-resistant complexes without caveolin. *J Cell Biol* **129**: 619-627
- Govaerts C, Wille H, Prusiner SB, Cohen FE (2004) Evidence for assembly of prions with left-handed beta-helices into trimers. *Proceedings of the National Academy of Sciences of the United States of America* **101**: 8342-8347
- Gu J, Gu X (2003) Natural history and functional divergence of protein tyrosine kinases. *Gene* **317**: 49-57

Haegel H, Larue L, Ohsugi M, Fedorov L, Herrenknecht K, Kemler R (1995) Lack of beta-catenin affects mouse development at gastrulation. *Development* **121**: 3529-3537

Harris D, Lele P, Snider W (1993a) Localization of the mRNA for a chicken prion protein by in situ hybridization. *Proceedings of the National Academy of Sciences of the United States of America* **90**: 4309

Harris DA, Huber MT, van Dijken P, Shyng SL, Chait BT, Wang R (1993b) Processing of a cellular prion protein: identification of N- and C-terminal cleavage sites. *Biochemistry* **32**: 1009-1016

Harris DA, Lele P, Snider WD (1993c) Localization of the mRNA for a chicken prion protein by in situ hybridization. *Proc Natl Acad Sci U S A* **90**: 4309-4313

Harrison SC (2003) Variation on an Src-like theme. *Cell* **112**: 737-740

Hartsock A, Nelson WJ (2012) Competitive regulation of E-cadherin juxtamembrane domain degradation by p120-catenin binding and Hakai-mediated ubiquitination. *PloS one* **7**: e37476

Heasman J, Crawford A, Goldstone K, Garner-Hamrick P, Gumbiner B, McCrea P, Kintner C, Noro CY, Wylie C (1994) Overexpression of cadherins and underexpression of beta-catenin inhibit dorsal mesoderm induction in early *Xenopus* embryos. *Cell* **79**: 791-803

Heasman J, Kofron M, Wylie C (2000) Beta-catenin signaling activity dissected in the early *Xenopus* embryo: a novel antisense approach. *Developmental biology* **222**: 124-134

Heasman SJ, Ridley AJ (2008) Mammalian Rho GTPases: new insights into their functions from in vivo studies. *Nature Reviews Molecular Cell Biology* **9**: 690-701

Hegde RS, Mastrianni JA, Scott MR, DeFea KA, Tremblay P, Torchia M, DeArmond SJ, Prusiner SB, Lingappa VR (1998) A transmembrane form of the prion protein in neurodegenerative disease. *Science* **279**: 827-834

Hegde RS, Tremblay P, Groth D, DeArmond SJ, Prusiner SB, Lingappa VR (1999) Transmissible and genetic prion diseases share a common pathway of neurodegeneration. *Nature* **402**: 822-826

Helwani FM, Kovacs EM, Paterson AD, Verma S, Ali RG, Fanning AS, Weed SA, Yap AS (2004) Cortactin is necessary for E-cadherin-mediated contact formation and actin reorganization. *The Journal of cell biology* **164**: 899-910

Holscher C, Delius H, Burkle A (1998) Overexpression of nonconvertible PrPc delta114-121 in scrapie-infected mouse neuroblastoma cells leads to trans-dominant inhibition of wild-type PrP(Sc) accumulation. *Journal of virology* **72**: 1153-1159

Hornshaw MP, McDermott JR, Candy JM, Lakey JH (1995) Copper binding to the N-terminal tandem repeat region of mammalian and avian prion protein: structural studies using synthetic peptides. *Biochemical and Biophysical Research Communications* **214**: 993-999

Hoschuetzky H, Aberle H, Kemler R (1994) Beta-catenin mediates the interaction of the cadherin-catenin complex with epidermal growth factor receptor. *The Journal of cell biology* **127**: 1375-1380

Howe K, Clark MD, Torroja CF, Torrance J, Berthelot C, Muffato M, Collins JE, Humphray S, McLaren K, Matthews L, McLaren S, Sealy I, Caccamo M, Churcher C, Scott C, Barrett JC, Koch R, Rauch GJ, White S, Chow W, Kilian B, Quintais LT, Guerra-Assuncao JA, Zhou Y, Gu Y, Yen J, Vogel JH, Eyre T, Redmond S, Banerjee R, Chi J, Fu B, Langley E, Maguire SF, Laird GK, Lloyd D, Kenyon E, Donaldson S, Sehra H, Almeida-King J, Loveland J, Trevanion S, Jones M, Quail M, Willey D, Hunt A, Burton J, Sims S, McLay K, Plumb B, Davis J, Clee C, Oliver K, Clark R, Riddle C, Elliott D, Threadgold G, Harden G, Ware D, Mortimer B, Kerry G, Heath P, Phillimore B, Tracey A, Corby N, Dunn M, Johnson C, Wood J, Clark S, Pelan S, Griffiths G, Smith M, Glithero R, Howden P, Barker N, Stevens C,

Harley J, Holt K, Panagiotidis G, Lovell J, Beasley H, Henderson C, Gordon D, Auger K, Wright D, Collins J, Raisen C, Dyer L, Leung K, Robertson L, Ambridge K, Leongamornlert D, McGuire S, Gilderthorp R, Griffiths C, Manthravadi D, Nichol S, Barker G, Whitehead S, Kay M, Brown J, Murnane C, Gray E, Humphries M, Sycamore N, Barker D, Saunders D, Wallis J, Babbage A, Hammond S, Mashreghi-Mohammadi M, Barr L, Martin S, Wray P, Ellington A, Matthews N, Ellwood M, Woodmansey R, Clark G, Cooper J, Tromans A, Grafham D, Skuce C, Pandian R, Andrews R, Harrison E, Kimberley A, Garnett J, Fosker N, Hall R, Garner P, Kelly D, Bird C, Palmer S, Gehring I, Berger A, Dooley CM, Ersan-Urun Z, Eser C, Geiger H, Geisler M, Karotki L, Kirn A, Konantz J, Konantz M, Oberlander M, Rudolph-Geiger S, Teucke M, Osoegawa K, Zhu B, Rapp A, Widaa S, Langford C, Yang F, Carter NP, Harrow J, Ning Z, Herrero J, Searle SM, Enright A, Geisler R, Plasterk RH, Lee C, Westerfield M, de Jong PJ, Zon LI, Postlethwait JH, Nusslein-Volhard C, Hubbard TJ, Roest Crolius H, Rogers J, Stemple DL (2013) The zebrafish reference genome sequence and its relationship to the human genome. *Nature* **496**: 498-503

Huber AH, Weis WI (2001) The structure of the beta-catenin/E-cadherin complex and the molecular basis of diverse ligand recognition by beta-catenin. *Cell* **105**: 391-402

Hundt C, Gauczynski S, Leucht C, Riley ML, Weiss S (2003) Intra- and interspecies interactions between prion proteins and effects of mutations and polymorphisms. *Biological chemistry* **384**: 791-803

Hynes RO (1996) Targeted mutations in cell adhesion genes: what have we learned from them? *Developmental biology* **180**: 402-412

Imai Y, Matsushima Y, Sugimura T, Terada M (1991) A simple and rapid method for generating a deletion by PCR. *Nucleic acids research* **19**: 2785

Ishiyama N, Lee S-H, Liu S, Li G-Y, Smith MJ, Reichardt LF, Ikura M (2010) Dynamic and Static Interactions between p120 Catenin and E-Cadherin Regulate the Stability of Cell-Cell Adhesion. *Cell* **141**: 117-128

-
- Ivanova L, Barmada S, Kummer T, Harris DA (2001) Mutant prion proteins are partially retained in the endoplasmic reticulum. *The Journal of biological chemistry* **276**: 42409-42421
- Jeong BH, Jeon YC, Lee YJ, Cho HJ, Park SJ, Chung DI, Kim J, Kim SH, Kim HT, Choi EK, Choi KC, Carp RI, Kim YS (2010) Creutzfeldt-Jakob disease with the V203I mutation and M129V polymorphism of the prion protein gene (PRNP) and a 17 kDa prion protein fragment. *Neuropathology and applied neurobiology* **36**: 558-563
- Jopling C, den Hertog J (2005) Fyn/Yes and non-canonical Wnt signalling converge on RhoA in vertebrate gastrulation cell movements. *EMBO Rep* **6**: 426-431
- Kanaani J, Prusiner S, Diacovo J, Baekkeskov S, Legname G (2005) Recombinant prion protein induces rapid polarization and development of synapses in embryonic rat hippocampal neurons in vitro. *Journal of Neurochemistry* **95**: 1373-1386
- Kane DA, McFarland KN, Warga RM (2005) Mutations in half baked/E-cadherin block cell behaviors that are necessary for teleost epiboly. *Development* **132**: 1105-1116
- Kelly C, Chin AJ, Leatherman JL, Kozlowski DJ, Weinberg ES (2000) Maternally controlled (beta)-catenin-mediated signaling is required for organizer formation in the zebrafish. *Development (Cambridge, England)* **127**: 3899-3911
- Kim M, Tezuka T, Tanaka K, Yamamoto T (2004) Cbl-c suppresses v-Src-induced transformation through ubiquitin-dependent protein degradation. *Oncogene* **23**: 1645-1655
- Kimmel CB, Ballard WW, Kimmel SR, Ullmann B, Schilling TF (1995) Stages of embryonic development of the zebrafish. *Dev Dyn* **203**: 253-310

-
- Klinghoffer RA, Sachsenmaier C, Cooper JA, Soriano P (1999) Src family kinases are required for integrin but not PDGFR signal transduction. *The EMBO Journal* **18**: 2459-2471
- Knaus KJ, Morillas M, Swietnicki W, Malone M, Surewicz WK, Yee VC (2001) Crystal structure of the human prion protein reveals a mechanism for oligomerization. *Nat Struct Biol* **8**: 770-774
- Knudsen KA, Soler AP, Johnson KR, Wheelock MJ (1995) Interaction of alpha-actinin with the cadherin/catenin cell-cell adhesion complex via alpha-catenin. *The Journal of Cell Biology* **130**: 67-77
- Korth C, Kaneko K, Prusiner SB (2000) Expression of unglycosylated mutated prion protein facilitates PrP(Sc) formation in neuroblastoma cells infected with different prion strains. *The Journal of general virology* **81**: 2555-2563
- Lambert MP, Barlow AK, Chromy BA, Edwards C, Freed R, Liosatos M, Morgan TE, Rozovsky I, Trommer B, Viola KL, Wals P, Zhang C, Finch CE, Krafft GA, Klein WL (1998) Diffusible, nonfibrillar ligands derived from Abeta1-42 are potent central nervous system neurotoxins. *Proceedings of the National Academy of Sciences of the United States of America* **95**: 6448-6453
- Larson M, Sherman MA, Amar F, Nuvolone M, Schneider JA, Bennett DA, Aguzzi A, Lesne SE (2012) The complex PrP(c)-Fyn couples human oligomeric Abeta with pathological tau changes in Alzheimer's disease. *The Journal of neuroscience : the official journal of the Society for Neuroscience* **32**: 16857-16871a
- Lauren J, Gimbel DA, Nygaard HB, Gilbert JW, Strittmatter SM (2009) Cellular prion protein mediates impairment of synaptic plasticity by amyloid-beta oligomers. *Nature* **457**: 1128-1132
- Le Pichon CE, Valley MT, Polymenidou M, Chesler AT, Sagdullaev BT, Aguzzi A, Firestein S (2009) Olfactory behavior and physiology are disrupted in prion protein knockout mice. *Nat Neurosci* **12**: 60-69

Le TL, Yap AS, Stow JL (1999) Recycling of E-cadherin: a potential mechanism for regulating cadherin dynamics. *The Journal of cell biology* **146**: 219-232

Lee G, Thangavel R, Sharma VM, Litersky JM, Bhaskar K, Fang SM, Do LH, Andreadis A, Van Hoesen G, Ksiezak-Reding H (2004) Phosphorylation of tau by fyn: implications for Alzheimer's disease. *The Journal of neuroscience : the official journal of the Society for Neuroscience* **24**: 2304-2312

Lehmann S, Harris DA (1997) Blockade of glycosylation promotes acquisition of scrapie-like properties by the prion protein in cultured cells. *The Journal of biological chemistry* **272**: 21479-21487

Lekven AC, Thorpe CJ, Waxman JS, Moon RT (2001) Zebrafish wnt8 encodes two wnt8 proteins on a bicistronic transcript and is required for mesoderm and neurectoderm patterning. *Developmental cell* **1**: 103-114

Leliveld SR, Dame RT, Wuite GJ, Stitz L, Korth C (2006) The expanded octarepeat domain selectively binds prions and disrupts homomeric prion protein interactions. *The Journal of biological chemistry* **281**: 3268-3275

Lemeer S, Ruijtenbeek R, Pinkse MW, Jopling C, Heck AJ, den Hertog J, Slijper M (2007) Endogenous phosphotyrosine signaling in zebrafish embryos. *Mol Cell Proteomics* **6**: 2088-2099

Leptin M (1991) twist and snail as positive and negative regulators during Drosophila mesoderm development. *Genes & development* **5**: 1568-1576

Lesne S, Koh MT, Kotilinek L, Kaye R, Glabe CG, Yang A, Gallagher M, Ashe KH (2006) A specific amyloid-beta protein assembly in the brain impairs memory. *Nature* **440**: 352-357

Levine E, Lee CH, Kintner C, Gumbiner BM (1994) Selective disruption of E-cadherin function in early Xenopus embryos by a dominant negative mutant. *Development* **120**: 901-909

-
- Li A, Christensen HM, Stewart LR, Roth KA, Chiesa R, Harris DA (2007) Neonatal lethality in transgenic mice expressing prion protein with a deletion of residues 105-125. *Embo J* **26**: 548-558
- Lin S, Wang J, Ye Z, Ip NY, Lin SC (2008) CDK5 activator p35 downregulates E-cadherin precursor independently of CDK5. *FEBS letters* **582**: 1197-1202
- Linden R, Martins VR, Prado MA, Cammarota M, Izquierdo I, Brentani RR (2008) Physiology of the prion protein. *Physiol Rev* **88**: 673-728
- Link V, Shevchenko A, Heisenberg CP (2006) Proteomics of early zebrafish embryos. *BMC Dev Biol* **6**: 1
- Llorens F, Carulla P, Villa A, Torres JM, Fortes P, Ferrer I, Del Rio JA (2013) PrP regulates epidermal growth factor receptor function and cell shape dynamics in Neuro2a cells. *Journal of neurochemistry*
- López Garcia F, Zahn R, Riek R, Wüthrich K (2000) NMR structure of the bovine prion protein. *Proceedings of the National Academy of Sciences of the United States of America* **97**: 8334-8339
- Lundmark K, Westermark GT, Nystrom S, Murphy CL, Solomon A, Westermark P (2002) Transmissibility of systemic amyloidosis by a prion-like mechanism. *Proceedings of the National Academy of Sciences of the United States of America* **99**: 6979-6984
- Lysek DA, Schorn C, Nivon LG, Esteve-Moya V, Christen B, Calzolari L, von Schroetter C, Fiorito F, Herrmann T, Guntert P, Wuthrich K (2005) Prion protein NMR structures of cats, dogs, pigs, and sheep. *Proc Natl Acad Sci U S A*
- Málaga-Trillo E, Sempou E (2009) PrPs: Proteins with a purpose: Lessons from the zebrafish. *Prion* **3**: 129-133
- Málaga-Trillo E, Solis GP, Schrock Y, Geiss C, Luncz L, Thomanetz V, Stuermer CA (2009) Regulation of embryonic cell adhesion by the prion protein. *PLoS biology* **7**: e55

Mallucci G, Dickinson A, Linehan J, Klohn PC, Brandner S, Collinge J (2003) Depleting neuronal PrP in prion infection prevents disease and reverses spongiosis. *Science* **302**: 871-874

Mange A, Milhavet O, Umlauf D, Harris D, Lehmann S (2002) PrP-dependent cell adhesion in N2a neuroblastoma cells. *FEBS Lett* **514**: 159-162

Manson J, West JD, Thomson V, McBride P, Kaufman MH, Hope J (1992) The prion protein gene: a role in mouse embryogenesis? *Development* **115**: 117-122

Manuelidis L (2003) Transmissible encephalopathies: speculations and realities. *Viral Immunol* **16**: 123-139

Massignan T, Stewart RS, Biasini E, Solomon IH, Bonetto V, Chiesa R, Harris DA (2009) A novel, drug-based, cellular assay for the activity of neurotoxic mutants of the prion protein. *J Biol Chem* **285**: 7752-7765

McCrea PD, Brieher WM, Gumbiner BM (1993) Induction of a secondary body axis in *Xenopus* by antibodies to beta-catenin. *The Journal of cell biology* **123**: 477-484

McLachlan RW, Kraemer A, Helwani FM, Kovacs EM, Yap AS (2007) E-cadherin adhesion activates c-Src signaling at cell-cell contacts. *Molecular biology of the cell* **18**: 3214-3223

McLennan NF, Brennan PM, McNeill A, Davies I, Fotheringham A, Rennison KA, Ritchie D, Brannan F, Head MW, Ironside JW, Williams A, Bell JE (2004) Prion protein accumulation and neuroprotection in hypoxic brain damage. *The American journal of pathology* **165**: 227-235

Medrano AZ, Barmada SJ, Biasini E, Harris DA (2008) GFP-tagged mutant prion protein forms intra-axonal aggregates in transgenic mice. *Neurobiology of disease* **31**: 20-32

Meyer-Luehmann M, Coomaraswamy J, Bolmont T, Kaeser S, Schaefer C, Kilger E, Neuenschwander A, Abramowski D, Frey P, Jaton AL, Vigouret JM, Paganetti P, Walsh DM, Mathews PM, Ghiso J, Staufenbiel M, Walker LC, Jucker M (2006) Exogenous induction of cerebral beta-amyloidogenesis is governed by agent and host. *Science* **313**: 1781-1784

Miyashita Y, Ozawa M (2007) A dileucine motif in its cytoplasmic domain directs -catenin-uncoupled E-cadherin to the lysosome. *Journal of Cell Science* **120**: 4395-4406

Montero J-A, Carvalho L, Wilsch-Bräuninger M, Kilian B, Mustafa C, Heisenberg C-P (2005) Shield formation at the onset of zebrafish gastrulation. *Development (Cambridge, England)* **132**: 1187-1198

Montero JA, Heisenberg CP (2004) Gastrulation dynamics: cells move into focus. *Trends Cell Biol* **14**: 620-627

Morel E, Fouquet S, Chateau D, Yvernault L, Frobert Y, Pincon-Raymond M, Chambaz J, Pillot T, Rousset M (2004) The cellular prion protein PrP^c is expressed in human enterocytes in cell-cell junctional domains. *J Biol Chem* **279**: 1499-1505

Moroncini G, Kanu N, Solfrosi L, Abalos G, Telling GC, Head M, Ironside J, Brockes JP, Burton DR, Williamson RA (2004) Motif-grafted antibodies containing the replicative interface of cellular PrP are specific for PrP^{Sc}. *Proceedings of the National Academy of Sciences of the United States of America* **101**: 10404-10409

Morrissey MP, Shakhnovich EI (1999) Evidence for the role of PrP(C) helix 1 in the hydrophilic seeding of prion aggregates. *Proceedings of the National Academy of Sciences of the United States of America* **96**: 11293-11298

Moser M, Colello RJ, Pott U, Oesch B (1995) Developmental expression of the prion protein gene in glial cells. *Neuron* **14**: 509-517

-
- Mouillet-Richard S, Ermonval M, Chebassier C, Laplanche JL, Lehmann S, Launay JM, Kellermann O (2000) Signal transduction through prion protein. *Science* **289**: 1925-1928
- Muramoto T, Scott M, Cohen FE, Prusiner SB (1996) Recombinant scrapie-like prion protein of 106 amino acids is soluble. *Proceedings of the National Academy of Sciences of the United States of America* **93**: 15457-15462
- Nada S, Okada M, MacAuley A, Cooper JA, Nakagawa H (1991) Cloning of a complementary DNA for a protein-tyrosine kinase that specifically phosphorylates a negative regulatory site of p60c-src. *Nature* **351**: 69-72
- Nagafuchi A, Ishihara S, Tsukita S (1994) The roles of catenins in the cadherin-mediated cell adhesion: functional analysis of E-cadherin-alpha catenin fusion molecules. *The Journal of cell biology* **127**: 235-245
- Nelson WJ (2008) Regulation of cell-cell adhesion by the cadherin-catenin complex. *Biochem Soc Trans* **36**: 149-155
- Neuendorf E, Weber A, Saalmueller A, Schatzl H, Reifenberg K, Pfaff E, Groschup MH (2004) Glycosylation deficiency at either one of the two glycan attachment sites of cellular prion protein preserves susceptibility to bovine spongiform encephalopathy and scrapie infections. *The Journal of biological chemistry* **279**: 53306-53316
- Niessen CM, Leckband D, Yap AS (2011) Tissue organization by cadherin adhesion molecules: dynamic molecular and cellular mechanisms of morphogenetic regulation. *Physiological Reviews* **91**: 691-731
- Nieto MA (2002) The snail superfamily of zinc-finger transcription factors. *Nature reviews Molecular cell biology* **3**: 155-166
- Nixon RR (2005) Prion-associated increases in Src-family kinases. *The Journal of biological chemistry* **280**: 2455-2462

Norstrom EM, Mastrianni JA (2005) The AGAAAAGA palindrome in PrP is required to generate a productive PrPSc-PrPC complex that leads to prion propagation. *The Journal of biological chemistry* **280**: 27236-27243

Norstrom EM, Mastrianni JA (2006) The charge structure of helix 1 in the prion protein regulates conversion to pathogenic PrPSc. *Journal of virology* **80**: 8521-8529

Okada M, Nakagawa H (1989) A protein tyrosine kinase involved in regulation of pp60c-src function. *The Journal of biological chemistry* **264**: 20886-20893

Orsulic S, Huber O, Aberle H, Arnold S, Kemler R (1999) E-cadherin binding prevents beta-catenin nuclear localization and beta-catenin/LEF-1-mediated transactivation. *Journal of Cell Science* **112 (Pt 8)**: 1237-1245

Owen F, Poulter M, Collinge J, Leach M, Lofthouse R, Crow TJ, Harding AE (1992) A dementing illness associated with a novel insertion in the prion protein gene. *Brain research Molecular brain research* **13**: 155-157

Ozawa M, Kemler R (1990) Correct proteolytic cleavage is required for the cell adhesive function of uvomorulin. *J Cell Biol* **111**: 1645-1650

Ozawa M, Ringwald M, Kemler R (1990) Uvomorulin-catenin complex formation is regulated by a specific domain in the cytoplasmic region of the cell adhesion molecule. *Proceedings of the National Academy of Sciences of the United States of America* **87**: 4246-4250

Palacios F, Tushir JS, Fujita Y, D'&Souza-Schorey C (2005) Lysosomal targeting of E-cadherin: a unique mechanism for the down-regulation of cell-cell adhesion during epithelial to mesenchymal transitions. *Molecular and Cellular Biology* **25**: 389-402

Pan T, Wong BS, Liu T, Li R, Petersen RB, Sy MS (2002) Cell-surface prion protein interacts with glycosaminoglycans. *The Biochemical journal* **368**: 81-90

Parham SN, Resende CG, Tuite MF (2001) Oligopeptide repeats in the yeast protein Sup35p stabilize intermolecular prion interactions. *The EMBO journal* **20**: 2111-2119

Pauly PC, Harris DA (1998) Copper stimulates endocytosis of the prion protein. *The Journal of biological chemistry* **273**: 33107-33110

Peifer M, Rauskolb C, Williams M, Riggelman B, Wieschaus E (1991) The segment polarity gene armadillo interacts with the wingless signaling pathway in both embryonic and adult pattern formation. *Development* **111**: 1029-1043

Petersen RB, Parchi P, Richardson SL, Urig CB, Gambetti P (1996) Effect of the D178N mutation and the codon 129 polymorphism on the metabolism of the prion protein. *The Journal of biological chemistry* **271**: 12661-12668

Piedra J, Martinez D, Castano J, Miravet S, Dunach M, de Herreros AG (2001) Regulation of beta-catenin structure and activity by tyrosine phosphorylation. *The Journal of biological chemistry* **276**: 20436-20443

Piedra J, Miravet S, Castaño J, Pálmer HG, Heisterkamp N, García de Herreros A, Duñach M (2003) p120 Catenin-associated Fer and Fyn tyrosine kinases regulate beta-catenin Tyr-142 phosphorylation and beta-catenin-alpha-catenin Interaction. *Molecular and Cellular Biology* **23**: 2287-2297

Pokutta S, Weis WI (2000) Structure of the dimerization and beta-catenin-binding region of alpha-catenin. *Molecular cell* **5**: 533-543

Pollard TD, Borisy GG (2003) Cellular motility driven by assembly and disassembly of actin filaments. *Cell* **112**: 453-465

Price DL, Sisodia SS, Gandy SE (1995) Amyloid beta amyloidosis in Alzheimer's disease. *Current opinion in neurology* **8**: 268-274

Priola SA, Chesebro B (1995) A single hamster PrP amino acid blocks conversion to protease-resistant PrP in scrapie-infected mouse neuroblastoma cells. *J Virol* **69**: 7754-7758

Prusiner SB (1982) Novel proteinaceous infectious particles cause scrapie. *Science* **216**: 136-144

Prusiner SB (1991) Molecular biology of prion diseases. *Science* **252**: 1515-1522

Prusiner SB (1998) Prions. *Proc Natl Acad Sci U S A* **95**: 13363-13383

Prusiner SB, Scott M, Foster D, Pan KM, Groth D, Mirinda C, Torchia M, Yang SL, Serban D, Carlson GA, et al. (1990) Transgenic studies implicate interactions between homologous PrP isoforms in scrapie prion replication. *Cell* **63**: 673-686

Prybylowski K, Chang K, Sans N, Kan L, Vicini S, Wenthold RJ (2005) The synaptic localization of NR2B-containing NMDA receptors is controlled by interactions with PDZ proteins and AP-2. *Neuron* **47**: 845-857

Puig B, Altmeyden HC, Thurm D, Geissen M, Conrad C, Braulke T, Glatzel M (2011) N-glycans and glycosylphosphatidylinositol-anchor act on polarized sorting of mouse PrP(C) in Madin-Darby canine kidney cells. *PLoS ONE* **6**: e24624

Raeber AJ, Muramoto T, Kornberg TB, Prusiner SB (1995) Expression and targeting of Syrian hamster prion protein induced by heat shock in transgenic *Drosophila melanogaster*. *Mech Dev* **51**: 317-327

Resenberger UK, Harmeier A, Woerner AC, Goodman JL, Muller V, Krishnan R, Vabulas RM, Kretzschmar HA, Lindquist S, Hartl FU, Multhaup G, Winklhofer KF, Tatzelt J (2011) The cellular prion protein mediates neurotoxic signalling of beta-sheet-rich conformers independent of prion replication. *The EMBO journal* **30**: 2057-2070

Riek R, Hornemann S, Wider G, Glockshuber R, Wuthrich K (1997) NMR characterization of the full-length recombinant murine prion protein, mPrP(23-231). *FEBS Lett* **413**: 282-288

Rivera-Milla E, Oidtmann B, Panagiotidis CH, Baier M, Sklaviadis T, Hoffmann R, Zhou Y, Solis GP, Stuermer CA, Malaga-Trillo E (2006) Disparate evolution of prion protein domains and the distinct origin of Doppel- and prion-related loci revealed by fish-to-mammal comparisons. *FASEB J* **20**: 317-319

Roche KW, Standley S, McCallum J, Dune Ly C, Ehlers MD, Wenthold RJ (2001) Molecular determinants of NMDA receptor internalization. *Nat Neurosci* **4**: 794-802

Rogers M, Taraboulos A, Scott M, Groth D, Prusiner SB (1990) Intracellular accumulation of the cellular prion protein after mutagenesis of its Asn-linked glycosylation sites. *Glycobiology* **1**: 101-109

Roskoski R, Jr. (2004) Src protein-tyrosine kinase structure and regulation. *Biochem Biophys Res Commun* **324**: 1155-1164

Roskoski R, Jr. (2005) Src kinase regulation by phosphorylation and dephosphorylation. *Biochem Biophys Res Commun* **331**: 1-14

Sambrook J, Maniatis T, Fritsch EF (1989) *Molecular cloning : a laboratory manual*, 2nd edn. Cold Spring Harbor, N.Y.: Cold Spring Harbor Laboratory.

Sandilands E, Serrels B, McEwan DG, Morton JP, Macagno JP, McLeod K, Stevens C, Brunton VG, Langdon WY, Vidal M, Sansom OJ, Dikic I, Wilkinson S, Frame MC (2012) Autophagic targeting of Src promotes cancer cell survival following reduced FAK signalling. *Nature cell biology* **14**: 51-60

Sanson B, White P, Vincent JP (1996) Uncoupling cadherin-based adhesion from wingless signalling in *Drosophila*. *Nature* **383**: 627-630

Santuccione A, Sytnyk V, Leshchyns'ka I, Schachner M (2005) Prion protein recruits its neuronal receptor NCAM to lipid rafts to activate p59fyn and to enhance neurite outgrowth. *J Cell Biol* **169**: 341-354

Sarnataro D, Paladino S, Campana V, Grassi J, Nitsch L, Zurzolo C (2002) PrPC is sorted to the basolateral membrane of epithelial cells independently of its association with rafts. *Traffic* **3**: 810-821

Schepis A, Nelson WJ (2012) Adherens junction function and regulation during zebrafish gastrulation. *Cell Adh Migr* **6**: 173-178

Schier AF, Talbot WS (2005) MOLECULAR GENETICS OF AXIS FORMATION IN ZEBRAFISH. *Annual review of genetics* **39**: 561-613

Schmitt-Ulms G, Legname G, Baldwin MA, Ball HL, Bradon N, Bosque PJ, Crossin KL, Edelman GM, DeArmond SJ, Cohen FE, Prusiner SB (2001) Binding of neural cell adhesion molecules (N-CAMs) to the cellular prion protein. *J Mol Biol* **314**: 1209-1225

Schneider S, Steinbeisser H, Warga RM, Hausen P (1996) Beta-catenin translocation into nuclei demarcates the dorsalizing centers in frog and fish embryos. *Mech Dev* **57**: 191-198

Sharma D, Holets L, Zhang X, Kinsey WH (2005) Role of Fyn kinase in signaling associated with epiboly during zebrafish development. *Dev Biol* **285**: 462-476

Shimizu T, Yabe T, Muraoka O, Yonemura S, Aramaki S, Hatta K, Bae YK, Nojima H, Hibi M (2005) E-cadherin is required for gastrulation cell movements in zebrafish. *Mech Dev* **122**: 747-763

Shmerling D, Hegyi I, Fischer M, Blattler T, Brandner S, Gotz J, Rulicke T, Flehsig E, Cozzio A, von Mering C, Hangartner C, Aguzzi A, Weissmann C (1998) Expression of amino-terminally truncated PrP in the mouse leading to ataxia and specific cerebellar lesions. *Cell* **93**: 203-214

Shyng SL, Lehmann S, Moulder KL, Harris DA (1995a) Sulfated glycans stimulate endocytosis of the cellular isoform of the prion protein, PrPC, in cultured cells. *The Journal of biological chemistry* **270**: 30221-30229

Shyng SL, Moulder KL, Lesko A, Harris DA (1995b) The N-terminal domain of a glycolipid-anchored prion protein is essential for its endocytosis via clathrin-coated pits. *The Journal of biological chemistry* **270**: 14793-14800

Simons K, Ikonen E (1997) Functional rafts in cell membranes. *Nature* **387**: 569-572

Solfrosi L, Bellon A, Schaller M, Cruite JT, Abalos GC, Williamson RA (2007) Toward molecular dissection of PrPC-PrPSc interactions. *The Journal of biological chemistry* **282**: 7465-7471

Solis GP, Radon Y, Sempou E, Jechow K, Stuermer CA, Malaga-Trillo E (2013) Conserved roles of the prion protein domains on subcellular localization and cell-cell adhesion. *PloS one* **8**: e70327

Solomon IH, Huettner JE, Harris DA (2010a) Neurotoxic mutants of the prion protein induce spontaneous ionic currents in cultured cells. *J Biol Chem* **285**: 26719-26726

Solomon IH, Khatri N, Biasini E, Massignan T, Huettner JE, Harris DA (2011) An N-terminal Polybasic Domain and Cell Surface Localization Are Required for Mutant Prion Protein Toxicity. *The Journal of biological chemistry* **286**: 14724-14736

Solomon IH, Schepker JA, Harris DA (2010b) Prion neurotoxicity: insights from prion protein mutants. *Curr Issues Mol Biol* **12**: 51-61

Spudich A, Frigg R, Kilic E, Kilic U, Oesch B, Raeber A, Bassetti CL, Hermann DM (2005) Aggravation of ischemic brain injury by prion protein deficiency: role of ERK-1/-2 and STAT-1. *Neurobiology of disease* **20**: 442-449

Steele AD, Emsley JG, Ozdinler PH, Lindquist S, Macklis JD (2006) Prion protein (PrP^c) positively regulates neural precursor proliferation during developmental and adult mammalian neurogenesis. *Proc Natl Acad Sci U S A* **103**: 3416-3421

Stein PL, Vogel H, Soriano P (1994) Combined deficiencies of Src, Fyn, and Yes tyrosine kinases in mutant mice. *Genes & development* **8**: 1999-2007

Stella R, Massimino ML, Sandri M, Sorgato MC, Bertoli A (2010) Cellular prion protein promotes regeneration of adult muscle tissue. *Mol Cell Biol* **30**: 4864-4876

Stewart RS, Harris DA (2001) Most pathogenic mutations do not alter the membrane topology of the prion protein. *The Journal of biological chemistry* **276**: 2212-2220

Sun G, Ramdas L, Wang W, Vinci J, McMurray J, Budde RJ (2002) Effect of autophosphorylation on the catalytic and regulatory properties of protein tyrosine kinase Src. *Archives of biochemistry and biophysics* **397**: 11-17

Sunyach C, Jen A, Deng J, Fitzgerald KT, Frobert Y, Grassi J, McCaffrey MW, Morris R (2003) The mechanism of internalization of glycosylphosphatidylinositol-anchored prion protein. *The EMBO Journal* **22**: 3591-3601

Takahashi F, Endo S, Kojima T, Saigo K (1996) Regulation of cell-cell contacts in developing *Drosophila* eyes by Dsrc41, a new, close relative of vertebrate c-src. *Genes & development* **10**: 1645-1656

Takahashi M, Takahashi F, Ui-Tei K, Kojima T, Saigo K (2005) Requirements of genetic interactions between Src42A, armadillo and shotgun, a gene encoding E-cadherin, for normal development in *Drosophila*. *Development* **132**: 2547-2559

Tank EM, Harris DA, Desai AA, True HL (2007) Prion protein repeat expansion results in increased aggregation and reveals phenotypic variability. *Molecular and Cellular Biology* **27**: 5445-5455

Taylor DR, Watt NT, Perera WS, Hooper NM (2005) Assigning functions to distinct regions of the N-terminus of the prion protein that are involved in its copper-stimulated, clathrin-dependent endocytosis. *Journal of cell science* **118**: 5141-5153

Tehrani S, Tomasevic N, Weed S, Sakowicz R, Cooper JA (2007) Src phosphorylation of cortactin enhances actin assembly. *Proceedings of the National Academy of Sciences of the United States of America* **104**: 11933-11938

Toni M, Spisni E, Griffoni C, Santi S, Riccio M, Lenaz P, Tomasi V (2006) Cellular prion protein and caveolin-1 interaction in a neuronal cell line precedes Fyn/Erk 1/2 signal transduction. *J Biomed Biotechnol* **2006**: 69469

Tsai WB, Zhang X, Sharma D, Wu W, Kinsey WH (2005) Role of Yes kinase during early zebrafish development. *Dev Biol* **277**: 129-141

Tsukita S, Nagafuchi A, Yonemura S (1992) Molecular linkage between cadherins and actin filaments in cell-cell adherens junctions. *Current opinion in cell biology* **4**: 834-839

Turnbaugh JA, Unterberger U, Saa P, Massignan T, Fluharty BR, Bowman FP, Miller MB, Supattapone S, Biasini E, Harris DA (2012) The N-terminal, polybasic region of PrP(C) dictates the efficiency of prion propagation by binding to PrP(Sc). *The Journal of neuroscience : the official journal of the Society for Neuroscience* **32**: 8817-8830

Turnbaugh JA, Westergard L, Unterberger U, Biasini E, Harris DA (2011) The N-terminal, polybasic region is critical for prion protein neuroprotective activity. *PLoS ONE* **6**: e25675

Uelhoff A, Tatzelt J, Aguzzi A, Winklhofer KF, Haass C (2005) A pathogenic PrP mutation and doppel interfere with polarized sorting of the prion protein. *The Journal of biological chemistry* **280**: 5137-5140

Ulrich F, Krieg M, Schotz EM, Link V, Castanon I, Schnabel V, Taubenberger A, Mueller D, Puech PH, Heisenberg CP (2005) Wnt11 functions in gastrulation by controlling cell cohesion through Rab5c and E-cadherin. *Dev Cell* **9**: 555-564

Um JW, Nygaard HB, Heiss JK, Kostylev MA, Stagi M, Vortmeyer A, Wisniewski T, Gunther EC, Strittmatter SM (2012) Alzheimer amyloid-beta oligomer bound to postsynaptic prion protein activates Fyn to impair neurons. *Nat Neurosci* **15**: 1227-1235

Uruno T, Liu J, Zhang P, Fan Y, Egile C, Li R, Mueller SC, Zhan X (2001) Activation of Arp2/3 complex-mediated actin polymerization by cortactin. *Nature cell biology* **3**: 259-266

Vagin O, Kraut JA, Sachs G (2009) Role of N-glycosylation in trafficking of apical membrane proteins in epithelia. *American journal of physiology Renal physiology* **296**: F459-469

Vincent B, Paitel E, Frobert Y, Lehmann S, Grassi J, Checler F (2000) Phorbol ester-regulated cleavage of normal prion protein in HEK293 human cells and murine neurons. *The Journal of biological chemistry* **275**: 35612-35616

Walsh DM, Klyubin I, Fadeeva JV, Cullen WK, Anwyl R, Wolfe MS, Rowan MJ, Selkoe DJ (2002) Naturally secreted oligomers of amyloid beta protein potently inhibit hippocampal long-term potentiation in vivo. *Nature* **416**: 535-539

Weaver AM, Heuser JE, Karginov AV, Lee WL, Parsons JT, Cooper JA (2002) Interaction of cortactin and N-WASp with Arp2/3 complex. *Current biology : CB* **12**: 1270-1278

Weaver AM, Karginov AV, Kinley AW, Weed SA, Li Y, Parsons JT, Cooper JA (2001) Cortactin promotes and stabilizes Arp2/3-induced actin filament network formation. *Current biology : CB* **11**: 370-374

Weinstein DC, Hemmati-Brivanlou AA (2001) Src family kinase function during early *Xenopus* development. *Developmental dynamics : an official publication of the American Association of Anatomists* **220**: 163-168

Weissmann C (2004) The state of the prion. *Nat Rev Microbiol* **2**: 861-871

Westerfield M (1993) *The Zebrafish book : a guide for the laboratory use of zebrafish (Brachydanio rerio)*, Eugene. Or.: University of Oregon Press.

Westergard L, Christensen HM, Harris DA (2007) The cellular prion protein (PrP(C)): its physiological function and role in disease. *Biochim Biophys Acta* **1772**: 629-644

Westergard L, Turnbaugh JA, Harris DA (2011a) A naturally occurring C-terminal fragment of the prion protein (PrP) delays disease and acts as a dominant-negative inhibitor of PrPSc formation. *The Journal of biological chemistry* **286**: 44234-44242

Westergard L, Turnbaugh JA, Harris DA (2011b) A nine amino acid domain is essential for mutant prion protein toxicity. *The Journal of neuroscience : the official journal of the Society for Neuroscience* **31**: 14005-14017

Whelock MJ, Johnson KR (2003) Cadherin-mediated cellular signaling. *Current opinion in cell biology* **15**: 509-514

Wille H, Michelitsch MD, Guenebaut V, Supattapone S, Serban A, Cohen FE, Agard DA, Prusiner SB (2002) Structural studies of the scrapie prion protein by electron crystallography. *Proceedings of the National Academy of Sciences of the United States of America* **99**: 3563-3568

Witzel S, Zimyanin V, Carreira-Barbosa F, Tada M, Heisenberg CP (2006) Wnt11 controls cell contact persistence by local accumulation of Frizzled 7 at the plasma membrane. *J Cell Biol* **175**: 791-802

Wodarz A, Nusse R (1998) Mechanisms of Wnt signaling in development. *Annu Rev Cell Dev Biol* **14**: 59-88

Wong BS, Liu T, Li R, Pan T, Petersen RB, Smith MA, Gambetti P, Perry G, Manson JC, Brown DR, Sy MS (2001) Increased levels of oxidative stress markers detected in the brains of mice devoid of prion protein. *J Neurochem* **76**: 565-572

Wu H, Parsons JT (1993) Cortactin, an 80/85-kilodalton pp60src substrate, is a filamentous actin-binding protein enriched in the cell cortex. *The Journal of cell biology* **120**: 1417-1426

Wu H, Reynolds AB, Kanner SB, Vines RR, Parsons JT (1991) Identification and characterization of a novel cytoskeleton-associated pp60src substrate. *Molecular and cellular biology* **11**: 5113-5124

Xing Y, Nakamura A, Chiba T, Kogishi K, Matsushita T, Li F, Guo Z, Hosokawa M, Mori M, Higuchi K (2001) Transmission of mouse senile amyloidosis. *Laboratory investigation; a journal of technical methods and pathology* **81**: 493-499

Yang JY, Zong CS, Xia W, Wei Y, Ali-Seyed M, Li Z, Broglio K, Berry DA, Hung MC (2006) MDM2 promotes cell motility and invasiveness by regulating E-cadherin degradation. *Molecular and Cellular Biology* **26**: 7269-7282

Zanata SM, Lopes MH, Mercadante AF, Hajj GN, Chiarini LB, Nomizo R, Freitas AR, Cabral AL, Lee KS, Juliano MA, de Oliveira E, Jachieri SG, Burlingame A, Huang L, Linden R, Brentani RR, Martins VR (2002) Stress-inducible protein 1 is a cell surface ligand for cellular prion that triggers neuroprotection. *The EMBO journal* **21**: 3307-3316

Zhang B, Xiong WC, Mei L (2009) Get ready to Wnt: prepatterning in neuromuscular junction formation. *Developmental cell* **16**: 325-327

Zhang J, Shemezis JR, McQuinn ER, Wang J, Sverdlov M, Chenn A (2013) AKT activation by N-cadherin regulates beta-catenin signaling and neuronal differentiation during cortical development. *Neural Dev* **8**: 7

9 Acknowledgements

First, I would like to extend my immense gratitude to my Ph.D. advisor Dr. Ed Málaga-Trillo for his outstanding scientific guidance, the uncountable hours he invested in my training and mentoring, and all his generous and kind support throughout my doctoral work. I will always remain grateful for having been given the opportunity to be part of this work.

Second, I want to thank Professor Dr. Stürmer for her generous support throughout my Ph.D. work and the opportunity to participate in some of the most stimulating conversations during lab meetings and Journal Clubs.

Third, I want to express my gratitude to my family (Michael, Ingrid and Georgia), who have never ceased to support me in my endeavors and have always been there for me when I have sought their help or advice.

Also, all my good friends in Konstanz and at home in Greece, especially Ursula Heins-Marroquin for always being there during the good and bad times in Konstanz. Many thanks also to my lovely lab mates Sarah, Nikola and Alejo for all the happy moments during lunch breaks and in the lab.

I would also like to thank Anette-Yvonne Loos, who took exceptional care of our zebrafish facility and provided our lab with embryos throughout my doctoral research. Also, to Marianne Wiechers and Ulrike Binkle for their great technical and moral support.

Finally, I would like to thank Dr. D.A. Harris for the months he hosted me in his laboratory in Boston in a wonderfully welcoming and stimulating environment.

